2-Dimensional Base Level Engineering (BLE) Report

HUC 1404: Upper Green - Great Divide Watershed, Wyoming

HUC8 Subbasins included: 14040101, 14040102, 14040103, 14040104, 14040105, 14040106, 14040107, 14040108, 14040109, and 14040200

Counties Included: Lincoln, Sublette, Sweetwater, and Uinta

MIP Case No: 23-08-0020S

Prepared by:

STARR II
PTS Zone 3

October 2025

Prepared for:

FEMA

Table of Contents

List of Tables

List of Figures

List of Acronyms

2D	Two-dimensional
AORC	Analysis of Record for Calibration
AWS	Amazon Web Services
BLE	Base Level Engineering
CNMS	Coordinated Needs Management Strategy
DEM	Digital Elevation Model
ENSO	El Niño-Southern Oscillation
FEMA	Federal Emergency Management Agency
FIRM	Effective Flood Insurance Rate Map
HEC-HMS	Hydrologic Engineering Center Hydrologic Modeling System
HEC -RAS	Hydrologic Engineering Center Hydrologic Modeling System
HEC-DSS	Hydrologic Engineering Center Hydraulic Modeling System
HMR	Hazardous Materials Regulations
HUC	Hydrologic Unit Code
IBTrACS	International Best Track Archive for Climate Stewardship
MFC	Multi-Frequency Calibration
NED	National Elevation Dataset
NetCDF	Network Common Data Form
NHD	National Hydrography Dataset
NFIP	National Flood Insurance Program
NOAA	National Oceanic and Atmospheric Administration
NRCS/USDA	Natural Resources Conservation Service
QPE	Quantitative Precipitation Estimates
PF	Precipitation Frequency
PRISM	Parameter-elevation Regressions on Independent Slopes Model
SNOTEL	Snowpack Telemetry Network

Sq mi	Square mile
SST	Stochastic Storm Transposition
SWE	Snow Water Equivalent
UGGD	Upper Green-Great Divide
USACE	U.S. Army Corps of Engineers
USBR	United States Bureau of Reclamation
USGS	United States Geological Survey
WSEL	Water Surface Elevation

1.0 Executive Summary

The two-dimensional (2D) Base Level Engineering (BLE) study conducted for the Upper Green-Great Divide Watershed (UGGD) in Wyoming focuses on hydrologic and hydraulic modeling to assess flood risk in the region. This study, part of the FEMA Risk MAP program, supports regulatory efforts and emergency management by providing scalable and cost-effective flood risk assessments.

This report serves as a technical record of the modeling approach, data sources, calibration processes, and workflow implementation, ensuring transparency, reproducibility, and consistency in flood hazard assessment and future applications.

The report documents the hydrologic and hydraulic modeling process used in the Region 8 Wyoming 2D BLE data production. It provides a comprehensive technical overview of the methodologies applied to develop, run, and troubleshoot the HEC-HMS hydrologic models and HEC-RAS hydraulic models, including the application of the Stochastic Storm Transposition (SST) methodology for generating synthetic storm events.

The HEC-HMS modeling focuses on generating inflow hydrographs using SST techniques, which serve as boundary conditions for the HEC-RAS hydraulic models. This approach, informed by recent USACE and FEMA watershed modeling pilots (Kanawha River Basin, West Virginia, 2022), addresses data gaps in the study area where traditional precipitation-frequency data and USGS regression equations are outdated or unavailable. By developing a suite of synthetic storms based on the gridded precipitation dataset over 40 years, the modeling process captures realistic spatial and temporal precipitation patterns. These synthetic storms are used to simulate runoff and generate probabilistic hydrographs representing a range of possible flood events, ensuring the resulting inflows reflect the basin's hydrologic response under varying conditions, rather than relying solely on outdated statistical relationships or design storms.

The HEC-RAS hydraulic modeling relies on inflow hydrographs from HEC-HMS models, with non-headwater domains receiving inflows from upstream HEC-HMS outflows. The final deliverables include terrain data, calibrated HEC-HMS and HEC-RAS models, water surface elevation and depth grids for multiple flood frequencies, velocity grids, and draft FIRM database products. Seamless, study-wide raster and polygon floodplain products will be created, with overlapping model domains to ensure consistency and facilitate final mapping.

2.0   Introduction

2.1   Purpose of Study

Through its Risk Mapping, Assessment, and Planning (Risk MAP) Program, the Federal Emergency Management Agency (FEMA) works with Federal, State, Tribal, and local partners to identify flood hazards and provide tools that help communities understand and manage their flood risks. The updated base-level flood risk information developed through this project, combined with insights and data gathered during the Discovery process, supports hazard mitigation efforts by providing communities with the information needed to raise awareness and take proactive measures to reduce the impacts of future flooding events.

2.2   Project Contacts and Stakeholders

Table 1 outlines the project contacts and stakeholders.

Table 1. The list of project contacts and stakeholders.

Organization	Title	Point of Contact	Email Address
FEMA	FEMA Project Monitor	Jamie Prochno	jamie.prochno@fema.dhs.gov
FEMA	FEMA Lead Engineer	Jaime Prochno	jamie.prochno@fema.dhs.gov
State	Wyoming NFIP Coordinator	Kim Johnson	kim.johnson@wyo.gov
STARR II	Project Manager	Jon Pink	Jpink@dewberry.com
STARR II	BLE Technical Lead	David Sutley	Dsutley@dewberry.com
STARR II	Discovery Lead	Jerri Daniels	jdaniels@dewberry.com
STARR II	BLE Subject Matter Expert	Curtis Smith	curtis.smith@stantec.com
STARR II	Hydraulics Project Manager	Jason Schneider	jason.schneider@stantec.com

2.3   Study Area Description

The study area covers the Upper Green–Great Divide (UGGD) Watershed, located in southwestern Wyoming. The area encompasses the full extent of the UGGD HUC4 watershed (HUC 1404), as shown in Figure 1, which is predominantly in Wyoming. The area of this watershed is approximately 21,000 square miles (sq mi). At a finer scale, the watershed is composed of:

- 81 HUC10 subwatersheds with a median size of ~250 sq mi.

- 485 HUC12 subwatersheds with a median size of ~42 sq mi.

Although the watershed extends into Utah and Colorado, this project focuses exclusively on the portions located within Lincoln, Sublette, Sweetwater, and Uinta Counties in Wyoming, which lie within the HUC4 watershed boundaries (outlined in red in Figure 1).

The UGGD watershed consists of ten HUC8 subbasins, identified as 14040101, 14040102, 14040103, 14040104, 14040105, 14040106, 14040107, 14040108, 14040109, and 14040200 (Figure 2).
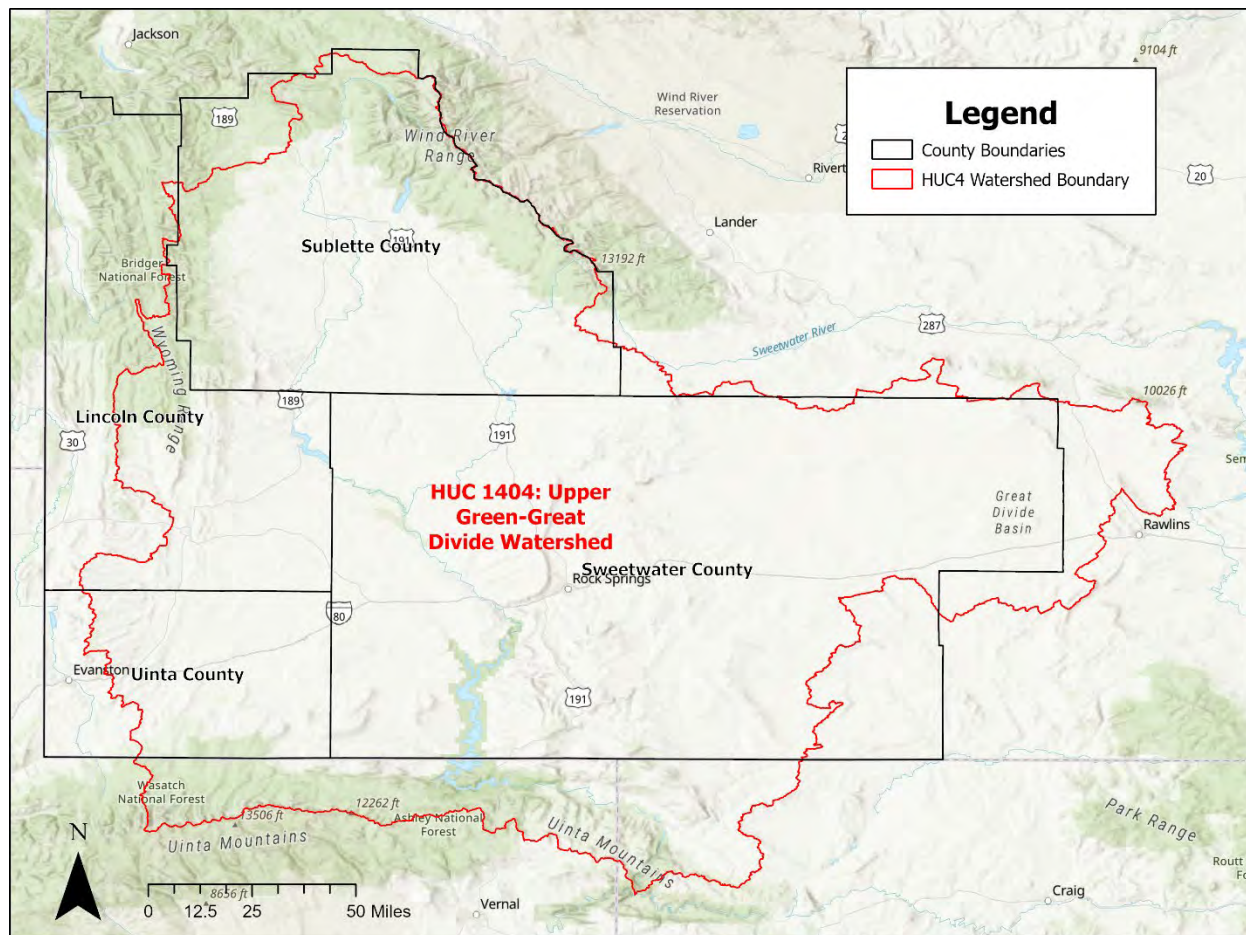
Figure 1. Upper Green- Great Divide study area

The UGGD watershed is part of the larger Colorado River Basin. Surface water from this watershed primarily drains south via the Green River, the largest tributary to the Colorado River. The Green River originates in the Wind River Range of Wyoming, flowing southward through Fontenelle Reservoir and Flaming Gorge Reservoir before continuing into Utah and Colorado, where it ultimately joins the Colorado River. This drainage system plays a critical role in supporting hydrologic and ecological processes, serving as a key water supply for agricultural, municipal, and environmental uses throughout the Upper Colorado Basin. Additionally, two major reservoirs, Fontenelle Dam on the Green River and Flaming Gorge Dam on the Green River near the Utah border (Figure 2), play significant roles in regulating streamflow within the UGGD watershed in

Wyoming. The U.S. Bureau of Reclamation (USBR) operates both reservoirs for purposes including water supply, hydropower, and flood control.

Figure 2. HUC8 subbasins, locations of Fontenelle and Flaming Gorge dams, and major rivers.

The project area includes fifteen communities across Lincoln, Sublette, Sweetwater, and Uinta Counties, all of which lie within the watershed boundary. These communities range from larger population centers, such as Rock Springs and Green River in Sweetwater County, to smaller rural communities including Kemmerer, Pinedale, La Barge, and Lyman. By incorporating both urban and rural communities, the project ensured that the flood risk products and modeling outputs would address a wide range of development patterns, land uses, and infrastructure vulnerabilities throughout the watershed. The list of Wyoming communities covered in the study area includes:

- Sweetwater County: Rock Springs, Green River, Granger, Superior, Bairoil, Wamsutter.
- Sublette County: Pinedale, Big Piney, Marbleton.
- Lincoln County: Kemmerer, La Barge, Diamondville, Opal.
- Uinta County: Lyman, Mountain View.

The UGGD watershed encompasses a variety of land uses that define the region's landscape. These land uses vary across Lincoln, Sublette, Sweetwater, and Uinta Counties, reflecting differences in development, land cover, and natural resource management. The watershed includes a mix of rangelands, forests, urban areas, and public lands, shaping the overall land use patterns within the region. The predominant land uses include:

- Agriculture and grazing: large portions of the watershed are used for livestock grazing and irrigated agriculture, especially in rural areas around Pinedale, Big Piney, Marbleton, Kemmerer, and La Barge.

- Forestry: the watershed contains extensive forest cover, particularly within the Bridger-Teton National Forest, which spans portions of Sublette and Lincoln Counties.

- Urban and municipal development: urbanized areas are limited but include Rock Springs, Green River, and Kemmerer, as well as smaller towns such as Lyman, Mountain View, and Diamondville. These communities contain residential, commercial, and municipal infrastructure.

- Public lands and recreation: large sections of the watershed, especially in Sweetwater and Lincoln Counties, are public lands, supporting outdoor recreation, hunting, and conservation efforts.

The total population of these four counties is 91,843 (U.S. Census Bureau, 2024). However, this number represents the population for the entire extent of all counties, not just the portions within the study watershed.

2.4 Topography

The UGGD watershed features diverse topography shaped by its position at the intersection of the Rocky Mountains and the high-elevation Wyoming Basin. The northern and western portions of the watershed include rugged mountain terrain, particularly in the Wind River Range and Wyoming Range, characterized by steep slopes, glacially-carved valleys, and extensive areas of exposed bedrock.

Descending from the mountains, the terrain transitions into broad alluvial valleys, rolling foothills, and high plains (USGS, 2023). The central and southern portions of the watershed, including the Great Divide Basin, are dominated by semi-arid plateaus, sagebrush steppe, and intermittent drainages, with a mixture of gentle slopes, isolated ridges, and ephemeral stream channels.

The Green River, which drains much of the watershed, flows southward through Fontenelle Reservoir and Flaming Gorge Reservoir, cutting through deep canyons in some areas and broadening into floodplains in others. The diverse topography influences hydrologic processes, with steep mountain headwaters contributing to rapid runoff, while lower-gradient areas provide opportunities for sediment deposition and temporary floodwater storage.

Overall, the combination of mountains, foothills, valleys, and arid plateaus defines the varied topography of the UGGD Watershed, influencing both surface water movement and the spatial variability of flood hazards across the study area.

Figure 3 displays the topography of the study area. The terrain data was sourced from NED 13 tiles using datasets from the USGS National Map Downloader (2023) and represents the same topography used for the hydrologic analysis. It is important to note that the topographic data used in the HEC-RAS hydraulic model has a finer resolution than the data shown in this figure. The primary purpose of this figure is to provide a general overview of the topographic features within the study area.
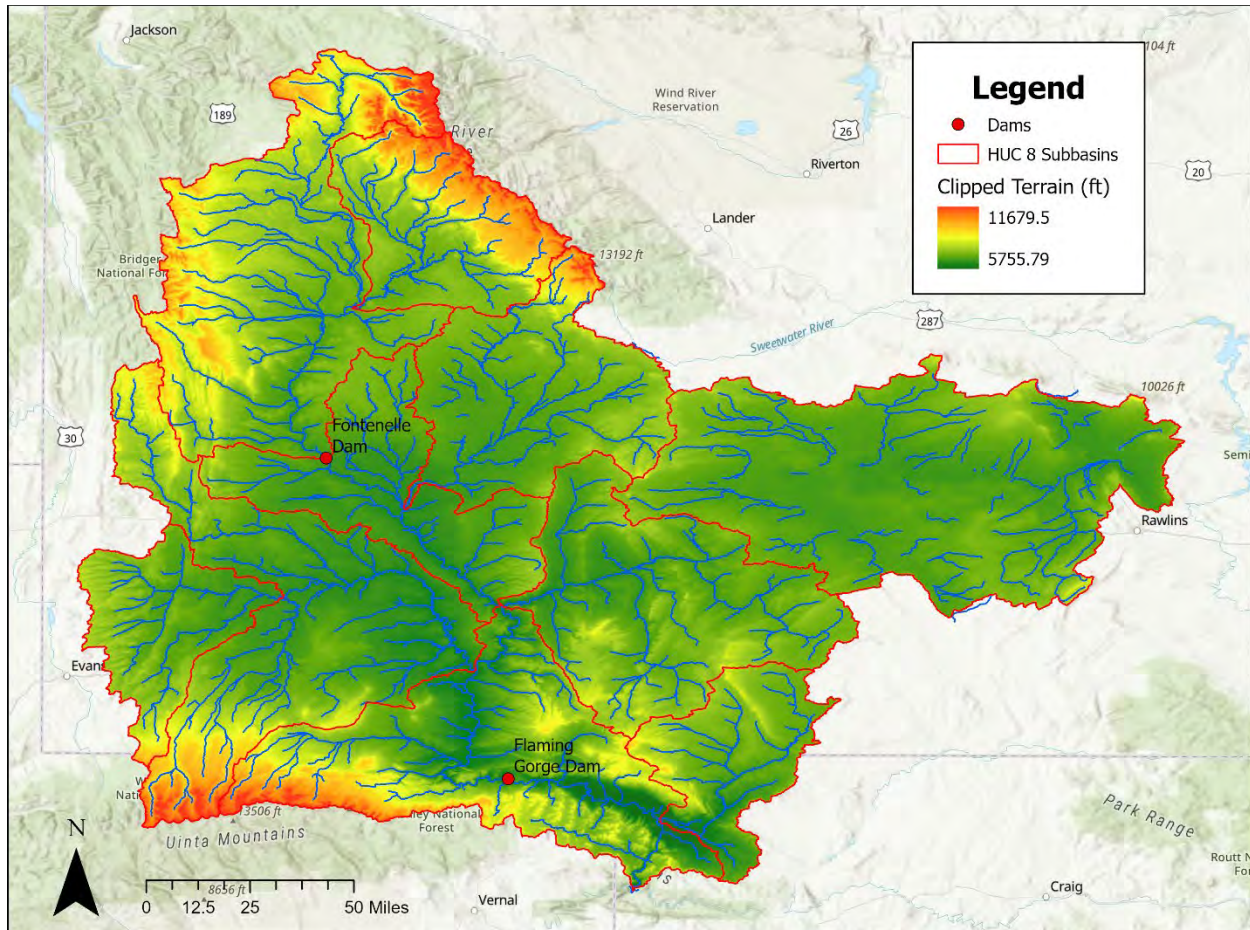
Figure 3. Clipped NED 13 terrain for the HUC4 study area.

2.5   Climatology

2.5.1   Precipitation

Southwest Wyoming has a semi-arid to arid climate, largely due to the rain shadow effect of the Rocky Mountains and its continental location far from maritime moisture sources. The UGGD Basin itself is surrounded by the Wind River Range to the northeast, the Wyoming Range to the west, and the Uinta Mountains to the south, while the Continental Divide bounds the eastern edge of the basin, including the Great Divide Closed Basin. This unique geography creates a high-elevation (greater than 5000 feet, 1600 meters) desert in the central valley of the basin as available moisture is blocked and reduced moving over the surrounding mountain ranges (up to 13,000 feet, 3980 meters).

The average annual precipitation in the Upper Green ranges from less than 7 inches (170 mm) in the dry, central valley and up to nearly 52 inches (1325 mm) in the high elevation mountain ranges that surround the basin, according to estimates from PRISM (Figure 4). Most of the precipitation in this region falls in the winter as snow along the mountain ranges, which supports the region's snowpack. Spring and summer rain showers and thunderstorms also occur but make up a much smaller portion of the region's annual precipitation total.
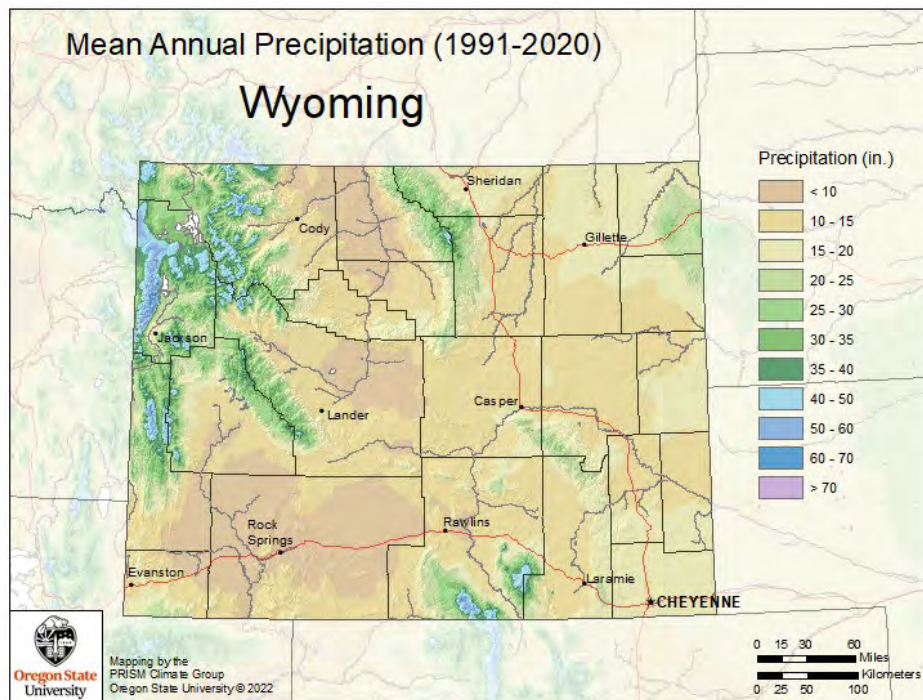
Figure 4. PRISM Mean Annual Precipitation in Wyoming from 1991-2020.

Basin average precipitation (Figure 5) derived from PRISM peaks in April-May with a secondary peak in September-October, and the lowest basin average precipitation is in July-August. However, basin maximum precipitation (Figure 6) shows a clear difference between the warm

season (~June-September) and cool season (October-~May), when the largest precipitation accumulation occurs in the cool season/winter months of November-February. This illustrates that while precipitation is more widespread across the basin during the shoulder months between the warm and cool seasons, the greatest precipitation totals occur during the cool season months but are constrained to the high elevation mountain ranges.
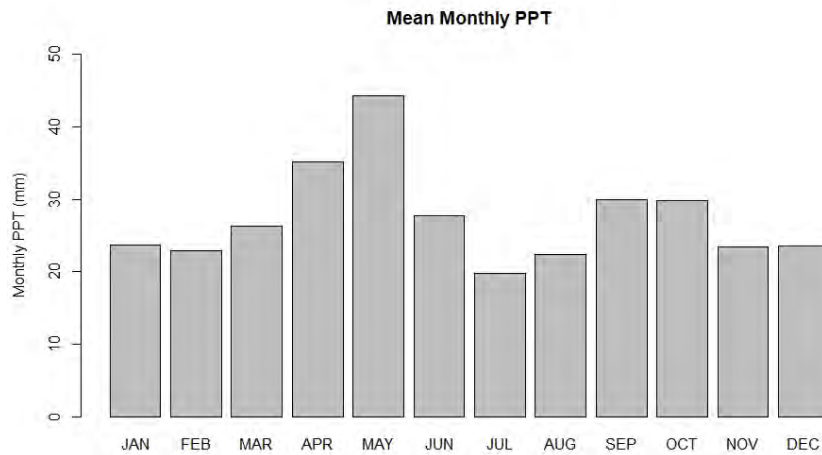
Figure 5. Basin average monthly precipitation for HUC 1404 (Upper Green) from PRISM.
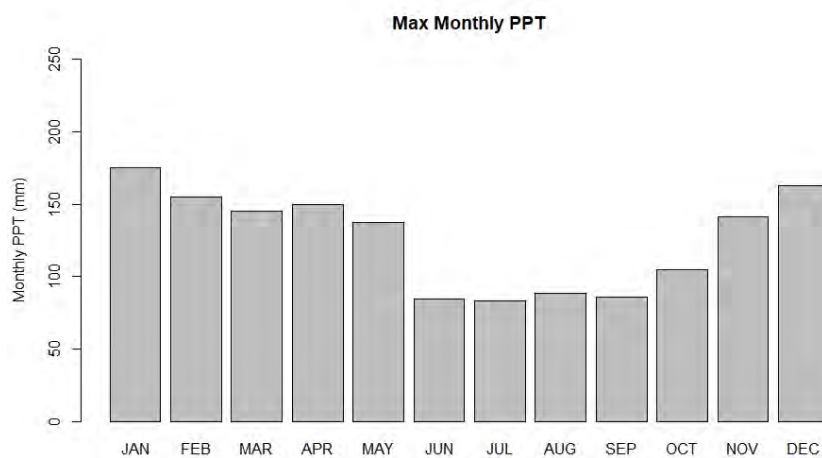
Figure 6. Basin maximum monthly precipitation for HUC 1404 (Upper Green) from PRISM.

El Niño (warm Eastern Pacific) events are typically associated with wetter than normal conditions in Southwest Wyoming, while conversely La Niña (cool Eastern Pacific) events are typically associated with dryer than normal conditions. The El Niño Southern Oscillation (ENSO) has a stronger impact on winter precipitation as distance to the Pacific decreases, as such ENSO has only a moderate impact on precipitation in the Upper Green.

2.5.2   Snowpack

Snow Water Equivalent (SWE) is a measure of how much water the snowpack contains. In the UGGD, snowpack generally begins to build up in October and reaches a peak in late spring. Snowmelt begins after peak SWE is reached, and typically takes until early summer for melt out. For the climatological period from 1991-2020, the median peak SWE occurs on April 10, with the snowpack containing approximately 14.5 inches of liquid equivalent (Figure 7), and is typically completely melted out by June 17 – a roughly two month period of rapid snowmelt. The greatest observed peak SWE for the UGGD (since SNOTEL observations began in the 1980s) was 24.1 inches on May 1, 1986, while the lowest observed peak SWE was only 9.8 inches on April 3, 2015. Annual total precipitation and snowpack are closely related; since most of the precipitation in the basin falls as snow, a higher than median precipitation year would result in a higher than median snowpack as well.
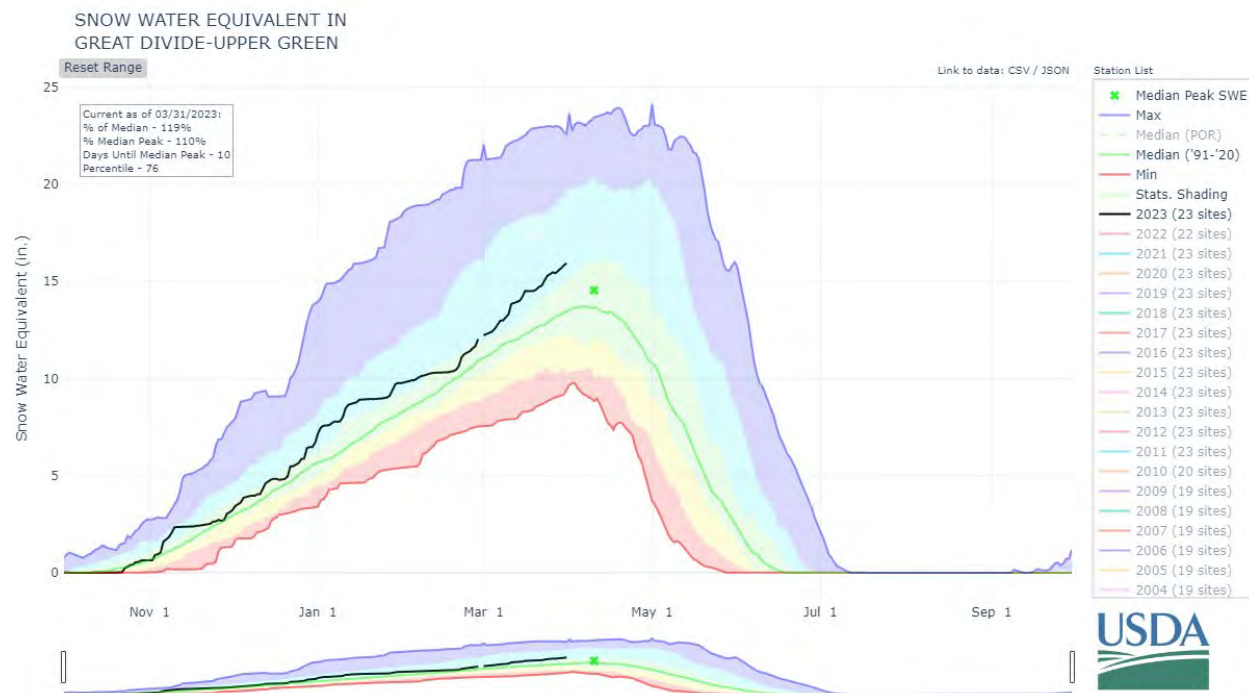
Figure 7. Median (green line), maximum (blue line), and minimum (red line) SWE for the Upper Green for the climatological period from 1991-2020. Statistical shading breaks are at the 10th, 30th, 50th, 70th, and 90th percentiles. The black line shows the 2023 water year, beginning October 1, 2022 as of March 31, 2023.

2.5.3   Riverine Flooding

Riverine flooding in Southwest Wyoming typically occurs in the late spring and early summer as a result of snowmelt but is also influenced by the meteorology of the region including temperature, humidity, and additional precipitation. Heavy precipitation as rainfall during the snowmelt season

(roughly April – June) is the most likely to result in rapid snowpack melt out and therefore riverine flooding, though warm temperatures and high relative humidity can also act to quickly melt out a snowpack without any actual rainfall.

While there is a clear relationship between annual precipitation and snowpack, the relationship between snowmelt season precipitation and the state of the snowpack is less obvious. For the 37-year period between 1986-2022, there were a total of 11 years where both peak SWE and snowmelt season precipitation were above the climatological median of each value. There were also 11 years in which both peak SWE and snowmelt season precipitation were below the climatological median (using the 1991-2020 normal from NRCS/USDA; Figure 7). This leaves 15 remaining years in which peak SWE was above the median and snowmelt season precipitation was below the median, or vice versa. Therefore, approximately 40% of the years in the period of record have an opposing relationship between snowpack and snowmelt season precipitation.
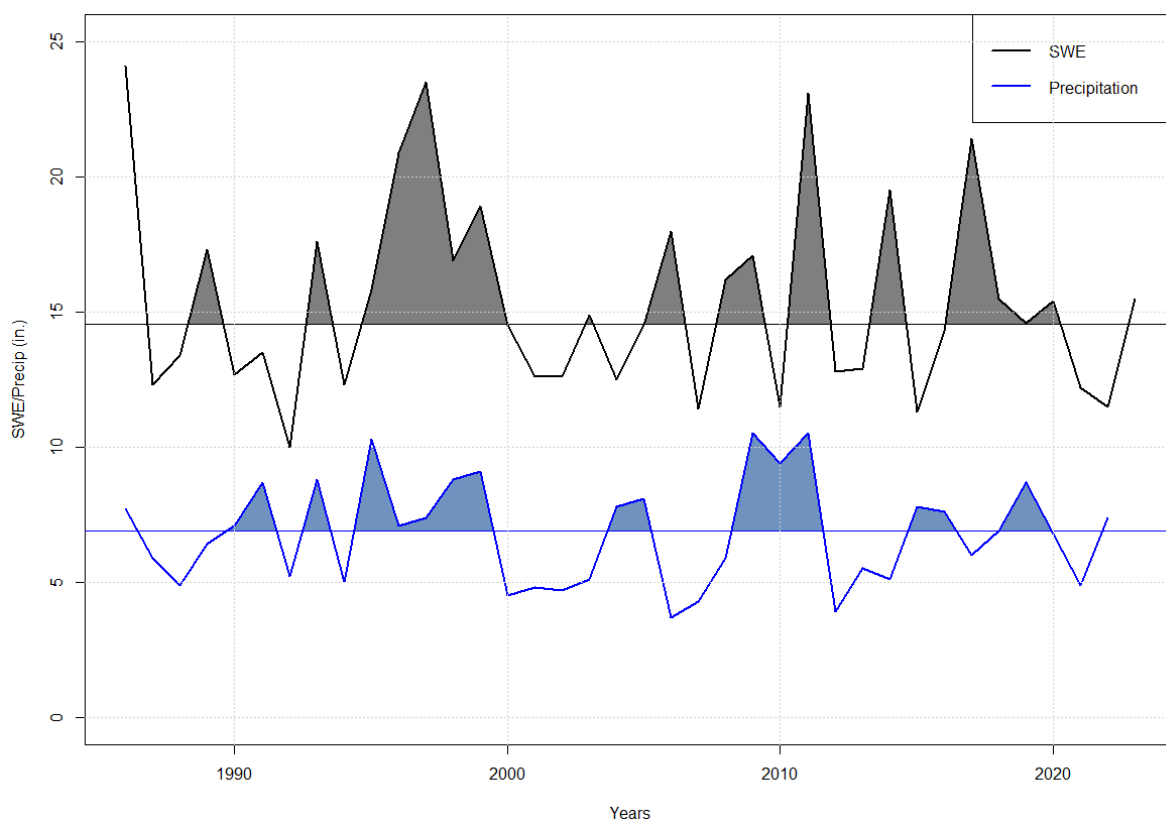
Figure 8. Time series plot of SWE (black) and snowmelt season precipitation (blue). The horizontal black line is the climatological median SWE, and the horizontal blue line is the climatological median snowmelt season precipitation. Periods where SWE or precipitation is above the median are shaded.

Southwest Wyoming has experienced notable flooding events over the years, impacting various communities across Sweetwater, Sublette, Lincoln, and Uinta Counties. Notable flooding events include:

- June 9, 1965 – Mountain View (Uinta County): Rain-on-snow runoff from the Uinta Mountains caused heavy flood damage to residents and ranches around Mountain View.

- May 17, 1984 – Lincoln County: Exceptionally warm days triggered rapid snowmelt, causing the Blacks Fork River to overflow and inundate several homes in low-lying areas.

- August 16, 1990 – Lincoln/Sublette Counties: A thunderstorm dropped up to five inches of rain in just two hours, generating flash floods with water depths of two to four feet in parts of Lincoln and southern Sublette Counties.

- August 17, 2007 – Sweetwater County: Intense thunderstorms dropped over an inch of rain in less than an hour, causing a surge of water and mud to rush into the southern part of the city via Dead Horse Canyon Creek.

- September 12, 2013 – La Barge Area (Lincoln/Sublette Counties): Heavy rainfall caused flash flooding and mudslides, damaging the Names Hill historical site near La Barge and closing U.S. Highway 189 temporarily.

- March 2023 – Blacks Fork River (Sweetwater County): Rapid snowmelt caused the river near Little America to crest at 11.1 feet, nearly a foot above flood stage, leading to moderate downstream flooding from Granger toward Flaming Gorge Reservoir.

2.6   Summary of Effective Studies

Table 2 presents the National Flood Insurance Program (NFIP) participation status and the most recent effective Flood Insurance Rate Map (FIRM) date for each community within the study area. This information helps document the current status of floodplain management across the counties and communities covered by this project.

For unincorporated areas, the county name followed by an asterisk (*) indicates that the NFIP status and map date apply to those unincorporated portions of the county.

This summary provides important context for understanding the current flood risk management landscape and identifying communities where updated flood hazard information from this project may support enhanced floodplain management and risk reduction efforts.

Table 2. The NFIP participation status and the most recent effective FIRM date for each community within the study area.

County	Community	NFIP Status	Current Effective Map Date
Lincoln	Diamondville, Town of	Participating	11/16/2011
	Kemmerer, Town of	Participating	11/16/2011
	Opal, Town of	Participating	11/16/2011
	La Barge, Town of	Not participating	11/16/2011

County	Community	NFIP Status	Current Effective Map Date
	Lincoln County *	Participating	11/16/2011
Sublette	Big Piney, Town of	Participating	-
	Marbleton, Town of	Not participating	-
	Pinedale, Town of	Not participating	3/18/1986
	Sublette County*	Participating	1/1/2008
Sweetwater	Bairoil, Town of	Not participating	-
	Granger, Town of	Not participating	2/26/1980
	Green River, Town of	Participating	6/20/2000
	Rock Springs, City of	Participating	7/20/1998
	Superior, Town of	Not participating	-
	Wamsutter, Town of	Not participating	-
	Sweetwater County*	Not participating	8/1/1978
Uinta	Lyman, Town of	Participating	2/17/2010
	Mountain View, Town of	Participating	2/17/2010
	Uinta County*	Participating	2/17/2010

3.0 Study Scoping and Key Assumptions

A full suite of hydrologic and hydraulic models was developed and independently calibrated. Hydrologic models were created at the HUC8 scale, while Hydraulic models were created for HUC10s. The study utilized an HEC-HMS model to simulate runoff and other hydrologic processes, which were then subject to application of a large number of stochastic events generated through SST. Then HEC-RAS 2D was used to capture the complexity of water movement across floodplains.

Final products were prepared in accordance with "Guidance for Flood Risk Analysis and Mapping: BLE Analysis and Mapping" (FEMA, 2023) and the BLE Draft FIRM Database Submittal Schema. The final deliveries included:

- Terrain data for each modeled domain
- HEC-HMS Models

- HEC-RAS Models

- 10, 4, 2, 1, 1+, 1-, 0.2% Water Surface Elevation (WSEL) grids

- 10, 4, 2, 1, 1+, 1-, 0.2% Depth grids

- 1% Velocity grid

- Draft FIRM Database, including:

  - S_Fld_Haz_Ar (1% and 0.2% flood hazard features)

  - S_Fld_Haz_Ln, S_Submittal_Info, and S_BFE layers

- Additional 1% flood area feature class

- Changes Since Last FIRM (only where modernized data existed)

All models were developed using the North American Vertical Datum of 1988 (NAVD 88) and the USGS Albers Equal-Area Conic Projection. Hydrology and hydraulic models resolution varied based on numerous factors, with refinement areas developed following 2D BLE Option A and Option C specifications.

Simulation time varied from model to model, based on the requirement that runoff travel time and inflow hydrograph arrival time from upstream watersheds allowed adequate time to simulate watershed response.

Hydraulic modeling and mapping were not performed within national forests, national wilderness areas, or other federal lands. However, these areas were included in HEC-HMS simulations to inform downstream hydrologic forcing.

3.1   Modeled Areas

A scoping exercise was performed for all HUC10s within the UGGD to determine what areas would be modeled. Each HUC10 was assigned a yes/no classification for the following:

- Did the HUC10 submit flow to another HUC10 (Figure 9)?

- Did the HUC10 receive flow from another HUC10 (Figure 10)?

- Did the HUC10 have effective Special Flood Hazard Areas (SFHA) from an existing FEMA flood study (Figure 11)?

- Did the HUC10 have CNMS S_Studies_Ln data (Figure 12)?

- Each HUC10 was then classified as "Scoped for Hydrology" and/or "Scoped for Hydraulics" based on the following criteria:

  - Hydrologic analysis was needed if the HUC10 submitted flow to another HUC10 or if it contained effective SFHA or CNMS S_Studies_Ln data (Figure 13).

  - Hydraulic analysis was needed if the HUC10 received flow from another HUC10 or if it contained effective SFHA or CNMS S_Studies_Ln data (Figure 14).

Treatment of Headwater HUC10s:

- For headwater HUC10s without effective studies, hydraulics and mapping were only performed where they impacted NFIP communities or where they were covered by existing Coordinated Needs Management Strategy (CNMS) S_Studies_Ln features.

- Hydrologic analysis was performed for headwater areas to produce inflows for dependent basins.

The results of these classifications are shown in Figures 9 to 14. For each of these classifications, engineering judgement was also applied to define the modeled analysis. Between scoping and additional engineering judgement, 66 HUC10s were scoped for Hydrology (modeled as 10 HUC8s) and 63 HUC10s were scoped for Hydraulics. Note that two HEC-HMS models were used to model HUC8 14040200. The final modeled hydrologic areas are shown in Figure 15.
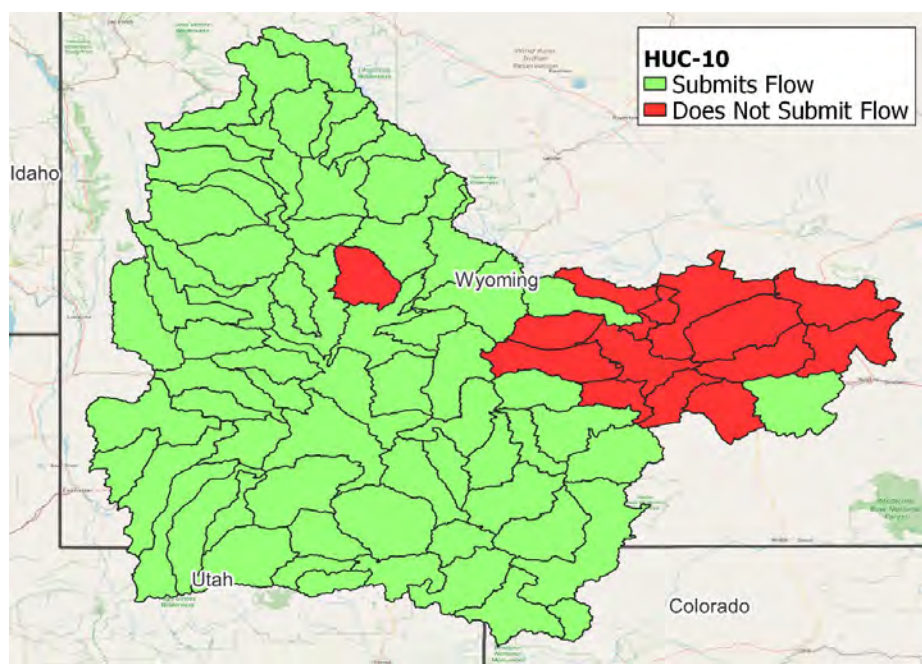
Figure 9. HUC10s submitting flow
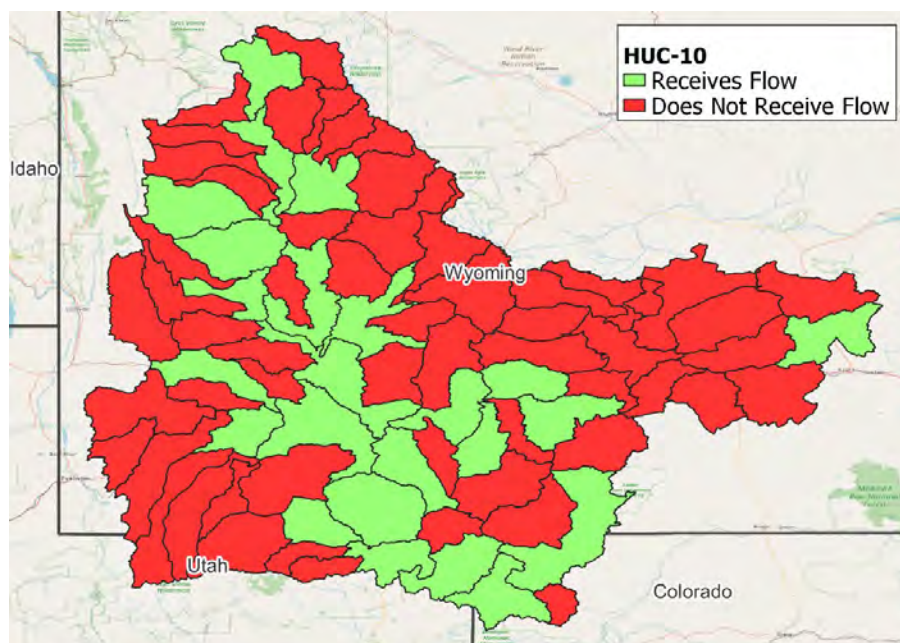
Figure 10. HUC10s receiving flow
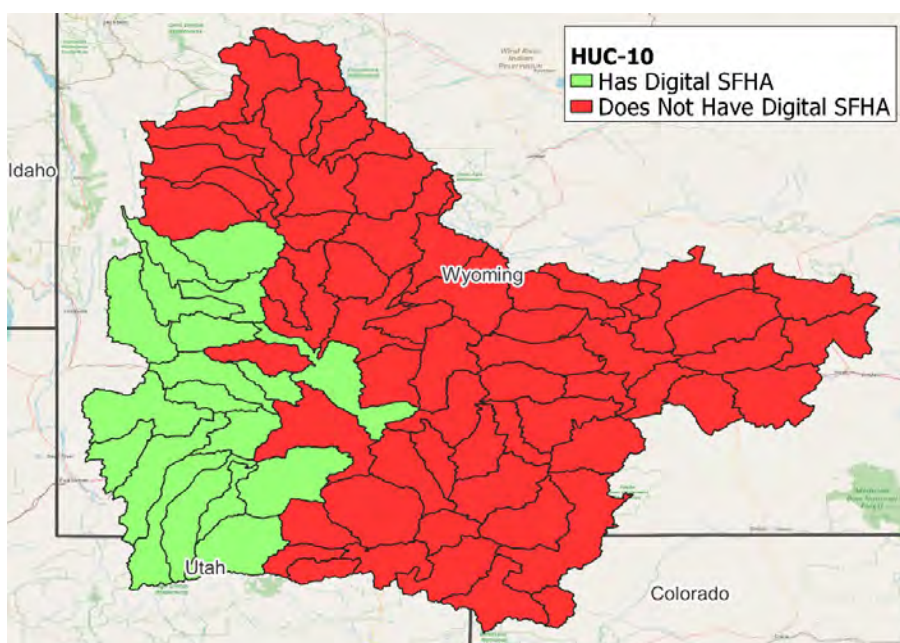
Figure 11. HUC10s with digital SFHA
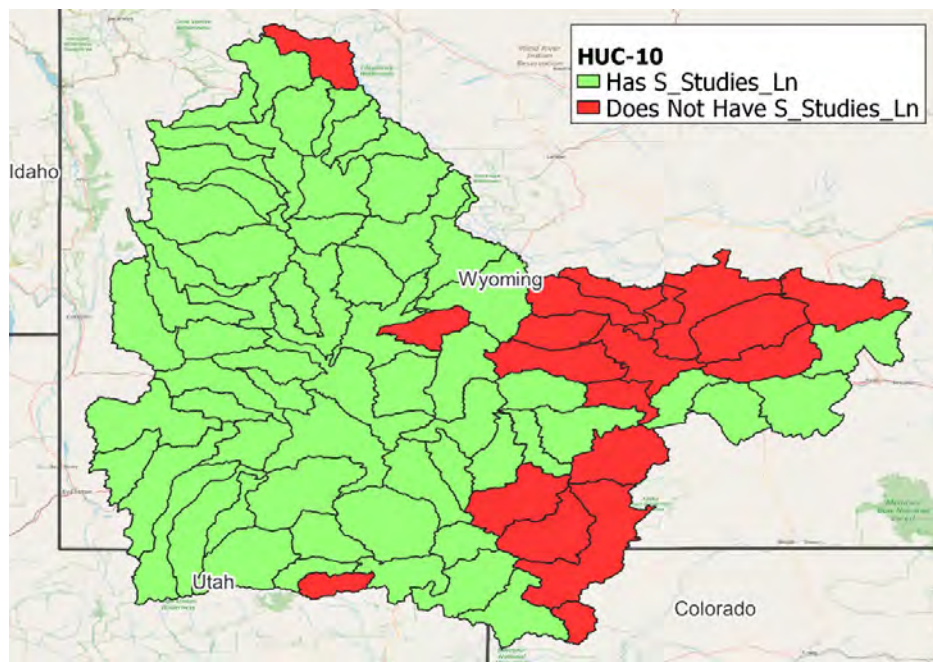
Figure 12. HUC10s with CNMS S_Studies_Ln
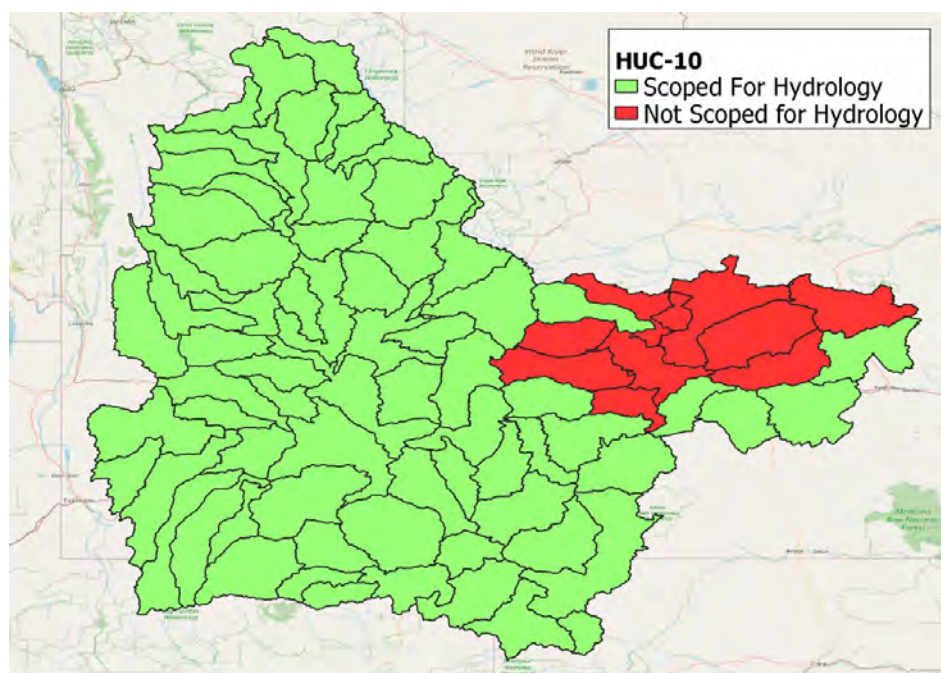
Figure 13. HUC10s for hydrologic analysis (submit flow or have SFHA or S_Studies_Ln)
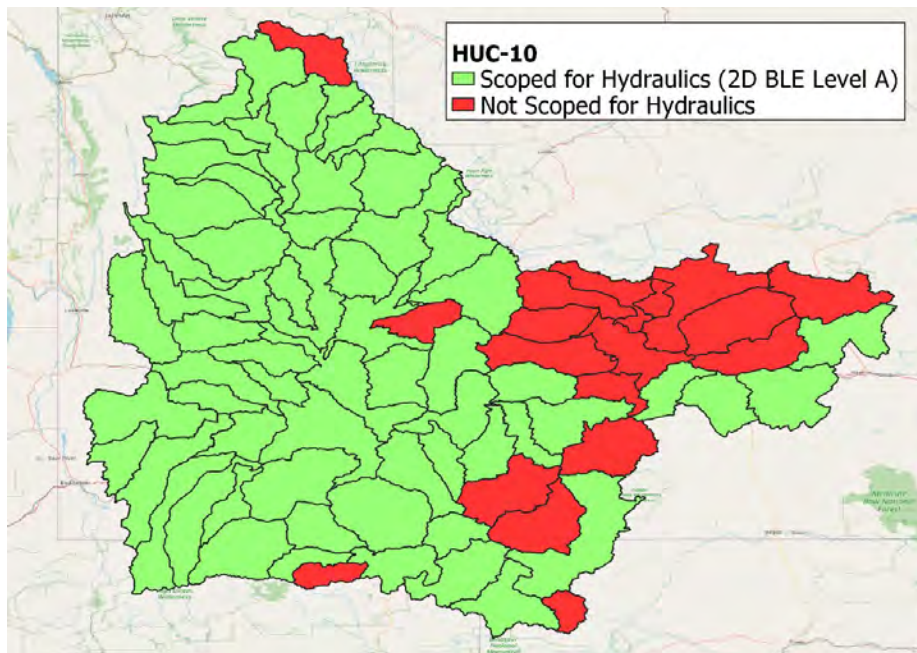
Figure 14. HUC10s for hydraulic analysis (receive flow or have SFHA or S_Studies_Ln)
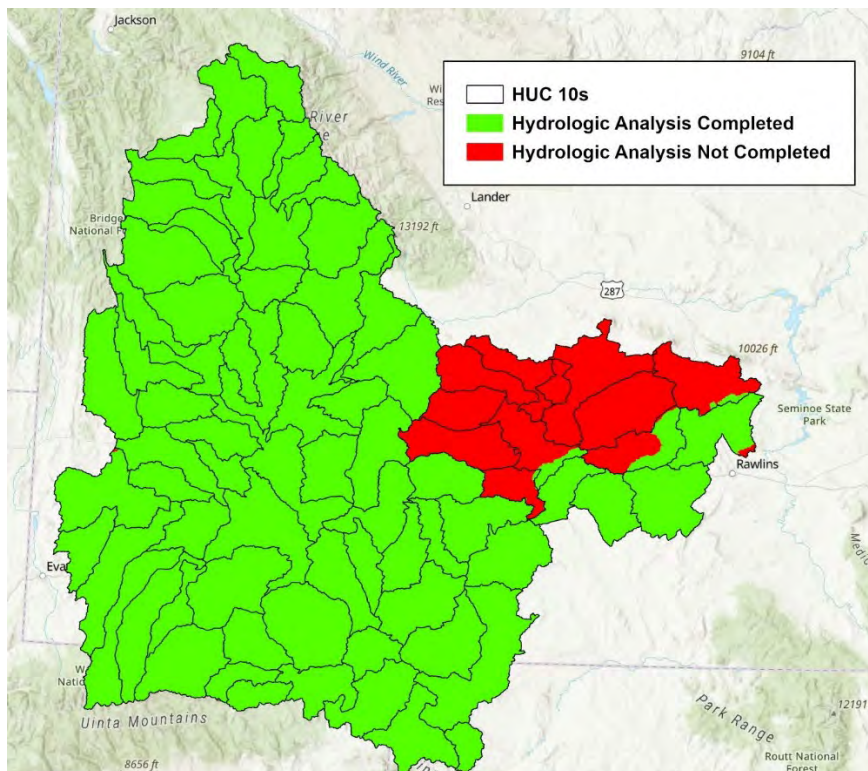
Figure 15. Final modeled hydrologic areas.

3.2   Refinement Regions

The majority of the study area was modeled as 2D BLE Option A (lower refinement). Option A areas included the National Hydrography Dataset (NHD) streamlines up to 5 square miles. The HEC-RAS mesh enforced breaklines at significant features in the terrain and hydro-connectors to approximate structures at roadway embankments. This was done to maintain appropriate flow patterns and continuity of flow.

2D BLE Option C (higher refinement) was applied to 28 refinement regions within the study area that impacted NFIP communities or contained existing Zone 'AE' classification in the CNMS S_Studies_Ln layer. Each refinement region was about the size of a HUC12, covering about 1,287 square miles in total. In these regions, the hydrology included NHD streamlines up to 1 square mile. At hydraulics, the hydrology regions were further refined using the National Structure Inventory (NSI) and the modeled floodplain, the HEC-RAS mesh was enhanced to meet Option C requirements according to engineering judgment.

Figure 16 and Figure 17 illustrate the final refinement regions of hydrology and hydraulics, respectively.
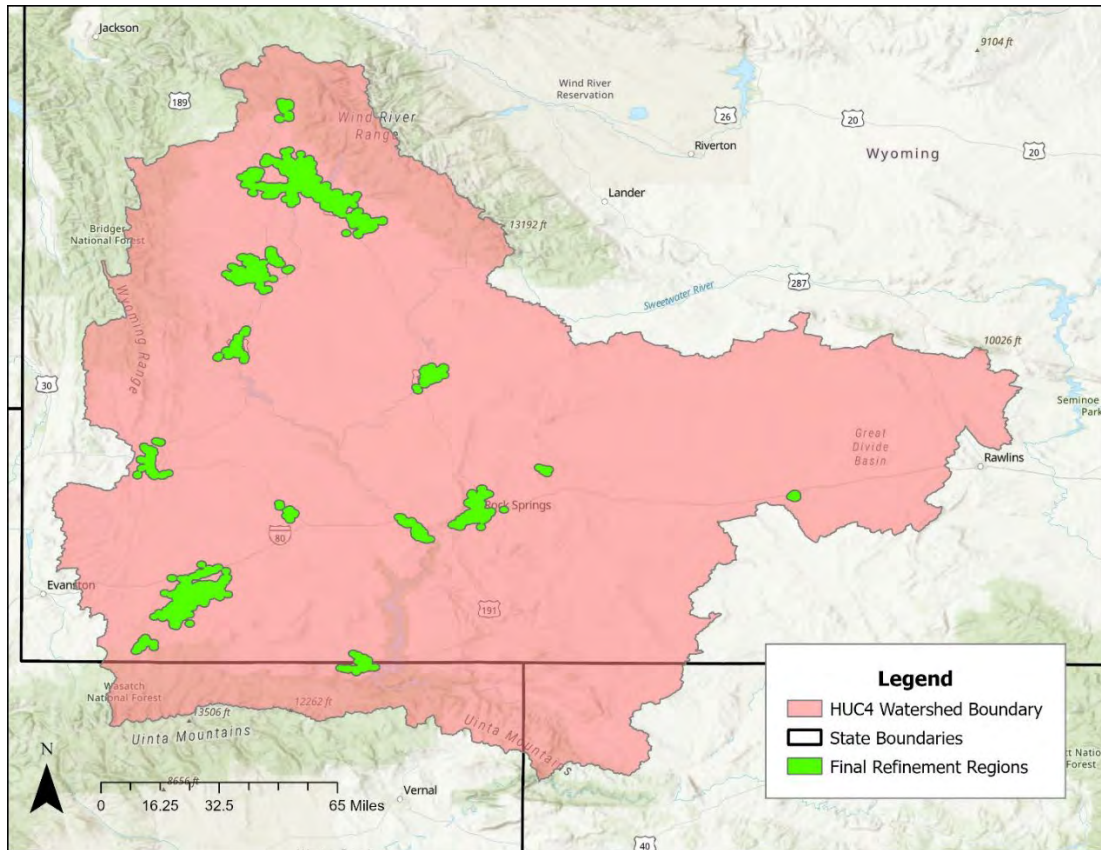
Figure 16. Final hydrologic refinement regions
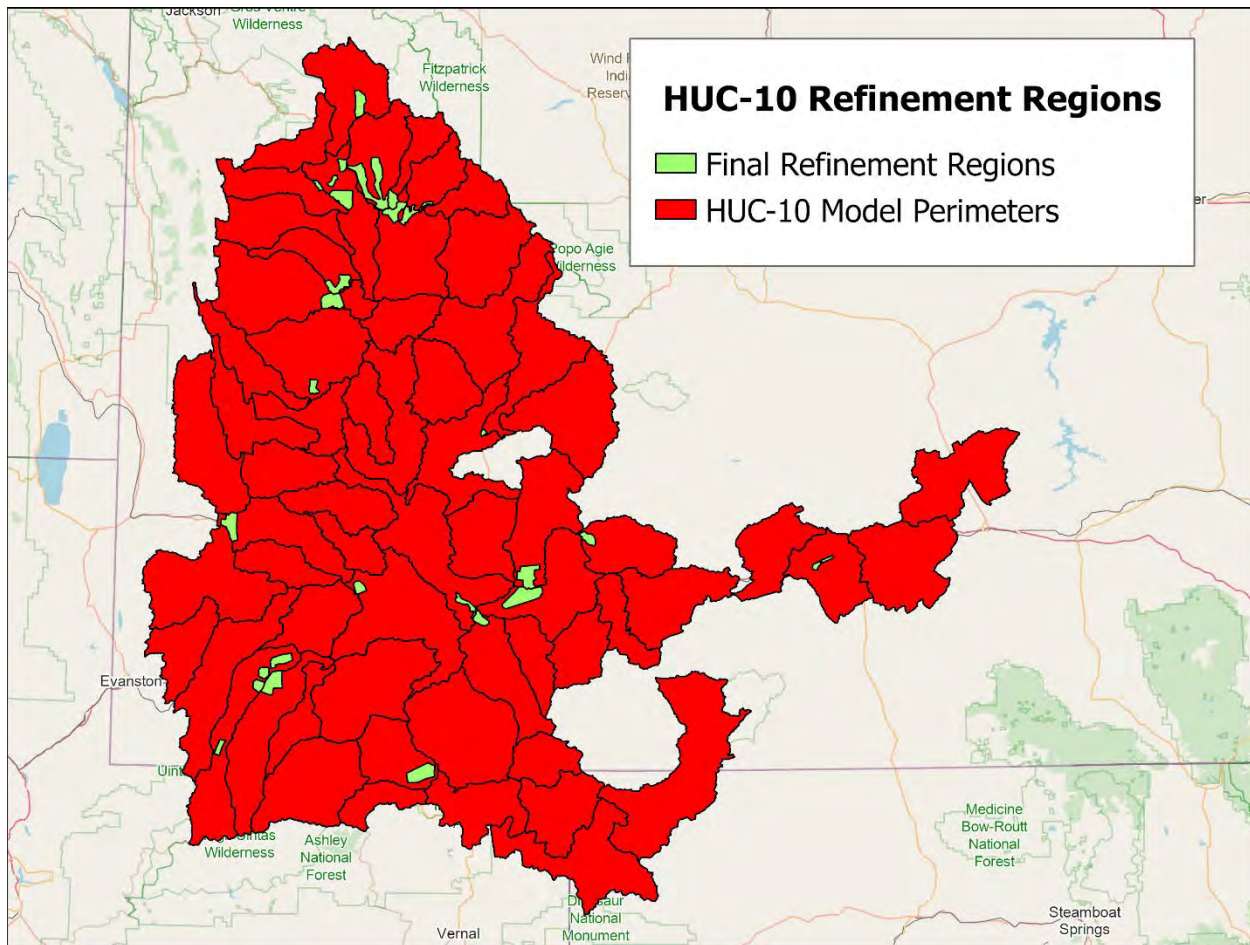
Figure 17. Final refinement regions of the hydraulic model.

3.3   Modeling Approach

Hydrology for this study was developed using SST to generate synthetic storm events, which were then simulated in HEC-HMS to produce basin hydrographs. These hydrographs served as inflow boundary conditions for HEC-RAS hydraulic models, ensuring a probabilistic approach to flood estimation.

This hydrology approach improved flood modeling accuracy, computational efficiency, and regulatory compliance by refining hydrologic conditions before hydraulic modeling. Traditional deterministic methods, including regional regression equations and stationary assumptions, have limitations that can misrepresent flood hazards.

To address these challenges, the study avoided reliance on outdated precipitation and peak flow regression datasets such as NOAA Atlas 2 (1973) and USGS regression equations (2003), which lacked coverage for recent climatic trends. Instead, high-resolution gridded precipitation data and SST-based probabilistic storm simulations provided a robust, data-driven hydrologic framework.

USACE and FEMA watershed modeling pilots in the Kanawha River Basin, West Virginia, informed some aspects of these methods (2022).

3.3.1　Hydrometeorology

The modeling team assessed the existing precipitation-frequency data and USGS peak flow regression equations applicable to the study area (USGS, 2003). Since the National Oceanic and Atmospheric Administration (NOAA) Atlas 14 did not provide coverage for this area, and the USGS regression equations were derived from streamflow data that did not cover the past 20–30 years of record, alternative approaches were evaluated.

To address the lack of traditional data in this project location, probabilistic methods were used to develop the hydrology required for hydraulic modeling. These techniques involved creating a suite of synthetic storms using gridded quantitative precipitation estimates (QPE) from the Analysis of Record for Calibration (AORC) dataset, developed by the National Weather Service. QPE was derived using remotely sensed precipitation, gauge-based observations, and other meteorological variables to estimate hourly precipitation across the continental United States.

The gridded simulated storms were then used to simulate events in HEC-HMS. The resulting simulations produced basin hydrographs, which were used to develop statistically sound outflows suitable for forcing the HEC-RAS hydraulic models.

A key advantage of this approach was that it did not assume a 1% annual chance precipitation event would necessarily result in a 1% annual chance watershed response (peak flow).

The probabilistic storm-generation framework established in this section provided the foundation for the Stochastic Storm Transposition (SST) methodology described in Section 4.1, which was applied to expand the range of realistic storm scenarios for hydrologic modeling.

3.3.1.1　Evaluation of Existing Precipitation Frequency Data

NOAA Atlas 14 Precipitation Frequency (PF) data was not available for this study area. NOAA Atlas 2 PF data was available, however it only covered two frequencies (50% and 1% annual chance) and two storm durations (6-hour and 24-hour). This dataset was published in 1973.

In 2014, the Wyoming Water Development Office (WWDO) published a study titled Probable Maximum Precipitation Study for Wyoming (WWDO, 2014). One of the study's main goals was to produce gridded Probable Maximum Precipitation (PMP) data. However, it also produced precipitation frequency (PF) grids as a secondary output in a digital appendix. The WWDO study provided PF data for nine frequencies: 50%, 20%, 10%, 4%, 2%, 1%, 0.5%, 0.2%, and 0.1% annual chance. The "rainfall-only" grids included one duration (24-hour), while the full "precipitation" grids included two durations (6-hour and 24-hour). This WWDO data was not approved as a replacement for NOAA Atlas 14 data for FEMA flood risk efforts.

3.3.1.2   Evaluation of Existing Peak Flow Regression Equations

The modeling team investigated the existing peak flow regression equations under USGS report WRIR-03-4107: Peak-Flow Characteristics of Wyoming Streams (USGS, 2003). For the hydrologic region of this project, the team assessed key attributes of the stream gages at the time the regression equations were developed, including:

- Number of gages

- Record length (median: 18 years)

- Recency (median latest year: 1981)

- Drainage area (median: 13 square miles)

- Average standard errors of prediction range from 35 to 135 percent

Due to these qualities, the study avoided reliance on the regression equations.

3.3.1.3   Stochastic Storm Transposition

In place of NOAA Atlas 14 precipitation estimates, SST was used to develop the forcing for HEC-HMS models in this study. The process included the following steps:

- Development of transposition regions: areas were identified based on shared hydro-meteorological characteristics, allowing storms from within the region to be transposed spatially.

- Identification of storms: historical anomalous storm events were cataloged and added to a storms database.

- Storm transposition and simulation: storms were selected, transposed (geospatially shifted), and simulated in HEC-HMS using probabilistic methods.

- Hydrograph development: results (hydrographs) from HEC-HMS simulations were statistically analyzed, and hydrographs were identified for the required frequency simulations in HEC-RAS.

The development of the transposition areas was guided by a meteorologist, while SST implementation followed approaches similar to those of USACE pilot study (Kanawha Pilot Project, 2022).

3.3.1.4   HEC-HMS

A HEC-HMS model was developed for each HUC8. Where gage records permitted, HMS models were calibrated to observed storms using gridded precipitation time series for the event(s), and adjustments were made using observed flow at USGS gage locations.

Literature review and historic peak flow hydrographs indicated that peaks were likely to occur during periods of high baseflow caused by snowmelt. The modeling incorporated baseflow and the snowmelt routines built into HEC-HMS.

The results of the suite of HEC-HMS runs were statistically analyzed to develop peak volume and shape parameters (i.e., hydrographs) representing each flood frequency scoped by the project. Uncertainty across the spectrum of HEC-HMS iteration results was quantified and applied directly to approximate the hydrographs for the 1% plus and 1% minus annual chance frequencies, as defined by FEMA.

3.3.2　　Hydraulics

HEC-RAS was forced using inflow hydrographs from HEC-HMS subbasin outlets. Non-headwater domains also received inflows directly from upstream HEC-RAS or HEC-HMS outflows where necessary. By default, 2D BLE Option A was used.

The hydraulic domains were informed by HUC10 boundaries and were sized similarly to HUC10s. The connectivity between HEC-HMS schematic files was utilized to create the domains for the hydraulic models.

First, a "Downstream Junction" from the HEC-HMS Junctions was assigned to HUC10s based on the WBD HUC10 boundaries. Junctions that lie towards the downstream end of a HUC10, were selected under the conditions that they are not located at confluences and that each HUC10 only has one assigned. These represent the outflow of the HUC10 domain and were used to create the inflow boundary conditions going into downstream HUC10 models.

Once assigned, each Downstream Junction was used as the start of a network for each HUC10. Given the connectivity between all the Junctions, Reaches, and Subbasins upstream were assigned to the same domain. The network continued upstream until another Downstream Junction was reached or once headwater has been reached. As a result, there are no overlaps in domain assignments.

The Subbasins assigned make up the basis of the final Model domain for each HUC10. Figure 18 illustrates how the Subbasins were assigned relative to the Downstream Junctions for two HUC10s.
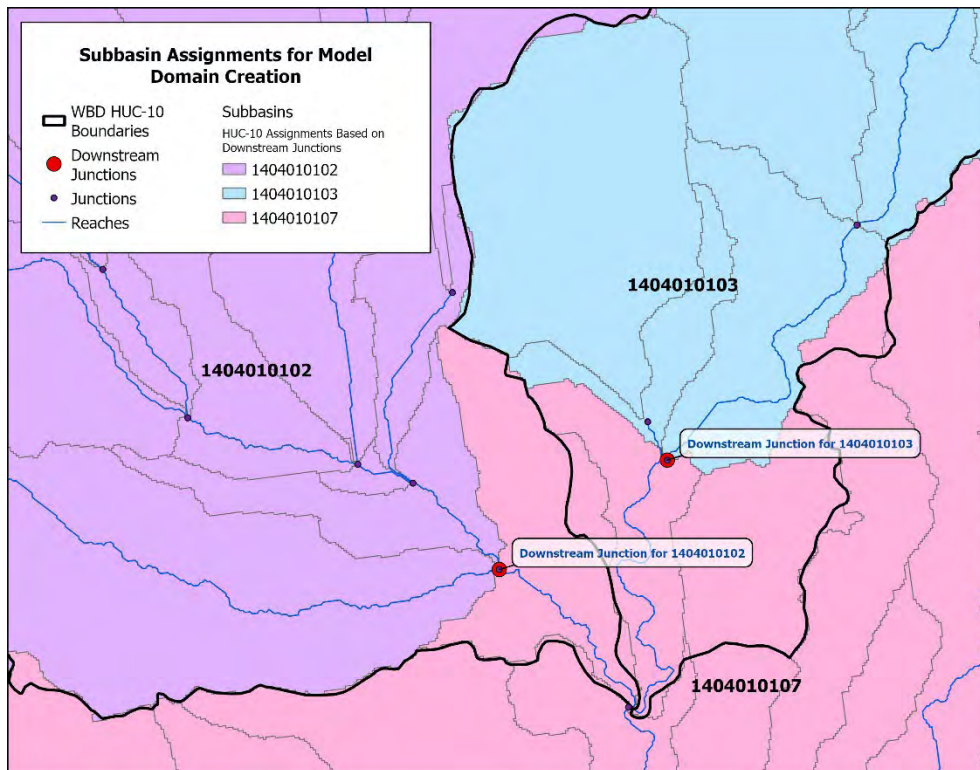
Figure 18. Subbasin Assignments Based on Downstream Junction Network

The grouped Subbasin features were then dissolved, smoothed, and adjusted to ensure no overlaps in boundaries nor gaps within/between Model Domains occurred (Figure 19). Additional adjustments were made for some Model boundaries in order to improve tie-ins, but they didn't deviate significantly from the shape formed by the grouped Subbasins.
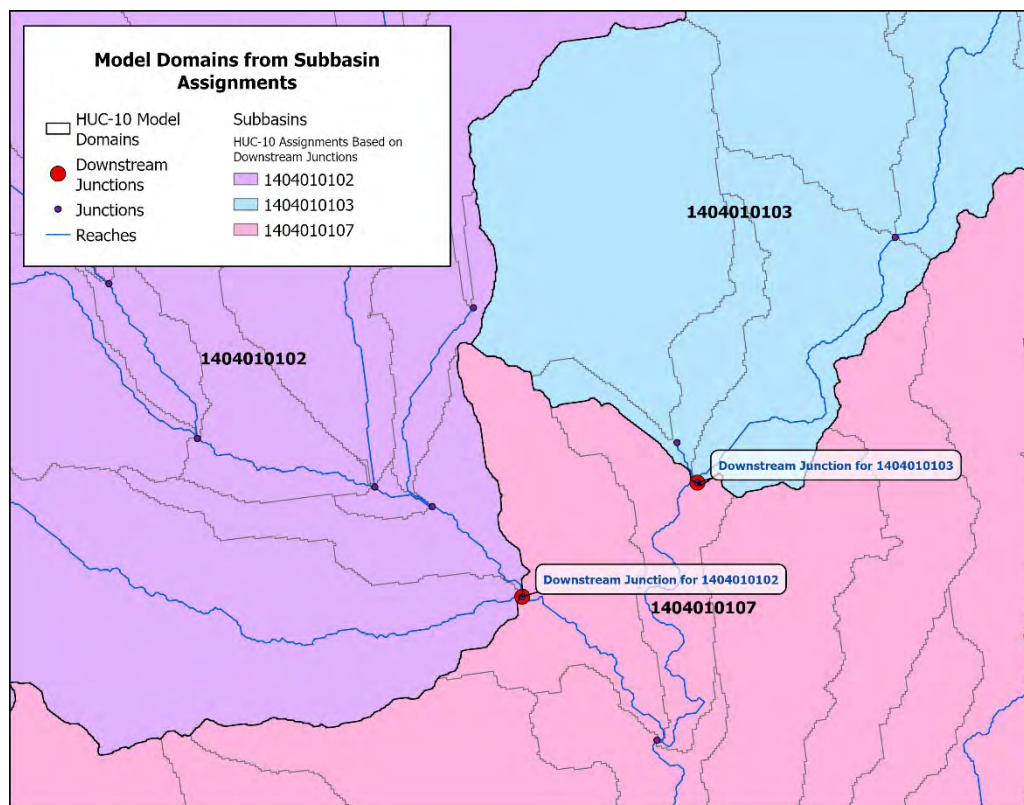
Figure 19. Updated Model Domains Based on Grouped Subbasins from HEC-HMS

The HEC-RAS simulation time was set long enough to attenuate an appropriate base flow, followed by allowing the primary flood wave to rise and begin to recede.

For lakes, storage effects were considered for hydrologic routing within the 2D model, with breaklines along spillways where available. Reservoir operations were only considered for Fontenelle Dam and Flaming Gorge Dam. An annual maximum series (AMS) was developed from the available USGS reservoir outflow record data. The AMS was randomly sampled and flow was applied to the hydraulic models as a constant flow hydrograph.

3.4 Mapping and Documentation

The HEC-RAS model domains were extended beyond their limits of applicability ("hydraulic base domains") upstream and downstream to alleviate instabilities near boundary conditions. This approach simplified the production of final, seamless, project-wide mapping products, as "tie-in" locations were selected along the significant overlap between HEC-RAS model domains.

No attempts were made to align, tie-in, or reconcile the results of this study with existing studies or previously developed mapping.

3.4.1 Floodplain Polygon Products

As previously stated, HEC-RAS was used exclusively for riverine modeling across most of the study area. Riverine floodplain polygons were generated by HEC-RAS using a Polygon Boundary Value of 0.0, meaning any depth of water was considered as inundation.

The raw inundation polygons from riverine models were expected to be adequate for final mapping, after identifying tie-in locations where model areas overlapped. However, additional smoothing was applied as needed.

3.4.2 Rater Products (Hydraulic Output)

Riverine floodplain polygon Raster products representing flood depth, water surface elevation, and velocity were produced for each HEC-RAS model. These raster datasets were combined into a study-wide tiled mosaic, with maximum values applied in areas of overlap.

4.0 Storm Catalog Development

4.1 Stochastic Storm Transposition

As introduced conceptually in Section 3.3.1, Stochastic Storm Transposition (SST) is a process that involves relocating observed storms from their original locations to new, randomly selected locations within a study area to increase the number of plausible storm scenarios available for analysis. Transposed storms should originate from a climatologically homogeneous region, meaning a region with similar meteorological and geographic characteristics to the study area. This homogeneous region is typically identified by comparing spatial data such as mean annual or seasonal precipitation, dewpoint temperatures, elevation, and proximity to moisture sources. For additional details on SST methodology and its application, refer to Lawler et al. (2024).

Dewberry has developed a storm catalog tool that objectively identifies large storm events within the designated transposition region. The tool leverages data from the AORC gridded QPE dataset, which spans from 1979 to the near present. This catalog serves as the basis for identifying candidate storms for transposition and ensures that the storms reflect the regional climate conditions relevant to the study area.

4.2 SST Region Development

As noted earlier, the UGGD watershed has an area of approximately 21,000 (sq mi). An SST region should be sufficiently large enough that when a storm from the region is transposed into the basin of interest (Wright et al., 2020), the entirety of the basin has grid coverage. It is also important to consider specific complications of the basin of interest. Complications taken into consideration in developing an SST region specifically for the UGGD included:

- The continental divide is the eastern edge of the basin. While storms regularly cross the continental divide, it is important to keep this boundary in mind as storms from the west will be on the windward/upslope side, while storms from the east will be leeward/downslope.

- The topography surrounding the basin and high-elevation desert interior is important to keep in mind because there is a nearly 7800 feet (2375 meters) difference in elevation from the lowest to the highest points.

- This part of the country has an arid to semi-arid climate and experiences very low mean annual precipitation in general.

- Atmospheric rivers are a major source of moisture and precipitation for the Western U.S. However, it is rare for intrusions all the way into Southwest Wyoming.

The transposition region was created by a meteorologist using GIS software (QGIS used here) and selected topographic, gridded meteorological, and other datasets to guide its determination. The following geospatial information was used to develop an understanding of the UGGD and the surrounding region for the development of an SST region:

- Continental Divide

- Mean Annual (Monthly) Precipitation

- Monthly precipitation used to compute warm season (May-September) and cool season (October-April) precipitation

- Mean Annual (Monthly) Dewpoint Temperature

- Monthly dewpoint temperatures used to compute warm season (May-September) and cool season (October-April) dewpoint temperatures

- Elevation

- Slope and aspect are also derived from the DEM

- Distance from coast (moisture source)

- International Best Track Archive for Climate Stewardship (IBTrACS) tropical cyclone tracks

Distance from the coast and tropical cyclone tracks were not applicable within the UGGD itself but were used to determine the limits of the western and southern boundaries. Ultimately, the final SST region was determined using warm and cool season precipitation and dewpoint temperatures, mean annual precipitation, and elevation. For each variable, the basin maximum and minimum values were determined, and a ± 20% buffer was added to create a range of potential values (Table 3). The gridded datasets were displayed in QGIS with only areas with values within each range symbolized (Figure 20). This informed a rough area of potentially homogenous conditions (potentially because of the very large range inherent within the basin) to draw the SST region from.

Table 3. Maximum and minimum values are used to symbolize variables in QGIS for drawing the SST region.

Variable	Minimum	Maximum
Warm season precipitation (mm)	70	490
Warm season dewpoint temperature (°C)	-11	3
Cool season precipitation (mm)	64	1185
Cool season dewpoint temperature (°C)	-22	-5
Mean annual precipitation (mm)	130	1600
Elevation (m)	1280	4780
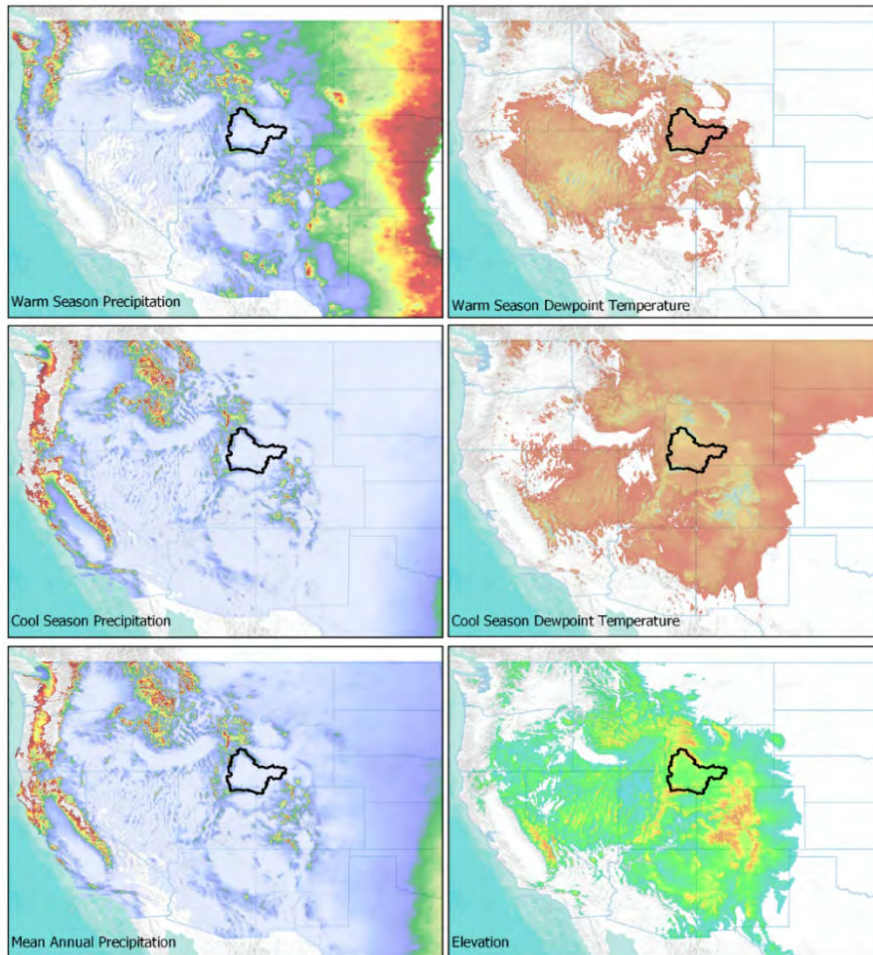
Figure 20. Metrological and geographical gridded datasets were used to draw the UGGD SST region. Only values within the range in Table 3 are symbolized on the map, and the values outside are transparent.

The final result is an impressively large SST region (Figure 21), spanning north to south from Montana to Arizona-New Mexico and east to west from Colorado to Nevada. Northern Arizona and New Mexico experience summer monsoonal thunderstorms, which are not transposable to the UGGD; the southern extent was ultimately included up to the edge of Mogollon Rim because the dry, high-elevation Colorado Plateau has similar mean annual precipitation and elevation as the interior of the UGGD. The Snake River Valley and the Great Salt Lake Basin were also included though they are lower in elevation than the UGGD and experience dryer dewpoints; these regions were included because they have comparable mean annual precipitation and are common intermountain west moisture pathways for atmospheric rivers.
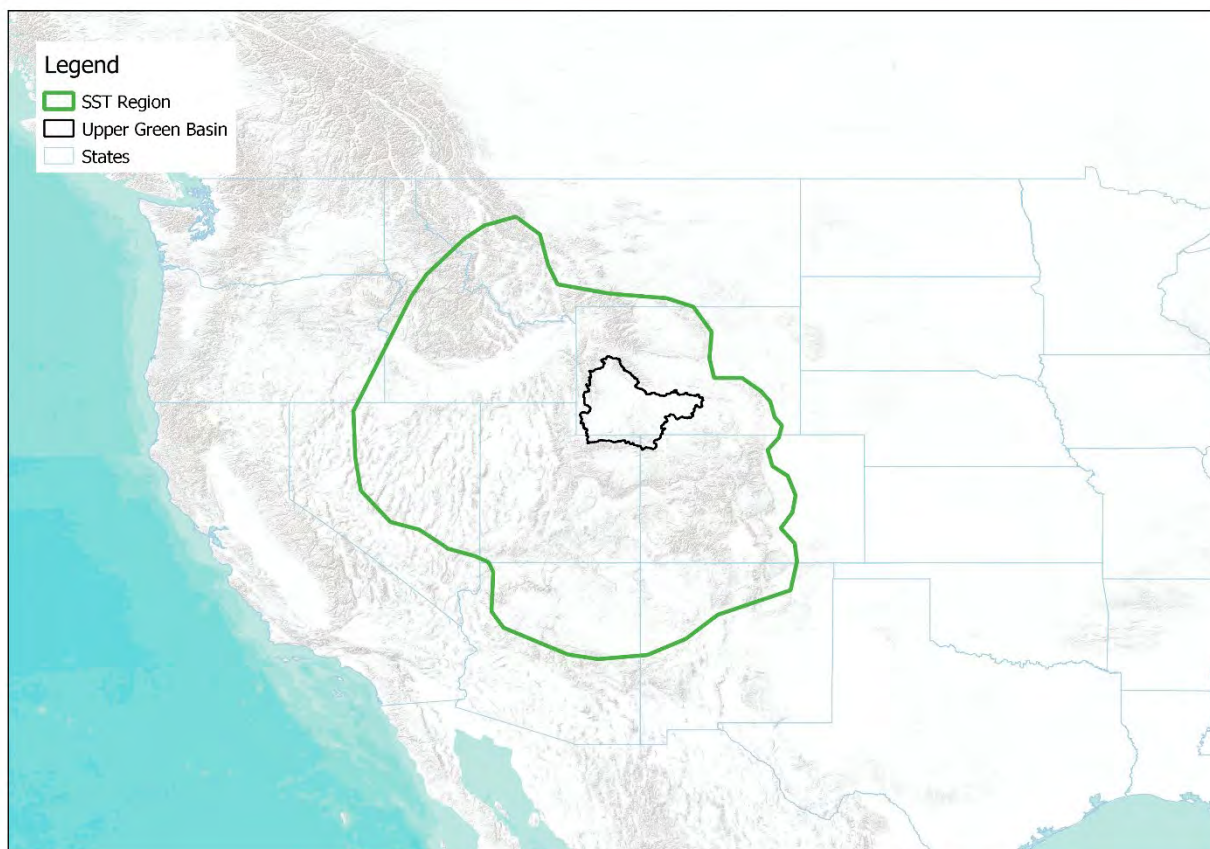
Figure 21. SST region drawn from meteorological variables for the UGGD basin.

4.2.1   Storms Database Viewer

Following the development of the transposition region, a storm catalog is developed that is unique to the transposition domain and watershed (UGGD), and then displayed in the storm database viewer. Each storm identified is then available for use in an SST analysis. The three main inputs to generate a storm catalog and view in the storms database viewer are:

1. Basin of interest – in this case the UGGD
2. SST region – drawn above
3. Duration of interest – in this case 72 hours

Hourly precipitation from the Analysis of Record for Calibration (AORC) dataset was summed within the transposition region for each 72-hour window in the dataset, beginning in 1979 to create an accumulation grid. Each 72-hour accumulation grid was scanned to identify events that would maximize precipitation over the UGGD if transposed to the watershed, establishing a storm precipitation field. Storm statistics were then computed for each 72-hour record, ranked, and displayed in the catalog.

The catalog can be sorted by mean, sum, and max precipitation as well as by season, and displays the basin location, potential storm location, and entire precipitation field for the

transposition area (Figure 22). Sorting by mean gives the largest areal coverage, which is important for a basin this large. Sorting by max can give very large point values but limited spatial coverage. These maximum point values may also be falsely high due to inaccuracies in the underlying QPE dataset. Depending on the time of year, this could be exacerbated as remotely sensed products tend to have difficulties with determining precipitation magnitude when the precipitation is frozen, as either snow, sleet, or freezing rain.
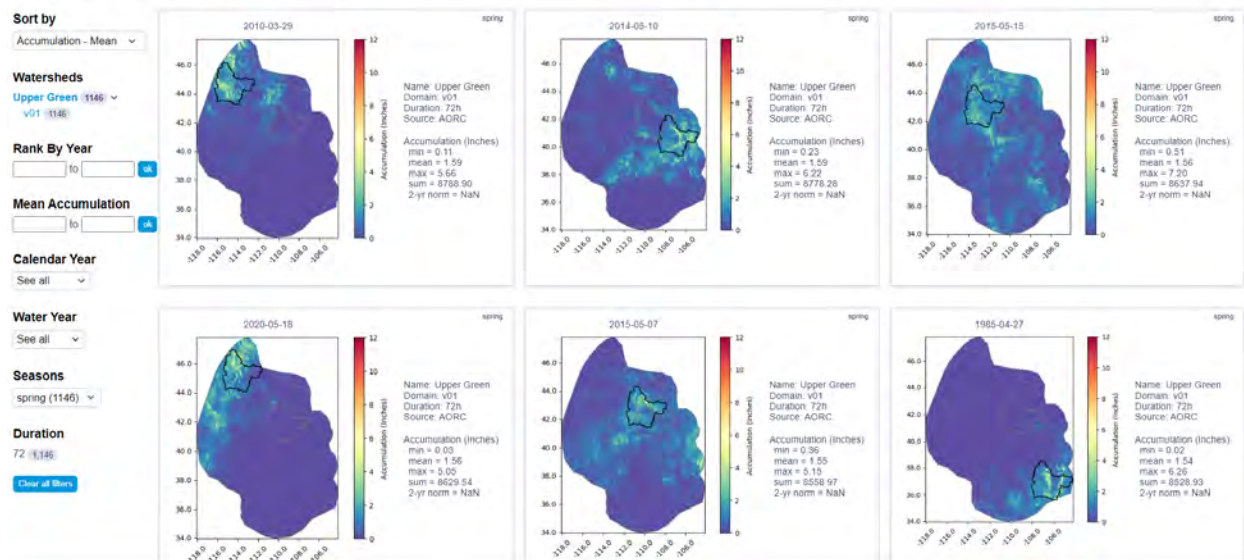
Figure 22. Screen capture of the Storms Database Viewer with the largest springtime events sorted by mean accumulation for the Upper Green.

4.2.2   HYSPLIT Back-Trajectory Analysis

The Hybrid Single-Particle Lagrangian Integrated Trajectory (HYSPLIT) model was run to compute the back-trajectories of several of the largest events identified in the storm database viewer to compare the moisture inflow source with that of the UGGD at the same time. This was done as an internal quality control measure and confirmation of the large extent of the transposition boundary. The storm database viewer was sorted by mean accumulation and not bound by any season (all year). Five of some of the largest storms from various seasons and locations were selected for HYSPLIT analysis, to consider a subset of possible storm seasonality and locations used in the SST analysis.

To run HYSPLIT, the starting height (in meters above ground level) of atmospheric pressure levels needs to be determined from atmospheric soundings. The 1000 mb (close to the surface), 850 mb, and 700 mb levels were chosen to represent the boundary layer through the lower-middle atmosphere. Skew-T diagrams from Boise, ID (BOI), Flagstaff, AZ (FGZ), and Albuquerque, NM (ABQ) were used depending on the storm location. HYSPLIT was run for 72-hours with two initial locations –the estimated maximum storm center and roughly the center of the UGGD. Table 4

below shows the storm information, HYSPLIT inputs, and notes from each model run. The basin centroid is roughly 42.0 N, -109.5 E. An example of the HYSPLIT output is seen for the April 1999 event in Figure 23. In this figure, the black stars on the map represent the two starting locations, the UGGD in WY and the storm center in CO. The red, blue, and green lines represent the moisture inflow vectors at the 1000 mb (surface), 850 mb, and 700 mb levels, respectively. This back-trajectory shows the moisture available in Southwest Colorado for this event originated from the same general location as the moisture in the UGGD.

Table 4. Summary table of HYSPLIT input information and notes from resulting back-trajectory analysis.

Storm Date	General Location/Sounding Site	1000 mb (m)	850 mb (m)	700 mb (m)	Lat.	Lon.	Notes
12/31/1996	Northwest/BOI	66	1429	3002	44.5	-116.0	Consistent moisture source but questionable precipitation magnitude
12/20/2010	Southwest/FGZ	85	1447	3024	38.0	-114.0	Consistent moisture sources
9/9/2013	South/ABQ	20	1477	3149	38.0	-111.5	Inconsistent surface moisture from low-pressure (cyclonic) rotation. National surface analysis and QPE suggest moisture coming from same system at least.
9/6/2003	South/FGQ	71	1507	3170	35.0	-113.0	Consistent moisture source from continental airmass (non-monsoonal)
4/29/1999	Southeast/ABQ	683	1412	3022	38.0	-107.0	Consistent moisture sources
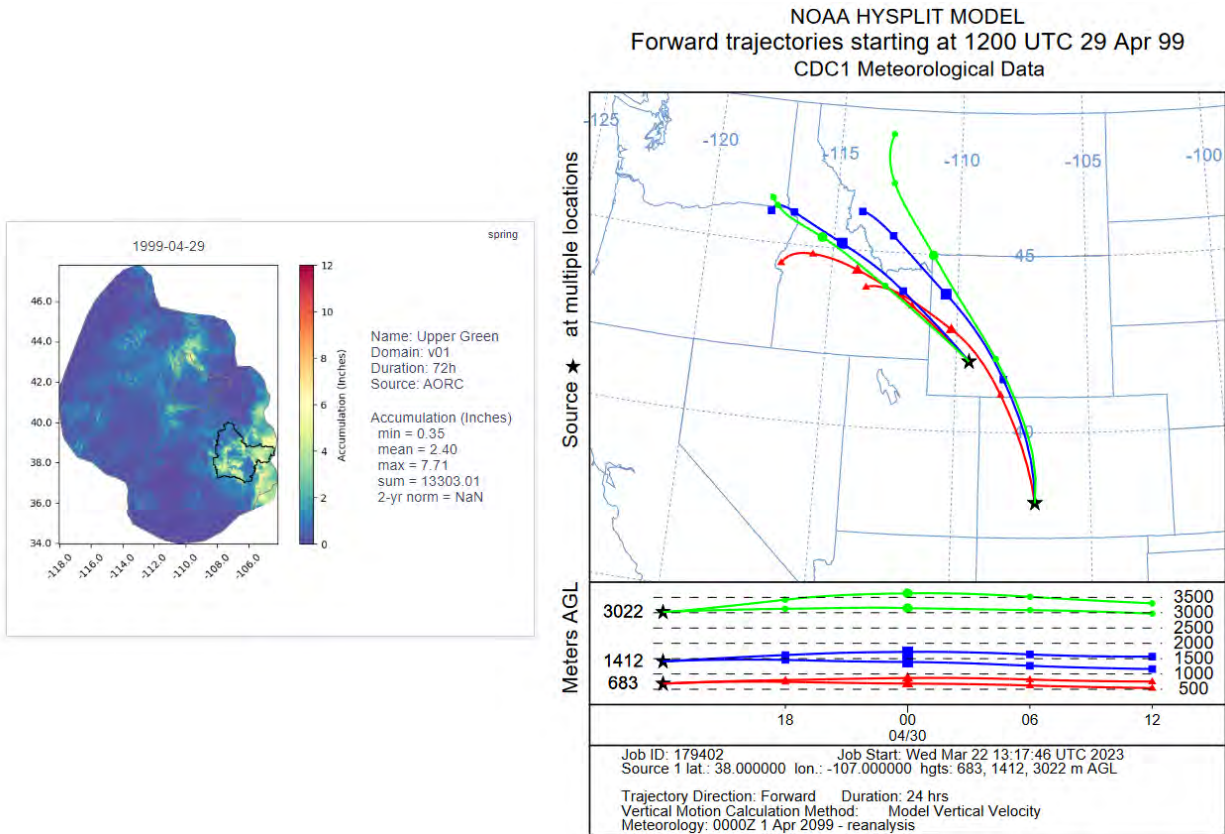
Figure 23. HYSPLIT output for the April 29, 1999 storm event in Southwest Colorado.

4.3 Guidelines for Incorporating Storm into the Storm Catalog

In summary, the following guidelines were established for incorporating storms into the storm catalog in the UGGD:

- Avoid selecting storms during winter months (October–March) to minimize errors in QPE estimates of frozen precipitation.

- Prioritize storms occurring during the snowmelt season (April–June) to align with riverine flooding patterns associated with rain-on-snow events.

- Sort storm entries by mean accumulation to focus on events with widespread precipitation coverage, reducing the impact of isolated extreme values that may stem from QPE uncertainties.

For guideline number 3, a normalized transposition approach was used (Hansen et al., 1977), in which the precipitation field was normalized by a climatological variable before transposing a dimensionless ratio grid to adjust the precipitation magnitude at the transposed location (details in the stochastic framework).

For this study area, it was determined that restricting storm selection to specific years was unnecessary. No clear relationship was found between snowpack depth and snowmelt season rainfall, and ENSO (El Niño-Southern Oscillation) was not identified as a primary driver of precipitation patterns in this region.

5.0   Hydrological Modeling

5.1   Model Development Overview

This BLE study utilized HEC-HMS (v4.11) to perform hydrologic simulations, estimating runoff based on watershed characteristics and forced with observed precipitation time series using the SST methodology. Hydrologic models were developed at the HUC8 level, ensuring consistent watershed delineation across the study area.

Subbasin delineation was performed using HEC-HMS with a 2.5 square mile drainage area threshold, selected as a practical choice to balance model resolution and computational efficiency for hydrologic modeling at the HUC4 scale. The threshold was informed by sensitivity analyses indicating that it produces representative subbasin sizes without excessive subdivision of the watershed. Future updates may refine this assumption as modeling needs and data availability evolve. ArcGIS Pro 3.1 was used for terrain preprocessing, watershed delineation, and visualization of model outputs.

To improve flood hazard characterization, SST was applied to select events from the catalog of synthetic storms, incorporating historical extreme events spatially transposed across the study region. This approach expanded the range of precipitation scenarios, improving rainfall-runoff representation and ensuring statistically sound flood risk estimates.

Model calibration was performed using both event-based (historical flood events) and multi-frequency-based techniques to refine runoff responses. The calibrated HEC-HMS models then simulated a suite of synthetic storm events, producing frequency-based hydrographs for various flood recurrence intervals.

These hydrographs were then spatially linked to HEC-RAS hydraulic models, ensuring accurate inflow conditions for simulating floodplain inundation and water surface elevations.

Figure 24. represents the hydrologic methodology diagram, which is detailed in the following subsections.
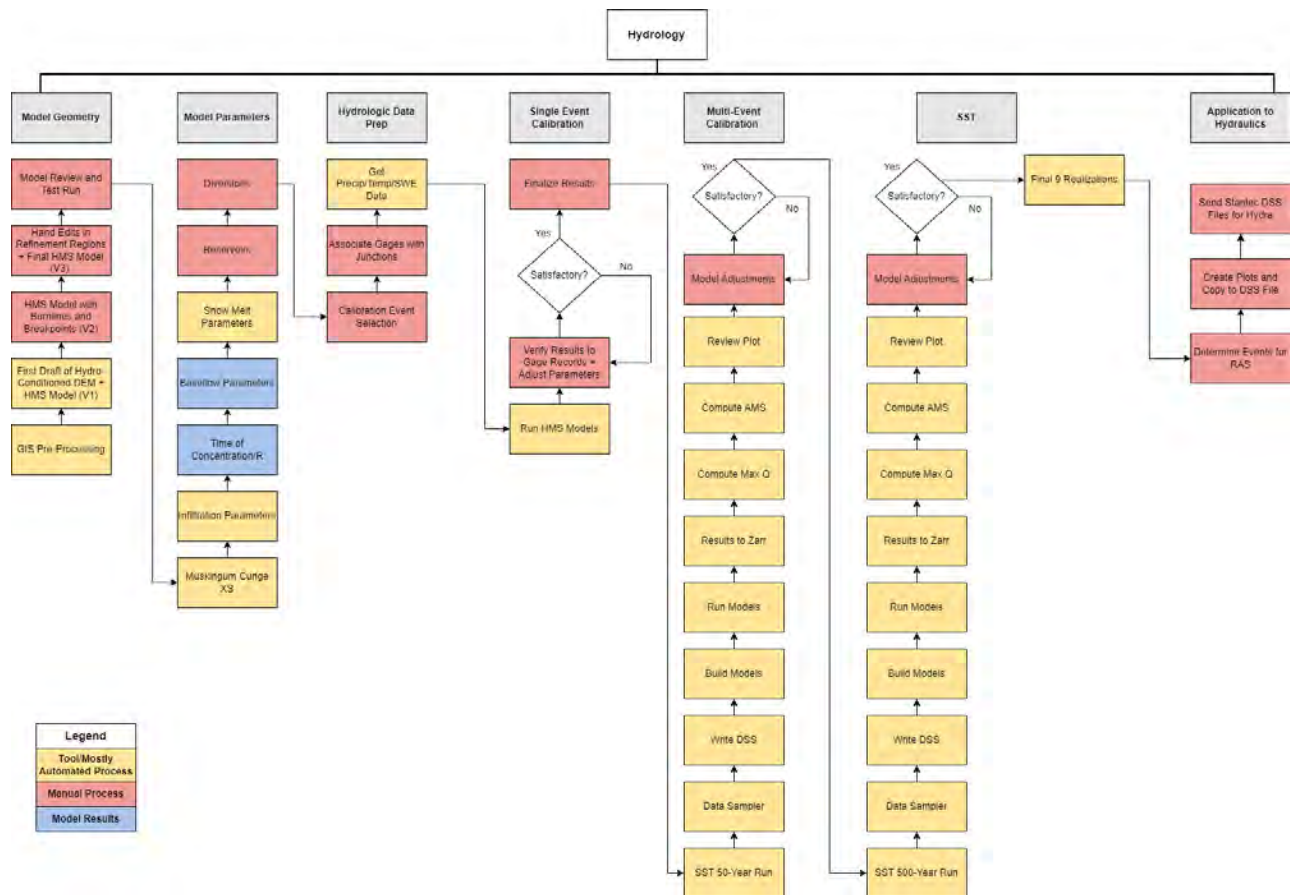
Figure 24. Hydrologic methodology diagram.

5.2   Terrain Development and GIS Data Processing

The DEM used for this project was obtained from the USGS National Map datasets (2023). The terrain included NED 13 (30-meter resolution) data, ensuring a detailed and accurate representation of topography. The projected coordinate system was U.S. Contiguous Albers Equal Area Conic, with both vertical and horizontal units set to 100 feet.

To enhance coverage, multiple DEM sources were assembled:

* USGS NED "1m" covered approximately 93% of the study area within Wyoming.

* USGS NED "Original Product Resolution" (OPR), specifically Project WY_SouthCentral_2020_D20, provided near-complete coverage, though some out-of-state areas remained uncovered.

* Additional NED sources were used to fill any remaining gaps.

To ensure accuracy, the DEM was clipped to the HUC4 study area and reviewed for elevation inconsistencies and boundary mismatches. Additionally, HUC8 boundaries were expanded three

miles upstream and downstream at basin inlets to maintain hydrologic continuity, except for headwater HUC8s, which did not receive upstream expansion.

To support hydrologic modeling, burnlines were incorporated to enforce flow paths over infrastructure, reservoirs, and lakes. Automated burnlines were generated across the HUC4 study area using the latest TIGER Line road and railroad shapefiles (2024) and the NHDPlus dataset (2023). NHD flowlines intersecting road buffers were clipped to define short line segments, reinforcing flow paths over roadways and other man-made structures. The Terrain Reconditioning tool in HEC-HMS was then applied to integrate these burnlines, ensuring that water flows correctly over infrastructure without artificial obstructions.

The terrain processing workflow included the following key steps:

1. Hydro Base DEM Development

   - Assembled DEM data from USGS sources, ensuring uniform projection and resolution.
   - Resampled NED tiles to create a 100-ft resolution terrain raster in USGS Albers projection.
   - Converted elevation units from meters to feet and reviewed DEM quality for anomalies.

2. HUC8 Area of Interest (AOI) Definition

   - Buffered raw HUC8 boundaries by 1600 feet to refine study extents.
   - Manually extended HUC8 boundaries approximately 3 miles upstream and downstream where applicable.

3. Clipping Study-Wide DEM for Each HUC8

   - Created HUC8-specific DEMs from the Hydro Base DEM, ensuring appropriate extents for each hydrologic model domain.

4. Burnline Creation for Flow Path Enforcement

   - Combined TIGER Line 2024 roads and 2022 railroads to create a road buffer layer (200-ft buffer width).
   - Selected NHDPlus flowlines that intersect buffered roads to define hydrologic burnlines.
   - Clipped NHD flowlines to buffered road areas, ensuring correct flow enforcement at crossings.
   - Manually refined burnlines for reservoirs, lakes, and critical flow pathways before integration into HEC-HMS terrain processing.

By integrating these terrain development and GIS data processing techniques, the project ensures that the hydrologic model operates with accurate topographic representation.

5.3   Watershed Delineation and Hydrology Network

A HEC-HMS model was developed for each HUC8 watershed within the study area, with the exception of HUC8 14040200, a closed basin which utilized two HEC-HMS models. The watershed and stream networks were delineated using burnlines to enforce hydrologic flow paths, with stream identification based on a 2.5 square mile drainage area threshold, consistent with the project scope. This initial configuration formed the basis of Version 1 (V1) of the HEC-HMS model.

To refine the hydrologic network, V1 models were imported into ArcGIS Pro using the Dewberry HMS2GIS tool, allowing for network review and correction. During this review, additional burnlines were added manually where necessary to ensure that flow paths aligned with the NHD stream network, terrain, or aerial imagery as appropriate. The model was then re-imported into HEC-HMS, reviewed, and refined through several iterations to improve network accuracy.

To support refinements in the 2D BLE Option A refinement regions, supplemental HEC-HMS reference models were developed using the final burnlines, but with a finer 0.5 square mile drainage area threshold resulting in smaller subbasins for stream identification. These finer-resolution models served as references to guide manual edits to add smaller subbasins in areas requiring additional adjustment, particularly in hydrologically complex or sensitive regions and to meet the Option A 1 square mile stream threshold.

5.3.1   Breakpoint Methodology for Hydrologic Control

HEC-HMS allows the automation of junction creation using breakpoints placed along identified streams. A breakpoint methodology was applied to establish hydrologic control points within each HUC8 model as follows:

- 5 square mile breakpoints were used in 2D BLE Option A areas (standard delineation).
- 1 square mile breakpoints were used in 2D BLE Option C areas (refinement regions) consistent with the BLE Analysis and Mapping Guidance Table 1 (FEMA, 2023).

Breakpoints were initially placed automatically at 5-square-mile intervals and then manually reviewed in ArcGIS Pro. Additional breakpoints were added at key hydrologic control points such as USGS major gage locations, major tributary junctions, and locations with known changes in flow conditions.

Once burnlines and 5- square mile breakpoints were incorporated, manual edits were performed within the 28 scoped refinement regions to enforce subbasin delineation up to the 1 square mile threshold.

5.3.2   Quality Control and Finalization

A quality control (QC) process was conducted before finalizing each model, including:

- Verifying federal land boundaries and ensuring junction placement along stream in proximity of federal land boundary

- Ensuring watershed delineation consistent with the quality of the input terrain
- Correcting schematic errors (e.g., subbasin delineation, stream reach flow path, model element placement and connectivity)
- Performing edge matching to prevent overlaps or gaps between adjacent models

These steps ensured that the final hydrologic models met all project requirements and provided a reliable foundation for subsequent hydrologic parameterization and hydraulic analyses.

5.4 Hydrologic Parameterization

Hydrologic parameterization defines the physical and hydrologic characteristics of subbasins and reaches in the watershed model. This step ensures that precipitation losses, runoff transformation, and flow routing are appropriately represented in the HEC-HMS model.

Initial hydrologic parameters were assigned to each HUC8 model based on standardized methodologies to maintain consistency across all subbasins. Key parameterization methods included:

- Deficit and Constant Loss for infiltration losses
- ModClark for runoff transformation
- Muskingum-Cunge for flow routing
- Linear Reservoir for baseflow simulation
- Gridded Temperature Index for snowmelt modeling

Evapotranspiration was applied to the HMS Meteorologic Model using the Gridded Hamon method and the default coefficient of 0.0065 in/g/m^3. For lakes, storage effects on hydrologic conditions were considered only for Fontenelle Dam and Flaming Gorge Dam, based on reservoir operation data obtained from the Bureau of Reclamation (USBR, 2021 and 2024).

The following subsections provide detailed descriptions of these parameterization methods, including their underlying equations, assumptions, and implementation in HEC-HMS. Initial parameterization was subject to adjustment during the calibration process.

5.4.1 Infiltration Losses

The Deficit and Constant Loss method was used to estimate infiltration losses, where parameters were derived from Gridded Soil Survey Geographic Data (gSSURGO 2023), Gridded National Soil Survey Geographic Database (gNATSGO), and the National Land Cover Database (NLCD) Imperviousness dataset. Parameters were assigned to each basin as follows:

Equation 1.

Maximum Deficit= (saturation storage−Wilting point storage) × active soil depth

Equation 2.

Initial Deficit= (saturation storage−field capacity storage) × active soil depth

where:

- Deficit (mm) = Soil water availability for infiltration.
- Soil water storage (mm³/mm³) = Volumetric measurement of water held in soil.
- Active soil depth (mm) = Depth contributing to infiltration.
- Wilting point storage = Soil moisture content at which plants permanently wilt.
- Field capacity storage = Maximum soil moisture content that soil can retain against gravity.
- Constant rate = Approximated by the hydraulic conductivity at the bottom of the active soil depth.

5.4.2   Runoff Transformation

The ModClark transform method was applied to all subbasins, allowing for a spatially distributed runoff response. Time of Concentration (T_c) was estimated using the HEC-HMS Calculator, based on the following Equation 3:

Equation 3.

$$T_C = 2.2 \left(\frac{LL_C}{\sqrt{slope_{10-85}}} \right)^{0.3}$$

where:

- T_c= time of concentration (hours).
- L= longest flow path (miles).
- L_C= centroidal flow path (miles).
- Slope10-85 = average slope between the 10% and 85% points along the longest flow path.

The additional Storage Coefficient (R) is required for the ModClark Unit Hydrograph and was defined by Equation 4.

Equation 4.

$$\frac{R}{(T_C + R)} = Ratio; \; Ratio \in (0,1)$$

The initial ratio was set at 0.5, meaning that R was initially equal to T_C.

5.4.3 Flow Routing

The Muskingum-Cunge method was applied to all reaches to model flow routing, using an 8-point cross-section approach. A uniform Manning's n value of 0.045 was assigned for channel roughness. Initial cross section placement was performed with an automated approach. This approach placed the cross section perpendicular to the midpoint of the channel. An algorithm was then applied to identify the 8 points needed to represent the overbanks and channel. This algorithm attempts to reduce the cross sectional area difference between station-elevation data sampled every 3 feet and station-elevation data of an 8 point cross section. The resulting cross sections were engineer reviewed and adjusted as needed.

Once the review was complete the cross sections were loaded into a HEC-DSS file and associated with the respective reaches in HEC-HMS using a Python script.

5.4.4 Baseflow Simulation

A two-layer linear reservoir model was applied to simulate baseflow and interflow, ensuring a realistic representation of groundwater contributions.

- The Groundwater Coefficients (GW1 and GW2) were assigned as follows:
  - *GW1* Coefficient = *3×R*
  - *GW2* Coefficient = *10×R*
- Baseflow Fractions = 0.5 for each layer
- Number of reservoirs per layer = 1

5.4.5 Snowmelt Modeling

The Gridded Temperature Index method was applied for snowmelt processes, using gridded initial conditions and the following standard melt parameters:

- PX Temperature = 34°F
- Base Temperature = 32°F
- ATI-Meltrate Coefficient = 0.98
- Wet Melt Rate = 0.1 in/day
- Rain Rate Limit = 0.5 in/hr
- Dry Melt Rate = set for each subbasin as an ATI meltrate function based on observed SWE data and accumulated temperature days.
- Cold Limit = 0.2 in/day
- ATI-Coldrate Coefficient = 0.5

A paired data set for the ATI-Coldrate function was created in HEC-HMS:

ATI (°F-Day)	Coldrate (in/°F-Day)
0	0.02
500	0.02
1000	0.02

5.4.6   Model Discretization

A structured discretization grid with a 2,000-meter cell size, based on the Standard Hydrological Grid (SHG) projection was generated to support the ModClark transformation. The SHG grid provides a spatial framework for mapping gridded precipitation, temperature, snow water equivalent and other snowmelt process inputs to the corresponding model subbasins, ensuring spatially distributed runoff computations across the watershed.

5.5   Calibration and Validation

Calibration and validation events were selected to ensure consistency and reliability across the study area. Events were chosen based on their historical significance, spatial coverage, and availability of complete datasets for precipitation, temperature, SWE, and streamflow records. The calibration process followed a two-step approach:

- Event-Based Calibration: Parameters were adjusted using observed streamflow from historical flood events.

- SST-Based Refinement: Parameters were further refined using SST events to enhance model accuracy across a range of flood scenarios.

This approach ensured that the models accurately represented both real-world flood responses and probabilistic event variability, improving overall hydrologic representation and predictive reliability.

5.5.1   Event-based Calibration

Calibration events were selected to ensure sufficient snowmelt contribution within the watershed, with a focus on capturing the transition from cold-season snowfall to peak runoff generation. The 2016 and 2018 flood events were selected, covering the period from May 1 to June 30. This timeframe was defined to account for both snowmelt-driven runoff and additional precipitation while considering the travel time required for flow movement across the study area.

Precipitation and temperature datasets were retrieved from AORC (V1.1), while SWE datasets were sourced from the University of Arizona climate database.

The USGS stream gages provided discharge records for calibration (Table 5). Reservoir discharge from USGS gage 09211200 (Fontenelle Reservoir) was applied as inflow to HUC 14040103 and USGS gage 09234500 (Flaming Gorge Reservoir) was used for HUC 14040106. For HUC 14040108, HUC 14040109, and HUC 14040200, where no direct USGS gage data was

available, calibration relied on regional parameter transfer, hydrologic similarity to adjacent gaged basins, and parameter adjustments to ensure consistency with observed data from nearby watersheds.

Table 5. The list of the USGS gage stations used for discharge calibration

HUC8	USGS Gage	Lat.	Lon.	Drainage Area (sq mi)	Datum
14040101	09188500	43°01'08.7"	110°07'07.9"	461	NAD83
	09209400	42°11'34"	110°09'45"	3,825	NAD27
14040102	09196500	43°01'37.4"	109°46'24.7"	76.3	NAD83
	09205000	42°34'02"	109°55'46"	1,255	NAD27
14040103	09211200	42°01'15.5"	110°02'59.3"	4,197	NAD83
14040104	09213500	42°19'46.56"	109°30'42.84"	315	NAD83
14040105	09217000	41°30'59"	109°26'54"	14,000	NAD27
14040106	09229500	41°00'16.3"	109°40'03.2"	520	NAD83
	09234500	40°54'30"	109°25'20"	19,400	NAD27
14040107	09217900	40°57'32.5"	110°34'47.0"	126	NAD83
	09218500	41°01'54"	110°34'43"	146	NAD27
	09220000	41°03'13.9"	110°23'55.1"	55.3	NAD83
	09223000	42°06'39.2"	110°42'33.9"	129	NAD83

The data was converted into .dss files using the HEC-HMS Gridded Data Import Wizard and HEC-DSSVue Data Entry Importer. To ensure data consistency, all sources were reviewed for timing alignment, and some datasets required time shifts to correct for differences in time zones. Additionally, datasets were clipped to a buffered study area to reduce file size.

Each HEC-HMS model was initialized with default parameters, but precipitation, temperature, and SWE gridsets were generated specifically for each calibration event. Unique initial conditions—including initial losses, baseflow, SWE grids, and ATI-Meltrate functions—were applied to each event. As a result, each event required a separate Basin Model and Control Specification, while other parameters remained consistent across models.

The following subsections discuss in more detail how the initial parameters were adjusted during calibration.

5.5.1.1   Snowpack Calibration

The first step in the calibration process focused on snowmelt parameter adjustments. Calibration was initially performed by reference to individual subbasins, and the resulting optimized parameters were then applied across all subbasins or subregions defined by gage calibration

points. In cases where mountainous or high-altitude regions exhibited different melt characteristics compared to lower elevations, adjustments were made while maintaining model homogeneity as much as possible.

The key snowmelt parameters adjusted during calibration included:

- PX Temperature – Controlling whether precipitation is classified as rain or snow.
- Wet Meltrate Constant – Governing snowmelt rates under wet conditions.
- Dry ATI-Meltrate Function – Modulating snowmelt rates under dry conditions.

The initial simulated SWE depth time series (Figure 25) was compared to observed SWE records (Figure 26). In this example, it was observed that the simulated SWE was not decreasing at an adequate rate, indicating a need for further refinements. Additionally, PX Temperature was reviewed to ensure the correct classification of precipitation as snow or rain, and necessary adjustments were made.
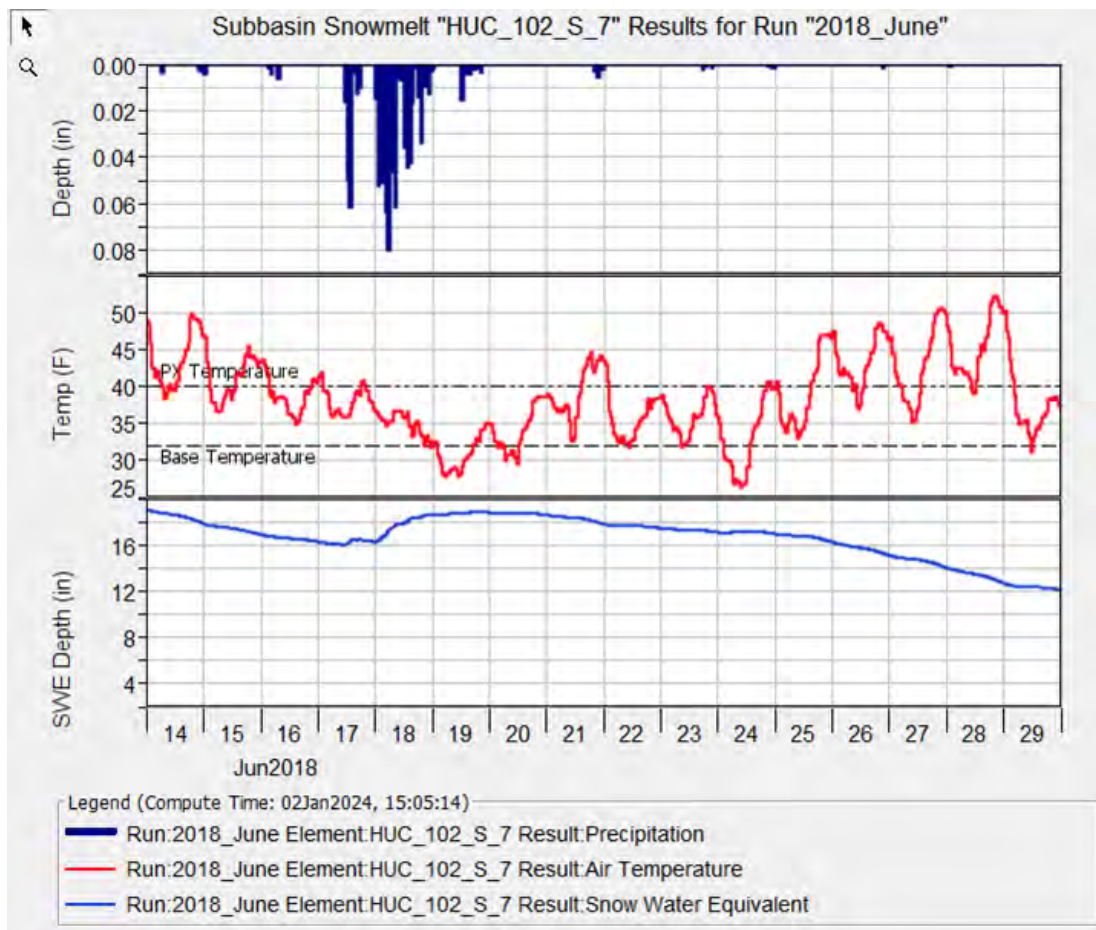
Figure 25. Initial SWE results prior to snowmelt parameter calibration.
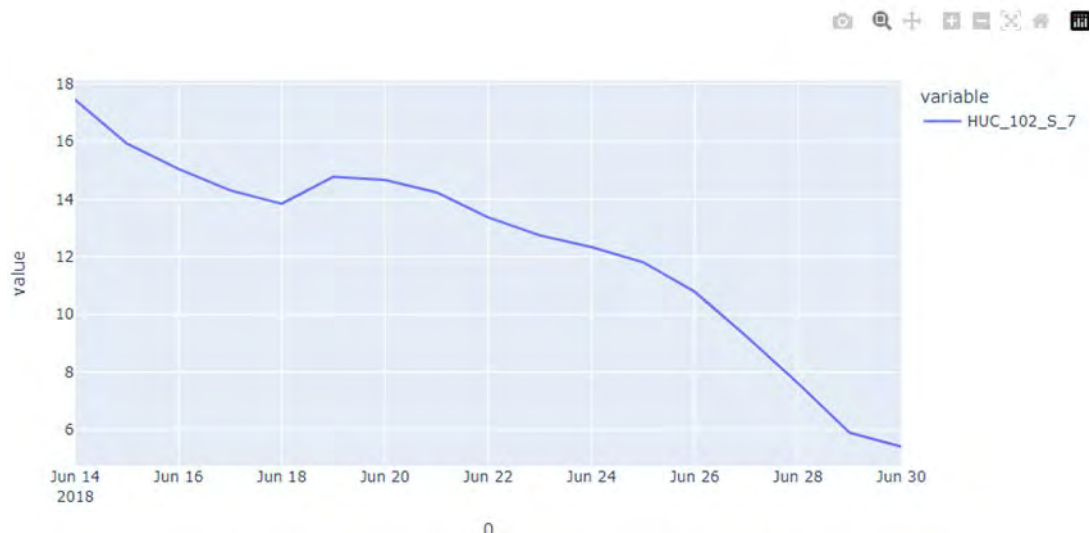
Figure 26. Record SWE.

To improve model accuracy, the ATI-Meltrate function was initially generated based on record data. A typical automated function is shown in Figure 27. However, in some cases, manual adjustments were required to better match the observed timing and intensity of snowmelt. Subbasin-level comparisons were conducted to ensure consistency across the model. Once snowmelt calibration was completed, the revised parameters produced a better fit between the simulated and observed SWE time series (Figure 28), achieving a representative balance across multiple subbasins.
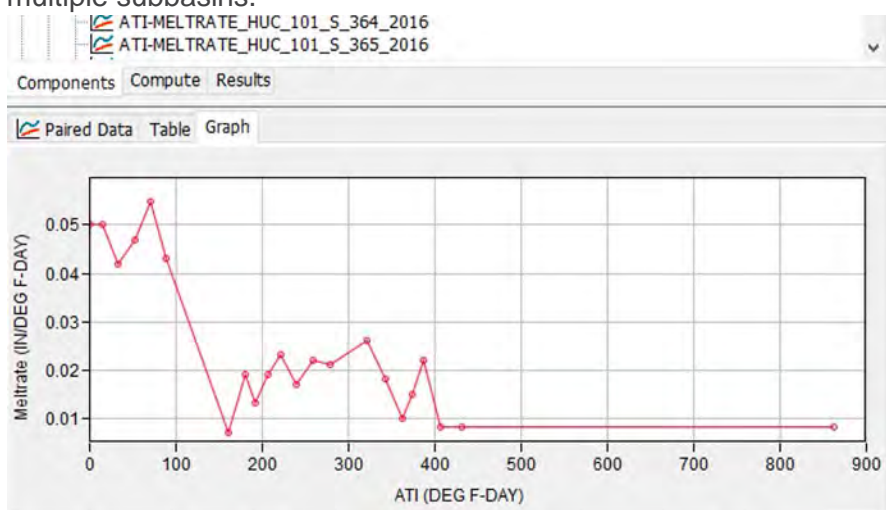
Figure 27. Automated dry ATI-Meltrate function.
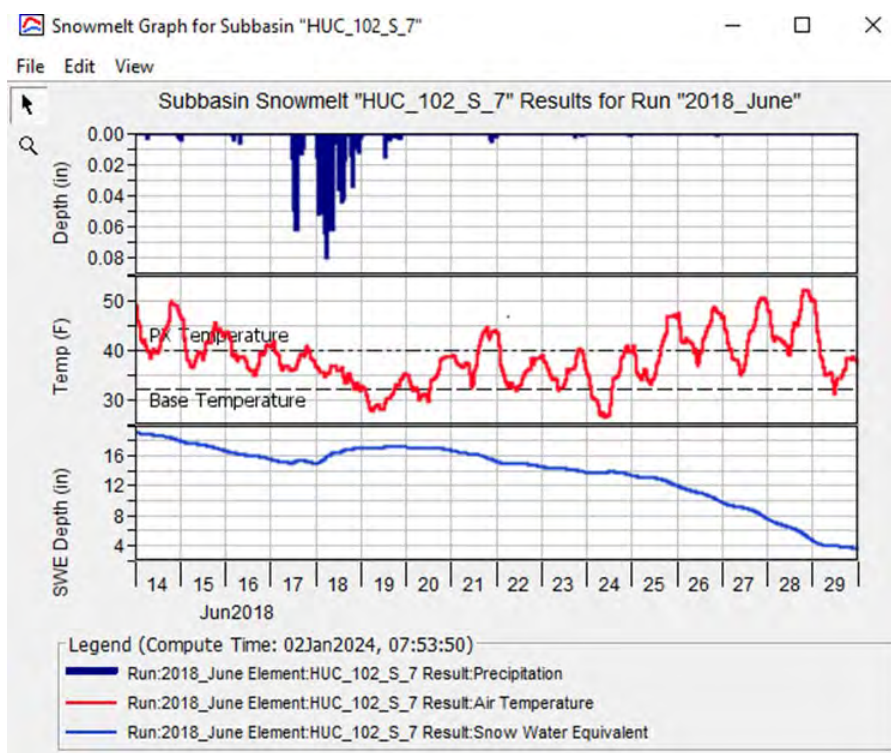
Figure 28. Initial SWE results after snowmelt parameter calibration.

Even after applying the calibrated parameters across the entire watershed, variations in SWE estimates were observed at the subbasin level, reflecting the natural complexity of hydrologic processes. While some subbasins exhibited slight differences in SWE magnitude, the overall trends and seasonal patterns were well captured. Additionally, minor fluctuations in recorded data, particularly short-lived variations, were not always pronounced in the simulation but remained within an acceptable range for hydrologic modeling. Achieving an exact match for every subbasin was not the objective; rather, the focus of calibration was to ensure that the general shape, magnitude, and timing of snowmelt were accurately represented across the watershed. This approach maintained hydrologic consistency while effectively capturing the key drivers of the system's response.

Following snowmelt calibration, the remaining model parameters were adjusted through an iterative process. Adjustments were made systematically, considering the interdependencies between parameters.

5.5.1.2 Routing Muskingum-Cunge Parameters

The timing of the flow hydrograph was refined by adjusting channel Manning's n values within a reasonable range while keeping slope values unchanged. Manning's n values ranged from 0.040 to 0.06. Cross-sections and reach lengths were generated from terrain data and remained unaltered, except where major reservoir influences were identified. For reaches passing through large reservoirs, routing parameters were removed by setting them to "no lag," effectively

eliminating attenuation effects in those sections. This approach ensured that routing adjustments were limited to hydraulically justifiable modifications while preserving model consistency across the watershed.

5.5.1.3 Loss Deficit and Constant Parameters

Initial losses were refined to reflect antecedent conditions, which significantly influence the shape and peak of the flow hydrograph. The Initial Deficit was adjusted between 0 to 1.2 times the default value, depending on event-specific conditions. The Constant Rate was calibrated as a fraction of the default value, typically ranging between 0.2 to 0.3 times the default rate, ensuring an accurate representation of infiltration losses.

The Maximum Storage and Impervious values remained at their default settings, as they were not expected to significantly impact calibration outcomes. This approachmaintained model consistency while allowing flexibility in loss parameter adjustments to match observed streamflow patterns.

5.5.1.4 Baseflow Linear Reservoir Parameters

Baseflow was modeled using a two-layer linear reservoir approach, where *GW1* and *GW2* values were adjusted to match recorded low-flow conditions. The initial baseflow was distributed between the two layers based on observed discharge data, ensuring an accurate representation of event-specific baseflow contributions.

The *GW1* and *GW2* fractions were typically set to 0.5, but minor adjustments were made to reflect local aquifer recharge contributions. Since aquifer recharge is known to affect certain areas of Wyoming, relevant data from the Wyoming State Geological Survey – GIS Groundwater Database was considered when applying GW fractions.

The *GW1* and *GW2* coefficients were initially set to $3 \times T_c$ and $10 \times T_c$, respectively, as default values. Rather than modifying these coefficients, adjustments were primarily made to the number of reservoirs, increasing storage time where necessary. The *GW1* parameters primarily influenced peak flow and hydrograph oscillations, while *GW2* parameters affected the overall shape and tail recession of the flow hydrograph.

This method ensured a balanced approach to baseflow calibration, maintaining consistency across models while allowing for site-specific refinements where necessary.

5.5.1.5 Transform ModClark Parameters

The ModClark transform parameters for time of concentration (T_c) and storage coefficient (R) had a subtle impact on the overall flow hydrograph, but minor adjustments were made to refine the final model output. In most cases, the default values provided a reasonable starting point, and significant deviations were avoided to maintain model reliability.

When adjustments were necessary, the relationship between T_c and R was preserved, as illustrated in Figure 29. By default, the two parameters were set equal, ensuring that the *Ratio* in

Equation 4 is equal to 0.5. Any modifications remained within hydrologically realistic limits to avoid instability. These refinements helped improve hydrograph timing and peak flow representation while maintaining model consistency.
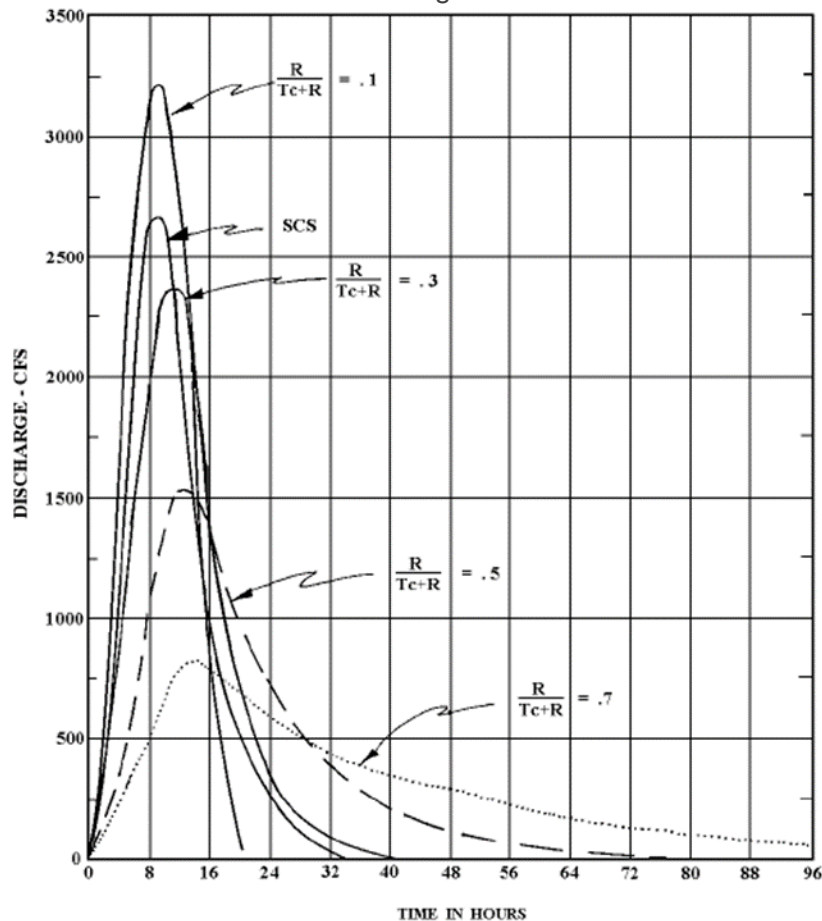
Figure 29. Discharge hydrograph and transform parameter relationship.

5.5.1.6   Reservoirs

In some regulated headwater areas, reservoirs played a significant role in the calibration process for recorded discharges and were evaluated on a case-by-case basis. For example, Figure 30 illustrates the location of reservoirs in HUC 102. Run-of-river reservoirs did not significantly impact discharges, as they did not provide substantial storage. However, in some instances, even smaller storage reservoirs had a notable effect on downstream gages, requiring explicit consideration in the calibration process when model results could not align without their inclusion.
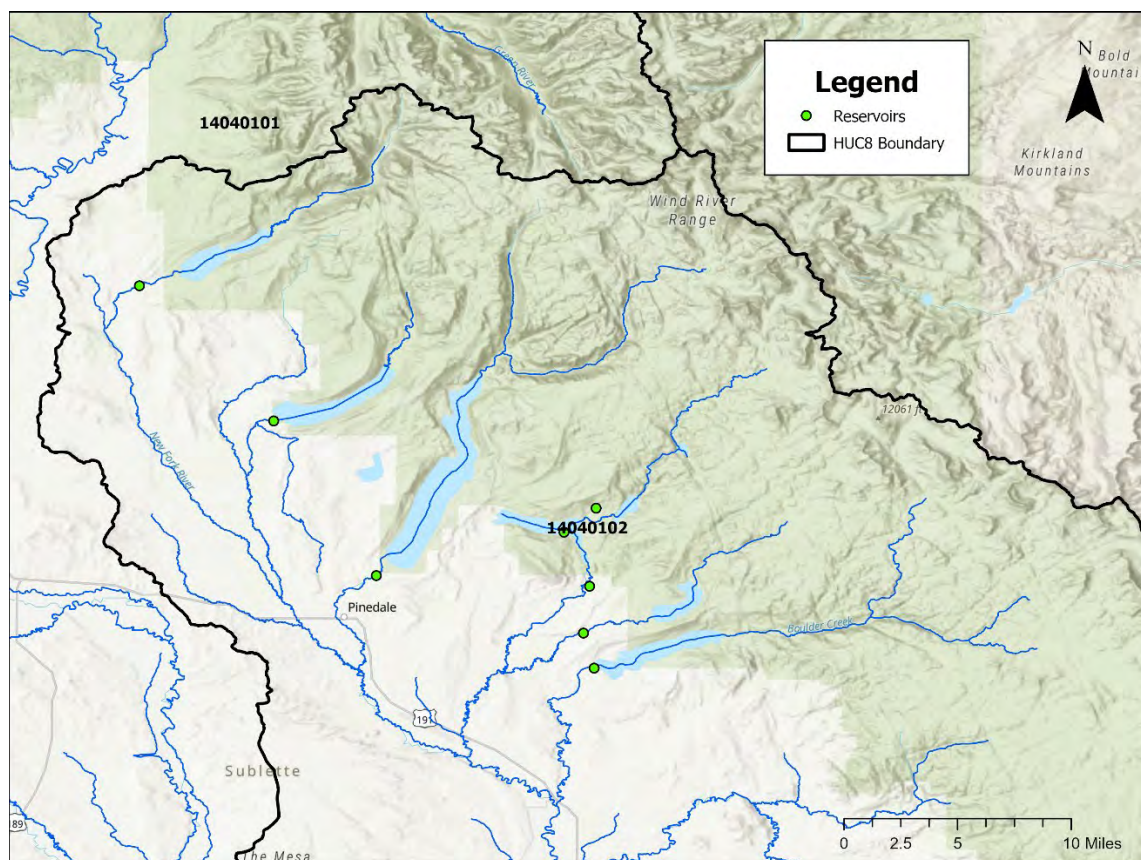
Figure 30. Locations of the reservoirs within HUC 102.

Reservoirs were modeled using simple HEC-RAS-derived stage-storage-discharge relationships. For reservoirs operating under a rule curve or in conjunction with other reservoirs, discharges were not always fixed for the same inflow conditions. In these cases, an average or generalized best-case discharge relationship, derived from multiple events, was applied to improve model performance and ensure hydrologic consistency.

5.5.1.7   Diversions

Agricultural diversions significantly impacted runoff in the study area, consistent with previous hydrologic modeling in Wyoming. Diversion records from the State Engineer's Office (WSEO, 2025) were reviewed and analyzed alongside topographic and aerial maps to determine where diversion losses should be applied in the model.

The Loss/Gain Constant Method was used to represent diversion losses within affected reaches. A threshold flow rate and a fractional loss were applied when flow exceeded this threshold. Based on previous modeling experience and a review of gaged diversions in the area, a 5 cfs flow rate with a 0.2 fraction was identified as a representative set of parameters for reaches subject to diversion losses. In addition, state records for the modeled area were carefully reviewed to confirm the appropriateness of these values. The magnitude of diversion flows was also

considered. While a 0.2 diversion fraction was reasonable for smaller tributaries, it was not appropriate for main stem reaches carrying hundreds or thousands of cfs during peak flow events. In such cases, lower diversion fractions (e.g., 0.01) were applied to ensure a realistic representation of flow conditions.

Although state records identified many diversions, some additional unmonitored or undocumented diversions were detected through a review of topographic maps and aerial imagery. As shown in Figure 31, the topographic map identified two named ditches (lighter blue lines with longer dashes) diverting streamflow in addition to the yellow square for an unnamed diversion monitored by the State Engineer's Office.

Figure 31. Topographic map showing diversions; this figure displays two named ditches (lighter blue lines with longer dashes) that divert streamflow, along with one unnamed diversion marked by a yellow square.

When multiple diversions affected the same reach, a single combined diversion loss based on the determined average rate was applied to simplify the modeling while maintaining hydrologic accuracy.

5.5.1.8   Model Performance

Calibrated model performance was evaluated using the matrix in Figure 32, with the goal of achieving a Satisfactory rating. Once the initial set of parameters was established, they were

tested on a second event for validation. Adjustments were made iteratively until a final set of parameters was obtained that provided Satisfactory results across all modeled events.

In some cases, less-than-ideal parameters for one event were kept to achieve consistent and reliable results across multiple events. This approach ensured that the model remained hydrologically realistic while maintaining acceptable performance for all calibration and validation events. Figure 33 shows an example of the calibration results.

Performance Rating ⬍	Color Code ⬍	R^2 (2015) ⬍	NSE (2015) ⬍	RSR (2007) ⬍	PBIAS (2015) ⬍
Very Good	Dark Green	$0.85 < R^2 \leq 1.00$	$0.80 < NSE \leq 1.00$	$0.00 < RSR \leq 0.50$	$PBIAS < \pm5$
Good	Light Green	$0.75 < R^2 \leq 0.85$	$0.70 < NSE \leq 0.80$	$0.50 < RSR \leq 0.60$	$\pm5 < PBIAS \leq \pm10$
Satisfactory	Orange	$0.60 < R^2 \leq 0.75$	$0.50 < NSE \leq 0.70$	$0.60 < RSR \leq 0.70$	$\pm10 < PBIAS \leq \pm15$
Unsatisfactory	Red	$R^2 \leq 0.60$	$NSE \leq 0.50$	$RSR > 0.70$	$PBIAS \geq \pm15$

Figure 32. Performance rating matrix.

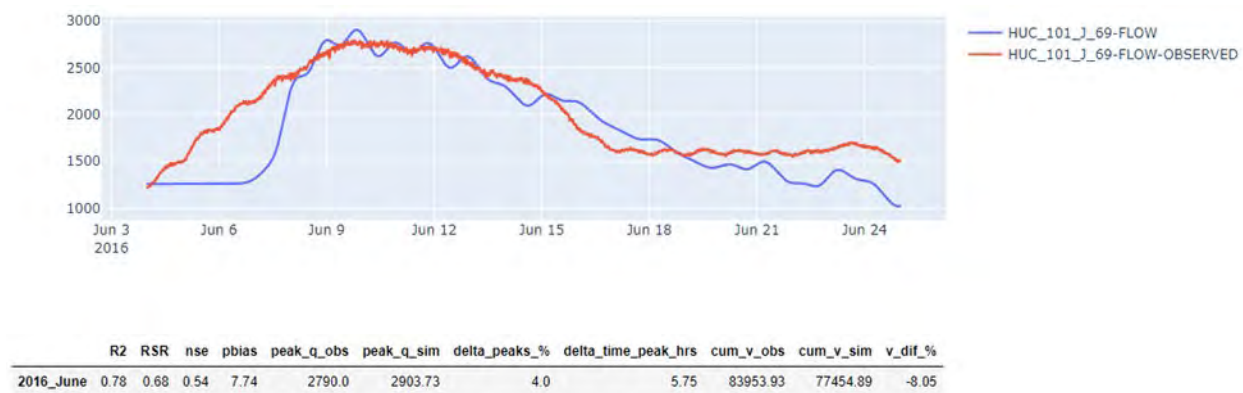|	R2	RSR	nse	pbias	peak_q_obs	peak_q_sim	delta_peaks_%	delta_time_peak_hrs	cum_v_obs	cum_v_sim	v_dif_%
2016_June	0.78	0.68	0.54	7.74	2790.0	2903.73	4.0	5.75	83953.93	77454.89	-8.05

Figure 33. An example of calibration results

5.5.2   Multi-Frequency Calibration

Following event-based model calibration, multi-frequency calibration (MFC) was performed wherein model parameters were further refined to align model results with gage observations across the spectrum of frequencies observed. Fifty synthetic years of events from the storm catalog were selected, transposed, and applied to the model, generating a set of peak discharge results, which were then compared to gage records. Ideally, the modeled peak results would closely align with the observed data at the gage. However, final parameter adjustments were often necessary to achieve the best possible fit between the simulated MFC results and observed data. As shown in Figure 34, the initial MFC model results (purple points and line) underestimated peak discharges compared to the gage observations (black points). These additional adjustments were necessary to account for epistemic uncertainty with the operations of reservoirs and agricultural

diversions in the study area, as well as typical soil moisture conditions not captured in the events selected for single event calibration.
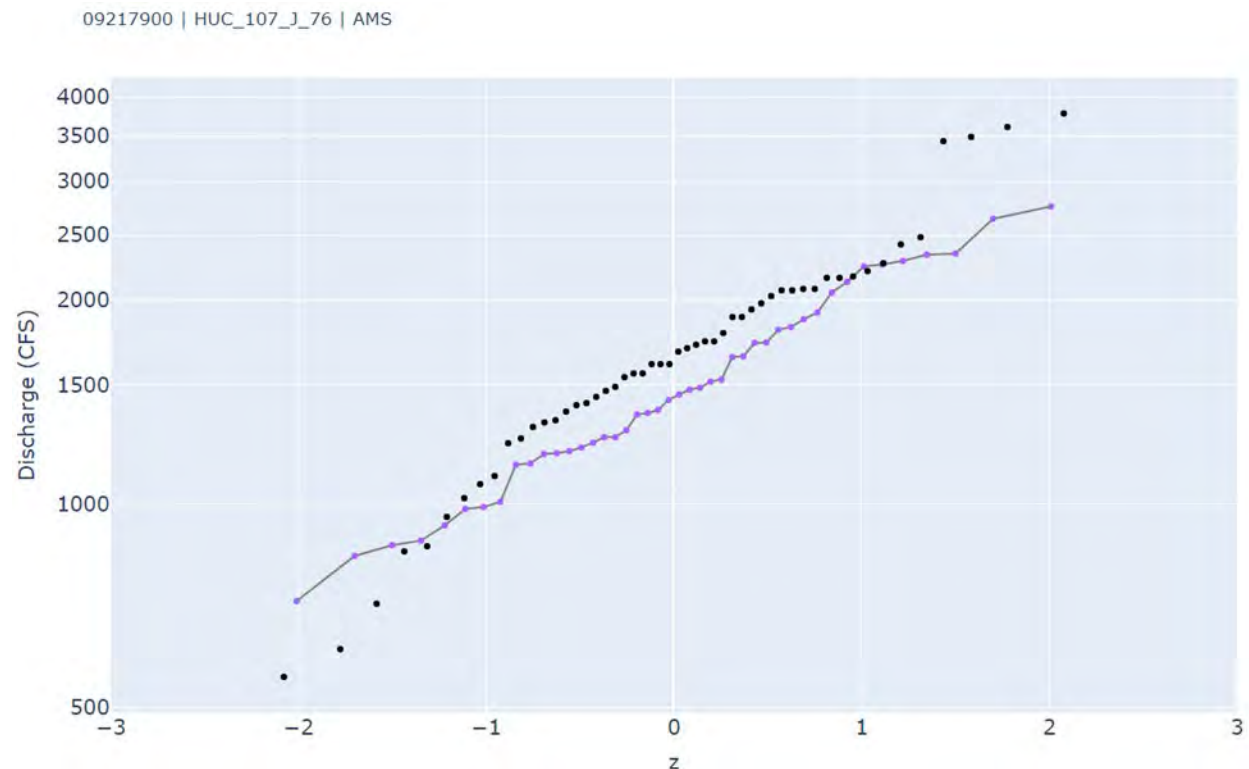

09217900 | HUC_107_J_76 | AMS

Figure 34. Initial SST comparison to gage analysis.

To ensure as comprehensive an assessment as possible, given the sparsity of gages, all gages with a significant period of record were reviewed within each HUC8. Additional intermediate gages—which were not ideal for calibration and validation—were also utilized as comparison points for MFC model results. In some cases, Wyoming State Engineer's Office gages provided supplementary peak discharge data, contributing to a more complete representation of the overall HUC response.

The goal of these adjustments was to match the HMS-modeled peak discharges to the gage-based analysis at the same vertical z parameter. For instance, if the initial SST model result at z = 0 was less than 1500 cfs, model parameters were adjusted to increase the peak flow to exceed 1500 cfs. Typically, two to four SST models from the same dataset provided sufficient information to refine the parameter set and achieve a better overall fit. Using the same models to adjust multiple gage comparison points improved efficiency in addressing the entire HUC calibration.

Once the parameter refinements were applied, the MFC events were re-simulated, and the results were compared again. As shown in Figure 35, the final adjustments produced a significantly improved fit. Adjustments affecting the results for the left tail (z < -1), while not necessarily relevant to the overall analysis, were crucial to ensure that the middle and upper portions of the plot were well aligned with the observed data.
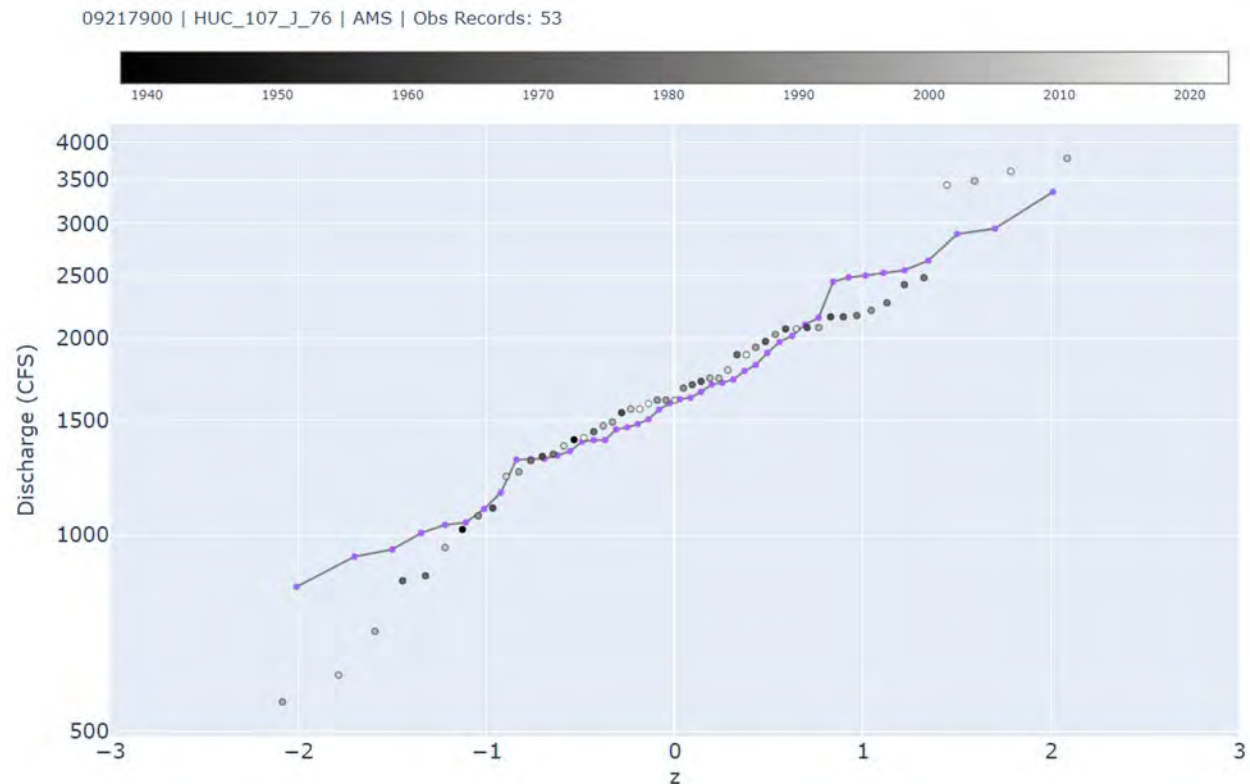
Figure 35. Comparison of final discharge: SST simulations vs. observed gage analysis.

These realizations of 50 synthetic years (s-years) were conducted in an iterative process to refine model parameters (Figure 36). This iterative approach ensured that model parameters were validated across the flood frequency space, improving confidence in the ability of the model to represent hydrologic conditions. The shape and scale of the synthetic results were evaluated against observed records, and adjustments were made as necessary. Each iteration aimed to achieve a reasonable fit between the synthetic and observed datasets, with parameter modifications triggering additional 50-year realizations until satisfactory results were obtained.

Figure 36. Iteration cycle for modeling in the stochastic framework.
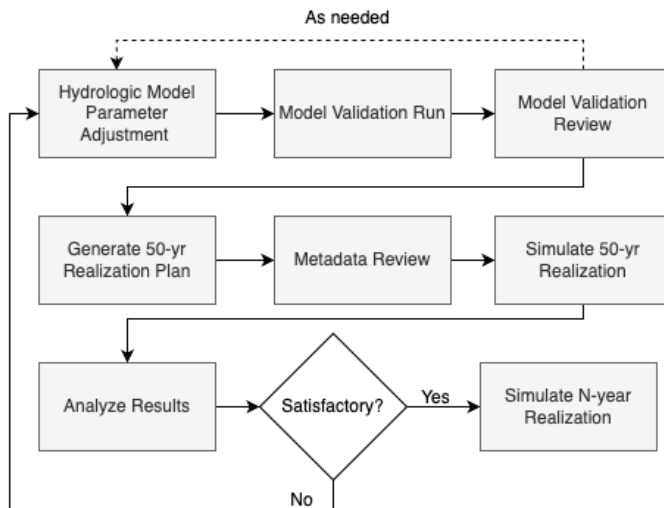
5.6   SST Simulation and Results

Following calibration, the suite of HEC-HMS simulations was executed using synthetic storms generated through SST, along with the final calibrated parameter sets. This produced a range of flow time series representing the full spectrum of flood frequencies required for the project.

From these simulations, hydrograph peaks corresponding to the 10%, 4%, 2%, 1%, 1% plus, 1% minus, and 0.2% annual exceedance chance events were identified through statistical analysis of the complete set of simulated results.

The final frequency-based hydrographs serve as the primary inflow inputs for subsequent hydraulic modeling and flood risk assessment, forming the foundation for floodplain mapping, flood risk characterization, and future mitigation planning within the study area.

5.6.1   Cloud-Based Stochastic Framework

A Python-based framework was developed to generate stochastic input data for 500-year realizations. As shown in the diagram below (Figure 37), for each year in a 500-year realization, a Poisson distribution was sampled to determine the number of storm events per year, resulting in k events per year.
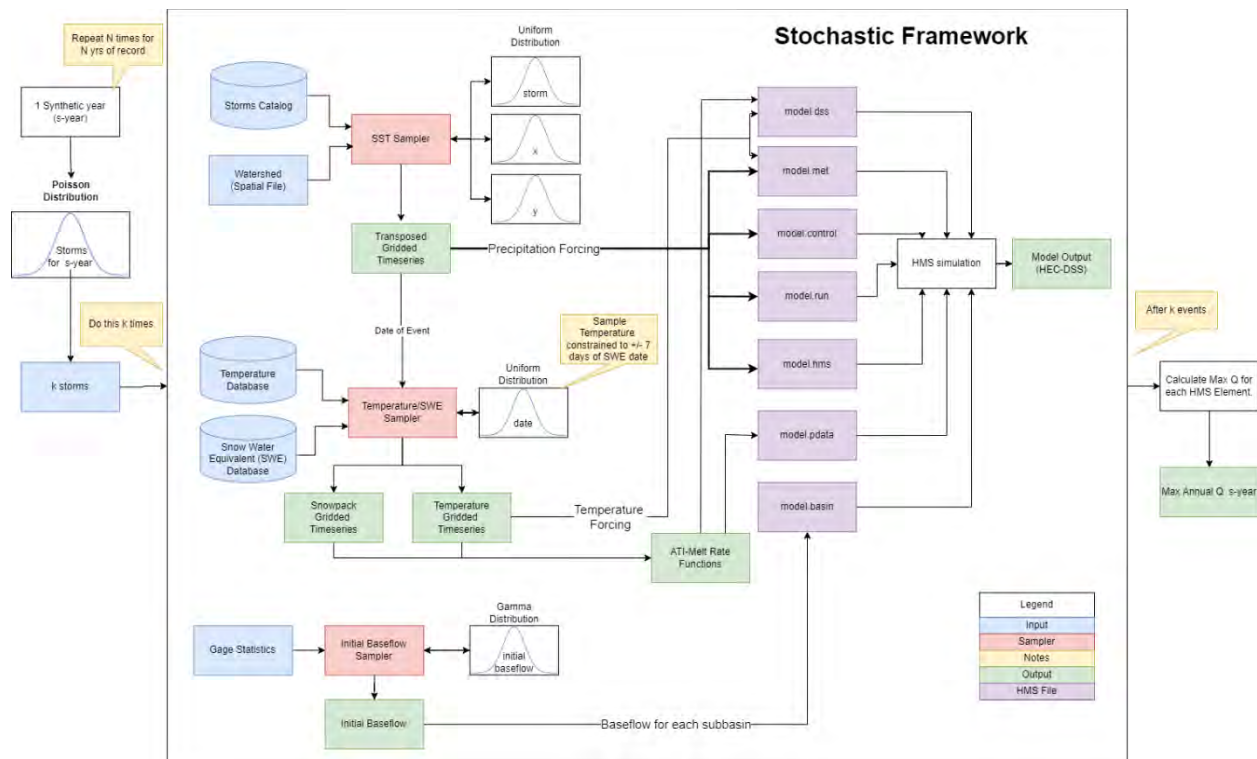
Figure 37. **Overview of the stochastic framework applied in this study.**

For each event, a storm was sampled from the storm catalog and transposed within the transposition region using a uniform distribution for selecting the event, x, and y location of the storm (Figure 38).
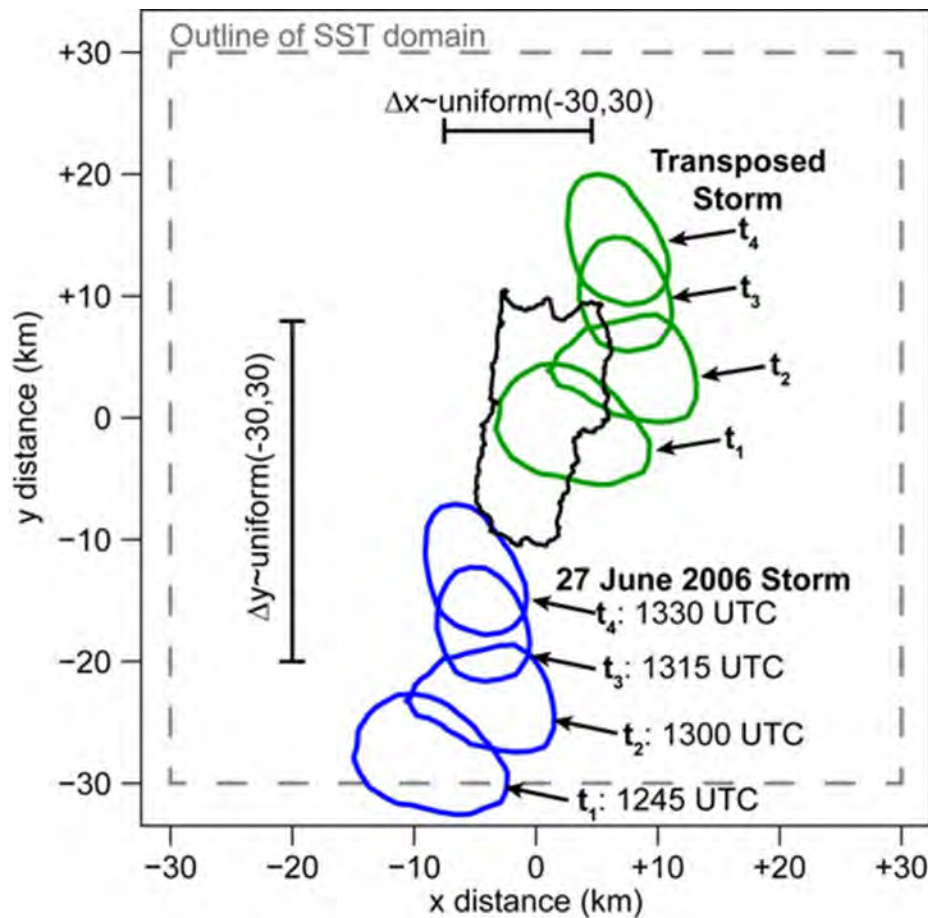
Figure 38. Depiction of stochastic storm transposition procedure for a single storm consisting of four time intervals. The blue ellipses show the time evolution of an arbitrary rainfall isohyet, while the green ellipses show the time evolution of transposed rainfall isohyets (Wright et al., 2017).

A metadata file (e.g., storm-E0001.json) was created for each storm event (Figure 39), containing key information such as:

- The random seed used for sampling
- Input/output summaries and statistics
- Timestamps for sampling execution
- Links to reference datasets

```
storm-E0001.json                                                    ⤢  ✕


{
  "id": "upper-green_v01_72h_20210714",
  "start": {
    "datetime": "2021-07-14 00:00:00",
    "timestamp": 1626220800,
    "calendar_year": 2021,
    "water_year": 2021,
    "season": "summer"
  },
  "duration": 72,
  "stats": {
    "count": 5535,
    "mean": 0.8543925881385803,
    "max": 5.484251976013184,
    "min": 0.031496062874794006,
    "sum": 4729.06298828125,
    "norm_mean": null
  },
  "metadata": {
    "source": "AORC",
    "watershed_name": "Upper Green",
    "transposition_domain_name": "v01",
    "watershed_source": "s3://tempest/watersheds/upper-green-1404/upper-green-1404.geojson",
    "transposition_domain_source": "s3://tempest/watersheds/upper-green-1404/upper-green-transpo-area-v01.geojson",
    "create_time": "2023-02-15 22:50:59.551839",
    "png": "https://tempest.s3.amazonaws.com/watersheds/upper-green-1404/upper-green-transpo-area-v01/72h/pngs/20210714.p
  },
  "geom": {
    "x_delta": -86,
    "y_delta": -132,
    "center_x": -113.53399200001331,
    "center_y": 38.099276
  },
  "ranks": {
    "true_rank": 39,
    "declustered_rank": 15
  },
  "categories": {
    "lv10": "Upper Green",
    "lv11": "Upper Green > v01"
  },
  "sst": {
    "input": {
      "grid_resolution": 2000,
      "event_number": 1,
      "synthetic_year": 1,
      "watershed": {
        "watershed_name": "Upper Green",
```

Figure 39. An example screenshot of the metadata file created for each storm event.

5.6.2   Sampling

Following storm event selection, the corresponding temperature and snowpack datasets were sampled. A historic snowpack year was randomly selected from the period of record using a uniform distribution, with the start date constrained to ±7 days from the precipitation start date. The temperature start date was then aligned with the snowpack start date to avoid unrealistic combinations (e.g., pairing an early April snowpack with a July temperature profile).

The baseflow for each subbasin was sampled independently of storm-based sampling using a gamma distribution (Figure 40). Similar to storm metadata, metadata files were also generated for each event's baseflow and temperature/snowpack sampling, documenting the sampling process and results.
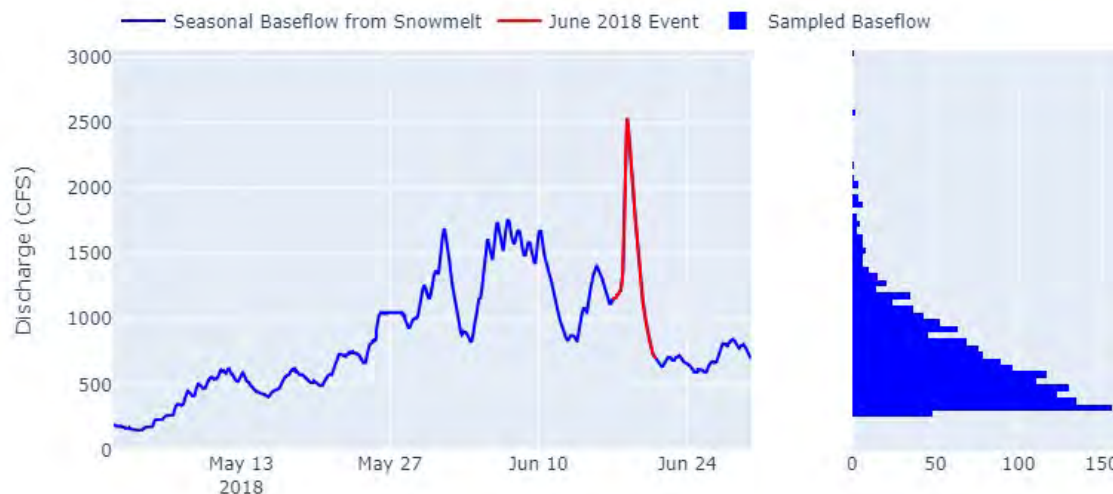
Figure 40. Baseflow sampling example using a gamma distribution.

5.6.3 Review and Validation of Stochastic Realization Plan

With sampling results and metadata in place, the sampling process was reviewed before simulating events in the realization. While this review was not required for every realization, it was a critical step during the initial setup of the computational infrastructure to ensure the accuracy and reliability of the stochastic framework.

For example, a review of discrete elements from the metadata—such as transposed storms plotted on a map (Figure 41)—allowed for verification of the realization plan. This step ensured that random sampling procedures were functioning as expected and provided an opportunity to identify and correct potential issues before initiating the full set of cloud-based hydrologic simulations that comprised the realization.
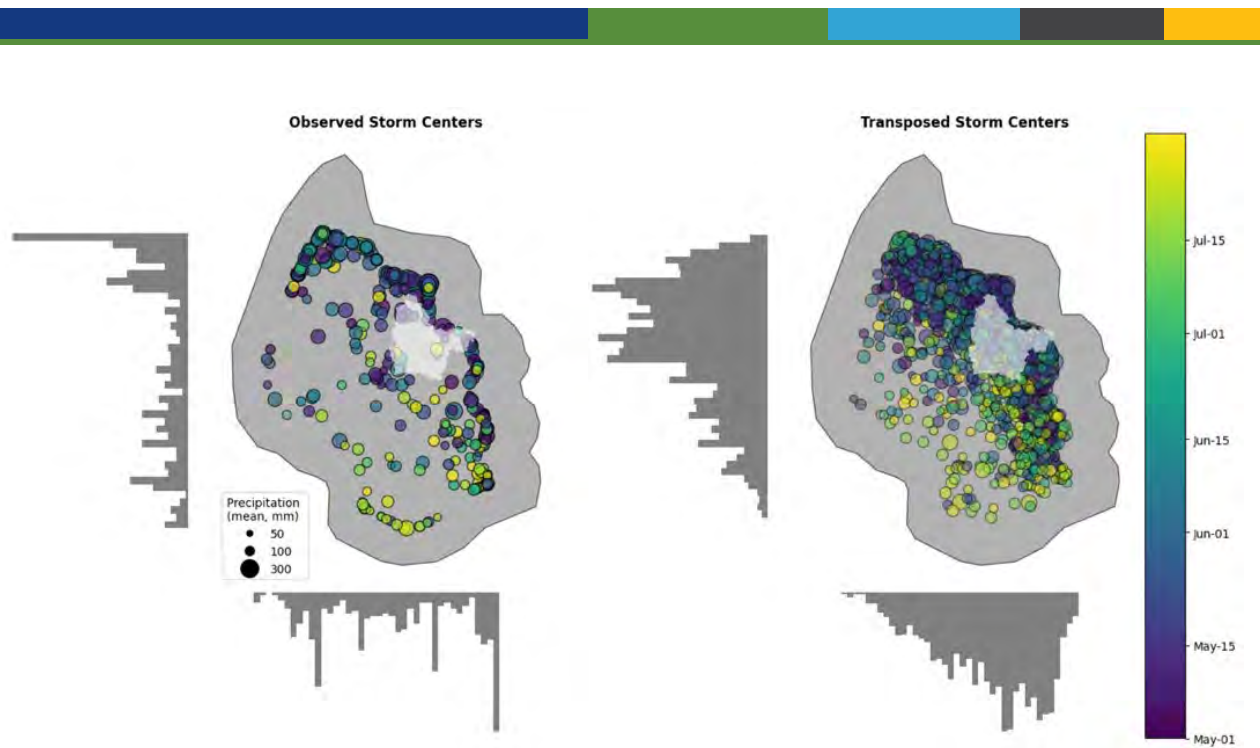
Figure 41. Example map showing transposed storm locations for a sample realization.

After finalizing the realization plan, a Python script processed each metadata file, generating the required event-based simulation files and initializing the hydrologic simulations in HEC-HMS. Upon completion of all simulations, a Python routine iterated over the simulation results, stored in HEC Data Storage System files (i.e., HMS output files). In addition, relevant datasets (primarily time series outputs from HMS elements) were extracted and stored in cloud-native Zarr files, ensuring efficient data access for large-scale analysis. By utilizing the Zarr format, data analysis and extraction could be performed directly in the cloud with minimal latency, eliminating the need for local file downloads.

5.6.4   Event Storm

With sampling results and metadata in place, a review of the sampling process was conducted before simulating events in the realization. As described by Wright et al. (2013) and outlined in the stochastic framework, the first step in developing the storm event catalog was determining the expected number of storms per year for a given watershed. This was achieved by analyzing discharge records at gage locations to estimate the average number of significant storms per year and multiplying this value by the total number of years in the precipitation dataset.

Consistent with the approach proposed by Wright et al. (2013), the Poisson distribution was used to determine the number of storms per synthetic year. The Lambda parameter for the Poisson distribution was estimated based on the frequency of significant streamflow events observed in the watershed (Figure 42).
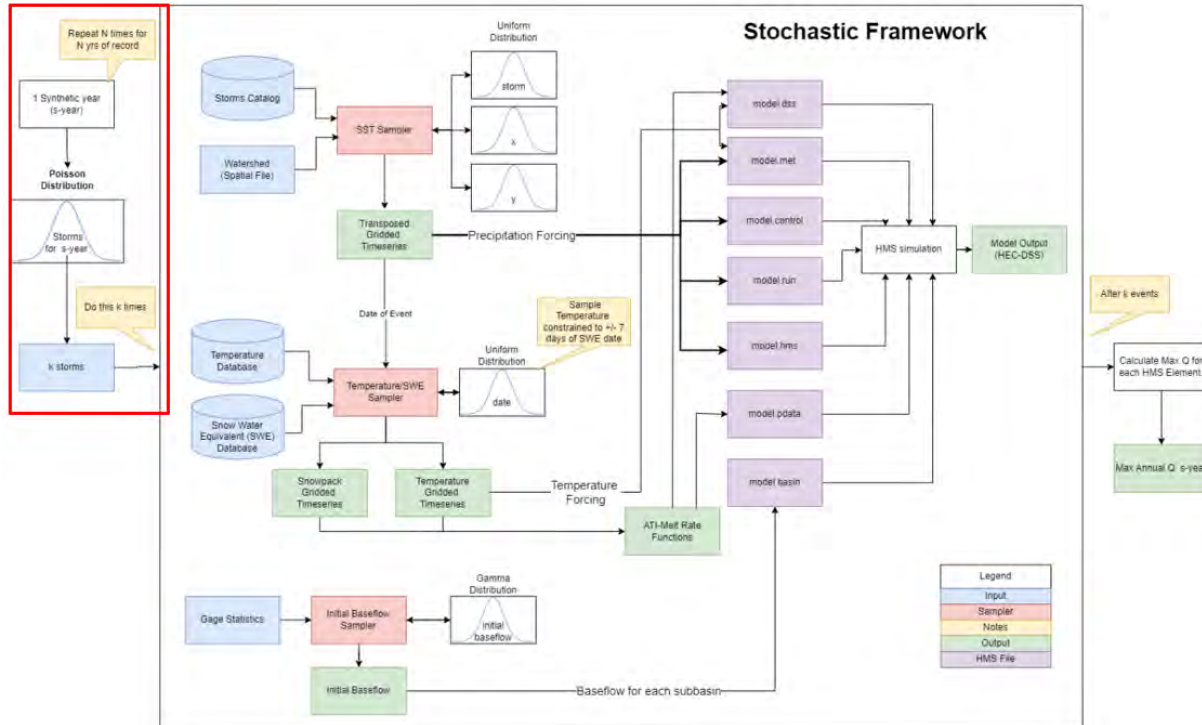
Figure 42. Stochastic framework.

For each simulated event, a storm was randomly selected from the storm catalog using a uniform distribution. Then, the storm was transposed within the x-y space of the transposition domain using uniform sampling. A quality control check ensured that 100% of the watershed area remained within the transposition region. If this check failed, the storm was re-transposed until it met the required criteria (Figure 43).
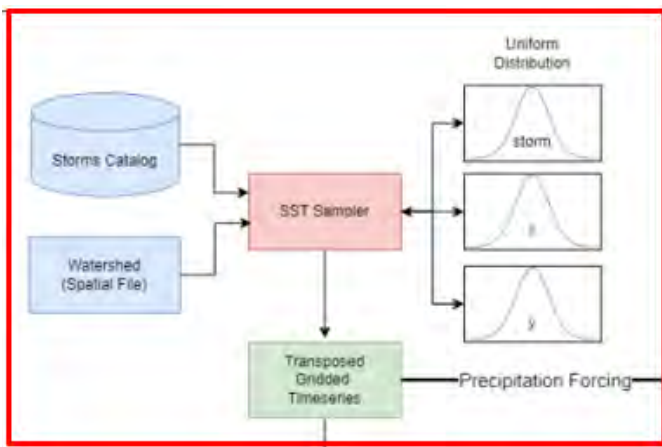

Figure 43. Precipitation event sampling and transposing procedure.

Unlike the approach used by Wright et al. (2013), an additional step was incorporated to account for orographic effects in mountainous regions. This method, known as dimensionless or

enhanced transposition, builds upon techniques used in Probable Maximum Precipitation (PMP) analysis in complex terrain, as established in HMR-49 (Hansen et al., 1977) and extended by Nathan et al. (2016). The process applies a normalization field, converting observed storms into a dimensionless space prior to transposition to account for terrain-induced precipitation variability (Micovic et al., 2015). After transposition, the normalization process was reversed, applying the same field at the transposed storm location.

The 30-year normal precipitation dataset from the PRISM Climate Group (OSU, 2024) was used as the normalization field. Since PRISM data is stored as monthly values, events that spanned multiple months were adjusted accordingly.

Significant snowpack accumulation occurs during the winter months in the UGGD watershed, contributing to baseflow and, in some years, generating peak flows at gages without concurrent rainfall events. To accurately incorporate snowpack into the hydrologic models, a snow water equivalent (SWE) dataset developed by the University of Arizona was used (NASA Earth Data, 2022). Following the conversion of AORC NetCDF data into cloud-optimized format, the SWE data was also converted from NetCDF to Zarr format and stored in the cloud. For each Poisson-sampled precipitation event, a uniform distribution was used to randomly select a starting date for the SWE dataset, constrained to ±7 days of the precipitation event's start date. Additionally, a random year was selected from the 40-year period of record (Figure 44). The selection process followed this workflow:

- Randomly select a starting date within ±7 days of the precipitation event.
    - Precipitation start date: June 7, 2001
    - Sampling range: June 4–10
    - Sampled value: June 5
- Randomly select a historical year from the 1980–2020 period of record.
    - Sampled year: 1993
- Extract SWE and temperature data for the selected date:
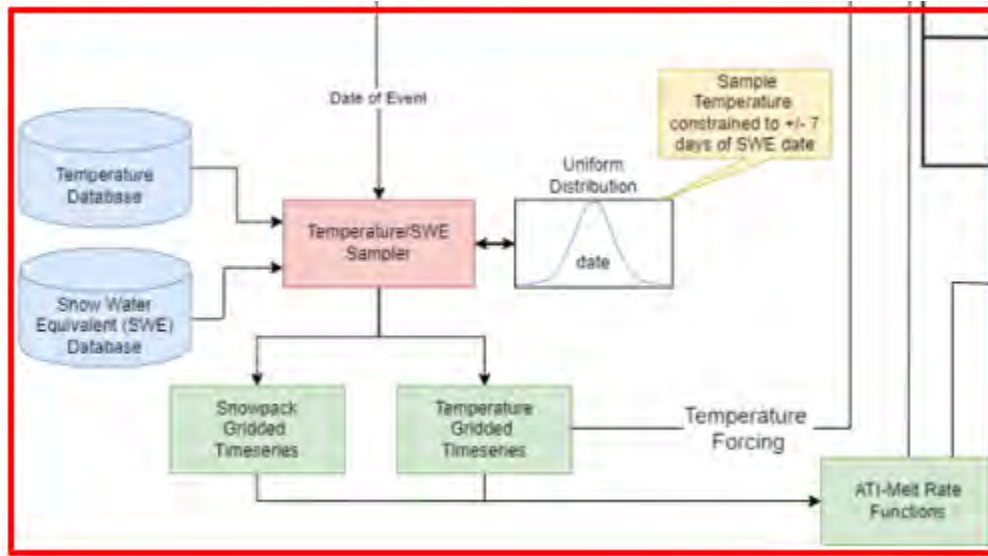   - SWE and Temp data retrieved for: June 5, 1993

Figure 44. SWE and temperature sampling procedure.

An additional function was incorporated into the HEC-HMS model configuration to account for seasonal variations in snowmelt rates for each simulation (Hydrologic Engineering Center, 2024). This function, referred to as the Antecedent Temperature Index – Meltrate (ATI-Meltrate) Function, was applied in combination with temperature data from the sampled event date and extended for the full simulation duration (up to 40 days). The ATI-Meltrate Function is governed by the following relationship:

Equation 6.

$$ATI_{(t-1)} = \left(ATIMR_{coeff} - ATI_t\right) + (T_a - T_{base}) * S$$

where:

- α = ATI-Meltrate Coefficient
- Ta = Input air temperature
- Tb = Base temperature
- S = Model time step (days)

If precipitation = 0 and ATI>0:

$$Cumulative\ Melt_t = SWE_{t-1} - SWE_t$$

Python scripts were developed to automate the sampling process, ensuring that event-specific ATI-Meltrate functions were generated for each subbasin in the model. Instead of applying a single bulk function across the entire watershed, this approach improved the model's accuracy by assigning meltrate values based on subbasin-specific characteristics. This enhancement

allowed for a more realistic representation of snowmelt processes across varied terrain and climatic conditions.

Due to the significant contribution of snowpack to baseflow in the fluvial channels of the watershed, initial baseflow conditions were incorporated into the stochastic process. This approach accounted for both baseflow dynamics and the expected snowmelt response in ungauged locations. To estimate the initial unit baseflow at the start of each simulation, a review of average daily and monthly discharge was conducted at available USGS gaging stations. The monthly discharge data was then used to fit a gamma distribution, providing a statistical basis for probabilistic baseflow sampling (Figure 45).
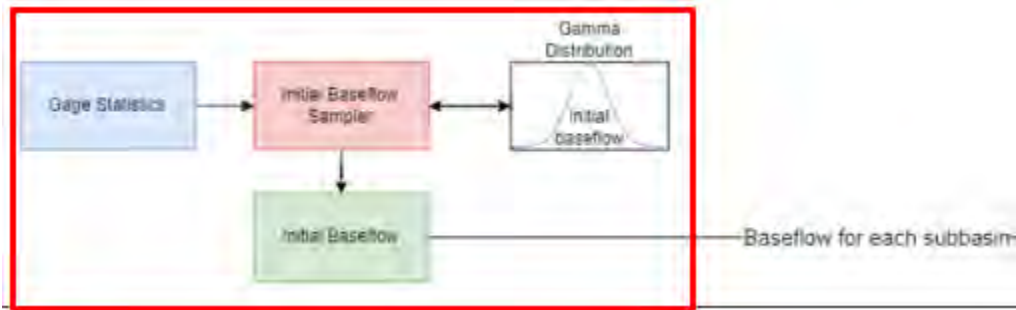
Figure 45. Baseflow sampling procedure.

The initial unit baseflow was randomly sampled from the probability space of the fitted gamma distribution, formulated as Equation 7:

Equation 7.

$$f(x|\alpha, \beta) = \frac{\beta^\alpha}{\Gamma(\alpha)} x^{\alpha-1} \exp(-\beta x)$$

Where:

- x = baseflow
- α = shape parameter
- β = scale parameter
- Γ(α) = gamma function

This probabilistic approach ensured that the baseflow conditions reflected natural variability, improving the model's representation of snowmelt-driven hydrology across the watershed (Figure 46).

Figure 46. Gage fitting for baseflow.
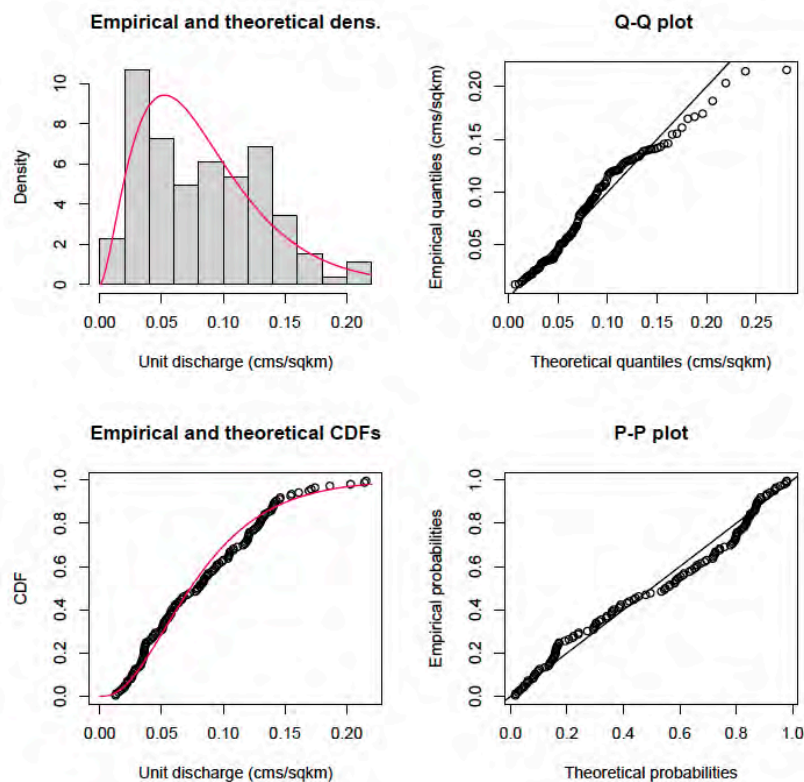
5.6.5   Flood Frequency Analysis

With sampling results and metadata in place, the sampling process was reviewed before simulating events in the realization.

The computational infrastructure played a critical role in enabling the development, execution, and review of hydrologic model results. To capture extreme event frequencies, such as 500-year floods, a realization length of 550 synthetic years was determined to be sufficient for each realization, with 10 realizations performed. A Python library was developed to manage random sampling, assembly, and adjustment of individual HEC-HMS model files, and the aggregation of results. The library included several key features, such as metadata tracking to link stochastic processes with results, seed tracking for random number generation to ensure the reproducibility of each event or realization, and automated execution of simulations in a cloud-based environment.

Hydrologic simulations were managed using an implementation of the process-API, as described by Lawler et al. (2024). Each hydrologic simulation job was submitted to the API, which launched a containerized execution environment on Amazon Web Services (AWS) serverless infrastructure. Each AWS container copied model files from an AWS Simple Storage Service (S3)

bucket, executed the hydrologic simulation using HEC-HMS binaries in a Linux environment, and stored the output files and metadata back in the S3 bucket (Figure 47).
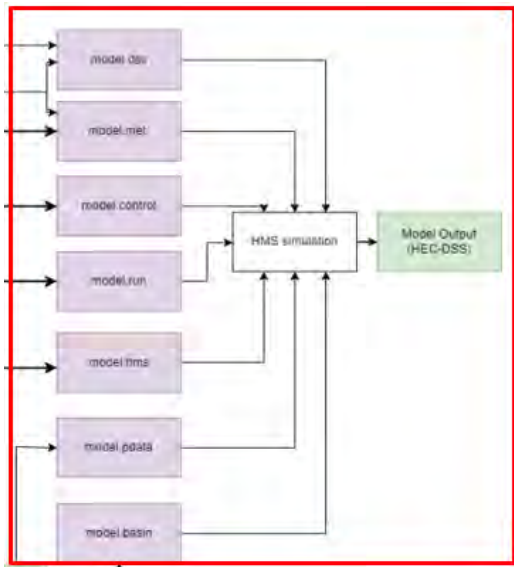

Figure 47. Files written to S3 for cloud execution of the hydrologic models.

A series of postprocessing routines was implemented to facilitate rapid evaluation of simulation results. The HEC-HMS results, stored in HEC-DSS files, were extracted and converted into Zarr format for more efficient retrieval and analysis. The annual maximum discharges for every element in the HMS model were computed for each year and stored in a separate Zarr array, allowing for streamlined access to results across all realizations (Figure 48).
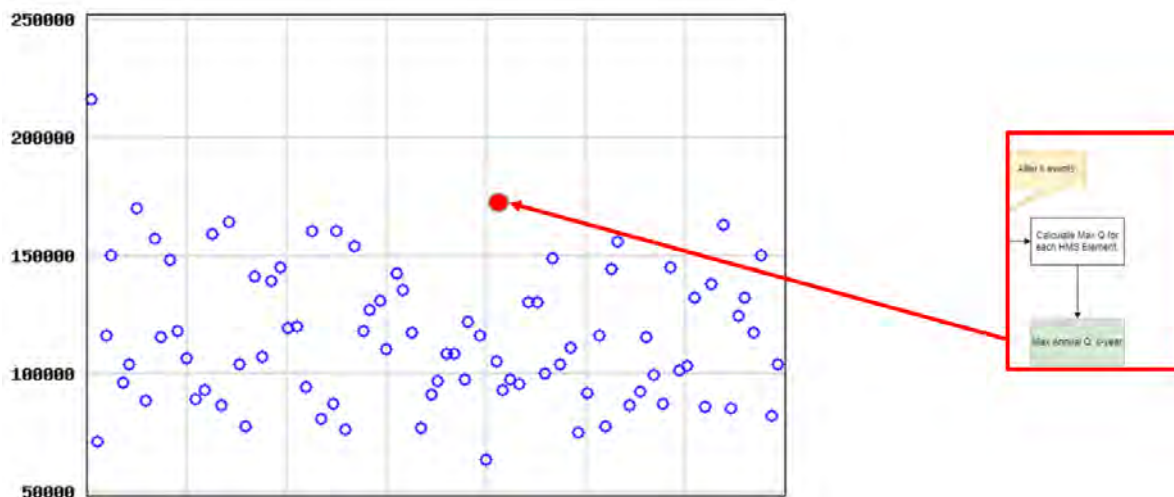

Figure 48. Example of creating a synthetic annual maximum series (AMS) at a point location in the watershed.

Once a 50-year realization produced satisfactory results, full 500-year realizations were executed, post-processed, and compared against observed annual maximum discharges at stream gage

locations. It was not necessary for a gauge to be active or to report high-frequency (e.g., 15-minute or 1-hour) discharge values as long as annual maximum discharge records were available. These historical data points provided valuable benchmarks for evaluating model performance. Consideration was also given to the age of the data and any watershed alterations that may have influenced flow conditions over the period of record (Figure 49).
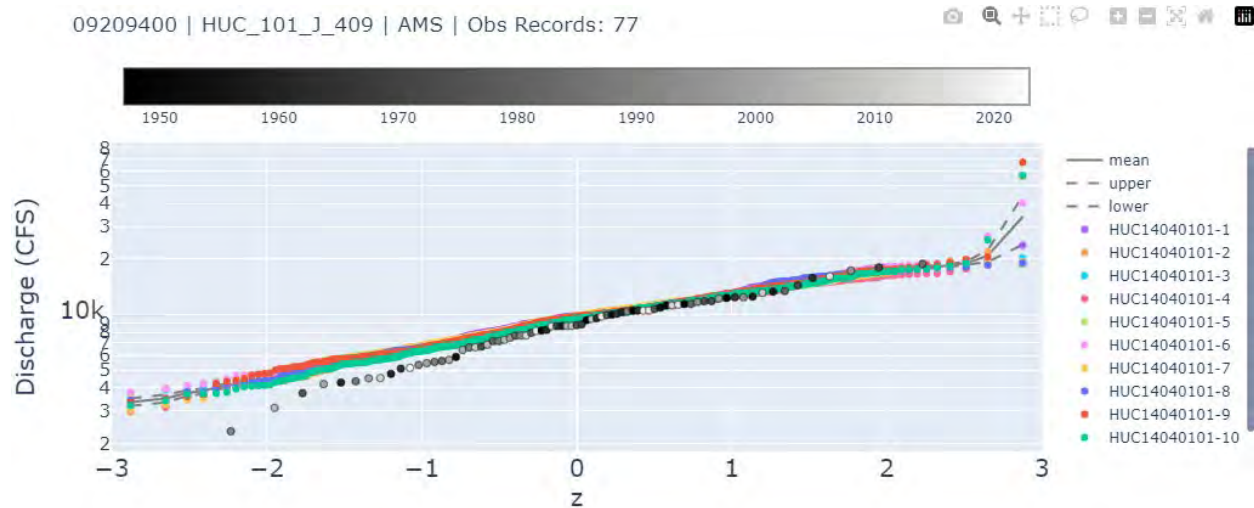

Figure 49. Synthetic AMS results compared to observed USGS AMS (black).

6.0 Hydraulic Modeling

6.1 Model Development Overview

This BLE study utilized two-dimensional (2D) unsteady hydraulic models within HEC-RAS (v6.4.1) to create floodplains that are based on the hydrograph inflows from hydrologic modeling performed in HEC-HMS. These hydrographs served as inflow boundary conditions for HEC-RAS hydraulic models. The initial mesh spacing in each domain was set to 400 feet.

The junctions from the HEC-HMS model were used as the location for the internal boundary conditions. Using the synthetic storms discussed in Section 5.0, inflow hydrographs were applied to these junctions. The inflow boundary conditions at each junction represented the additional inflows from each upstream sub-basin so that flow accumulation was accounted for throughout the watershed. Routing of these flows was handled by the 2D computational mesh in HEC-RAS.

Since the hydrologic flow for a specific annual exceedance probability (AEP) is derived from several storm events, multiple plans were processed for each AEP. Each junction has a specific storm event attributed to it for each AEP. Therefore, a certain AEP might have more than one storm event attributed to it. All associated plans need to be processed. For 10%, 4%, 2%, 1%, 1%+, 1%-, and 0.2% AEP, there will be a minimum of 7 plans. The maximum number of plans is 58 for HUC10 1404010306.

Figure 50 shows a 1% map for 1404010206 and the storm events that are associated with each junction. Figure 51 shows how the discharge rates compare for each storm event.
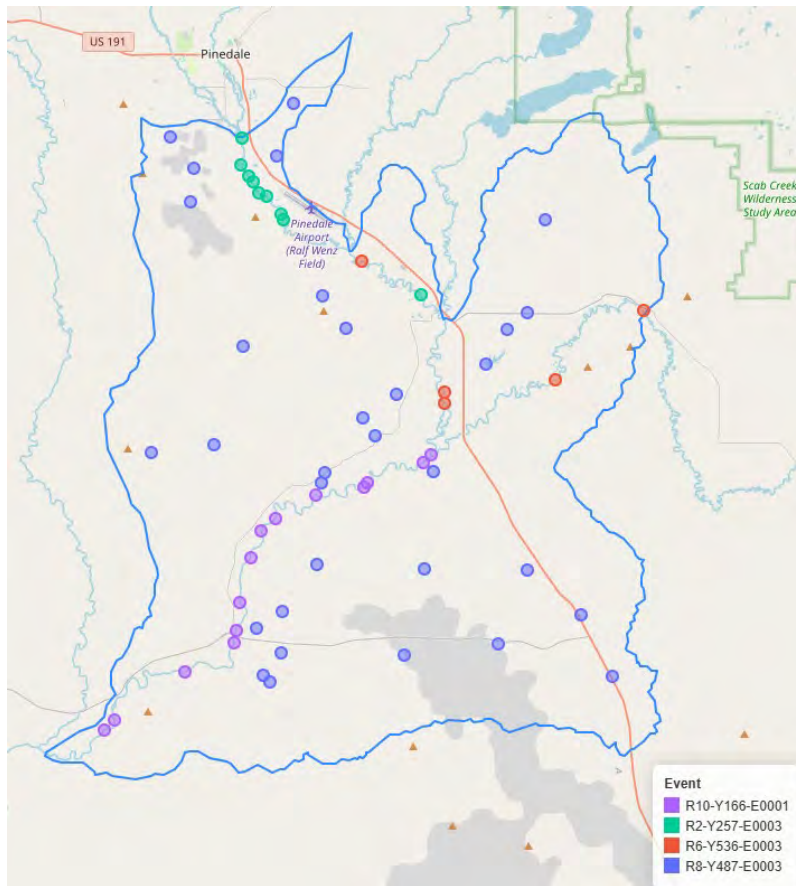

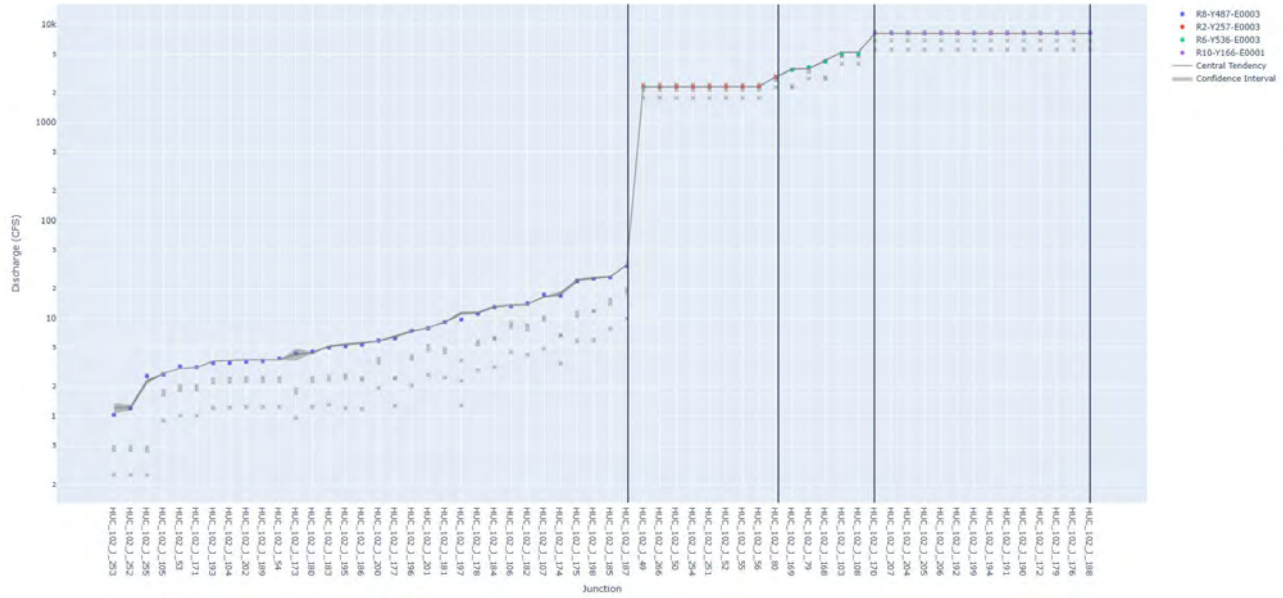**Figure 50. HUC10 1404010206 1% Storm Event Map**

Figure 51. HUC10 1404010206 1% Storm Event Plot

6.2   Terrain Development

The DEM used for this project was obtained from USGS National Map datasets. The terrain included NED (1-meter resolution) QL2 data, to provide a detailed and accurate representation of the physical topography. The projected coordinate system used was U.S. Contiguous Albers Equal Area Conic, with both vertical and horizontal units set to feet.

To provide coverage, multiple DEM sources were assembled:

- USGS NED "1m" covered approximately 93% of the study area.

- USGS NED "Original Product Resolution" (OPR), was utilized for the areas of Utah, which were not yet integrated into the NED "1m" dataset, specifically Project UT_FlamingGorge_3_2020, was utilized in its OPR format.   Please note the OPR has a higher resolution of 0.5m.

The DEM was clipped to the domain areas and reviewed for elevation consistency and boundary mismatches. Missing DEM data occurred in a few basins. In those cases, the mesh was adjusted to exclude the areas missing DEM areas if it was outside the area of influence of the hydrologic flow input. For example, 1404010610 had the mesh modifications to remove a missing DEM area that was outside the flooding area, as shown in Figure 52.
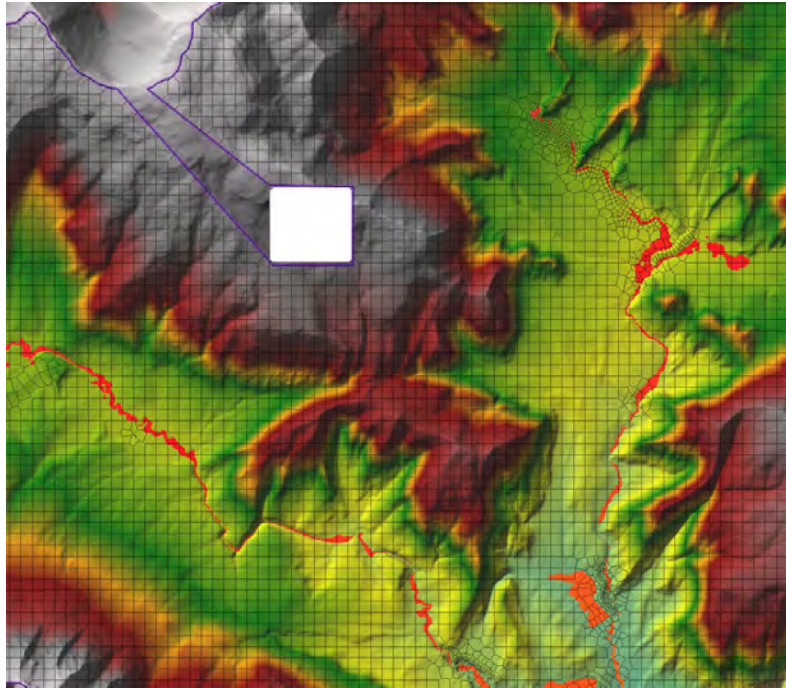
Figure 52. Adjusted Mesh Due to Missing DEM Areas

6.3 Model Development Overview

Breaklines were utilized to properly align cells to embankments, high grounds, and roads located within the floodplain area. The cell mesh spacing along the breaklines varied from 200 to 400 feet, depending on the location and the level of detail needed. The cell mesh along breaklines varied from 100 to 200 feet in refinement regions.

6.3.1 Hydraulic Structures

Structures were identified from the DEM and ortho-imagery; no survey was conducted. Cell mesh was aligned to high ground using breaklines and a hydro connector was used to pass flow through the structure. "Hydro connectors" were added by using terrain modifications as shown in Figure 53 to reflect the approximate stream invert slope and opening size to allow flow conveyance within reason through the structure. The approximate opening of a structure was based on aerials and DEMs.
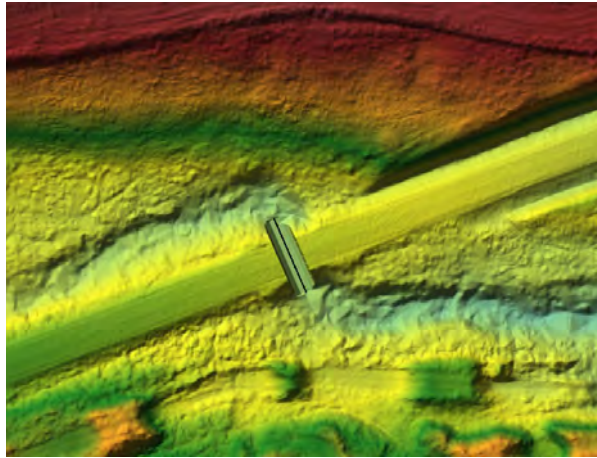
Figure 53. Example of Hydro-Connector Terrain Modification

Dams were identified using the National Inventory of Dams (NID). All high or significant hazard dams were captured using a 2D connection. For all other dams, the cell mesh was aligned using breaklines along the dam crest.

Two of the High-Risk classified dams were located at the perimeter outlet, which required a unique model perimeter adjustment. Instead of a 2D connection, the perimeter was modified to follow the dam crest, and a v-notch was made to allow for regular flow to pass from the upstream model to the downstream model. This would prevent an unrealistically high WSEL.

Models HUC10 1404010204 and 1404010401 had a perimeter outlet that followed this procedure, as can be seen in Figure 54 .
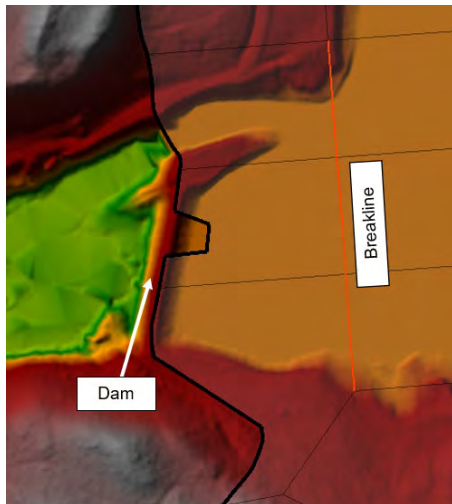

Figure 54. Example of Hydro-Connector Terrain Modification

6.3.2 Manning's 'N' Roughness Coefficient

The National Landcover Database (NLCD) 2019 (Yang et al., 2018) was primarily used to determine land use and corresponding roughness values. Regarding overbanks, the Manning's values were set to the average values from the HEC-RAS reference document (as listed in Table 6).

Table 6. Manning's 'n' Roughness Coefficients Corresponding to NLCD 2019 Dataset

Land Cover Description	Manning's 'n' Roughness Coefficient
Open Water	0.03
Perennial Snow/Ice	0.01
Developed, Open Space	0.04
Developed, Low Intensity	0.08
Developed, Medium Intensity	0.10
Developed High Intensity	0.15
Barren Land (Rock/Sand/Clay)	0.025
Deciduous Forest	0.16
Evergreen Forest	0.16
Mixed Forest	0.16
Shrub/Scrub	0.10
Grassland/Herbaceous	0.035
Pasture/Hay	0.03
Cultivated Crops	0.035
Woody Wetlands	0.12
Emergent Herbaceous Wetlands	0.07
Palustrine Forested Wetland	0.12
Palustrine Scrub-Shrub Wetland	0.07
Palustrine Emergent Wetland	0.07

6.3.3 Computational Settings

The computational timestep was selected to balance between model runtimes, model stability, and model accuracy. Diffusion Wave Equations (DWE) were selected, the HEC-RAS Hydraulic Reference Manual states that the combination of timestep, flood wave velocity and cell size should result in a peak Courant number ideally less than six tenths (0.6) and not to exceed two (2). An Advanced Time Step Control was utilized with Courant Velocity/Length Methodology and parameter values based upon the Equation Set and model run time considerations. If 1% velocities were too high, the timestep was further reduced.

6.3.4 Boundary Condition

6.3.4.1 Downstream Boundary Condition

A 'normal depth' boundary condition was used as a default downstream boundary condition except for the events that represented tie-ins for recurrence intervals. Normal depth slopes were approximated by the generalized slope of the terrain at the downstream end of the model. Stage hydrographs or rating curves were used for tie-in events. More information about this approach is provided in Section 6.3.6. There were two models (see Section 6.3.4.4) that were closed basins and therefore did not have a downstream boundary condition.

6.3.4.2 Internal Boundary Condition

Inflow boundary conditions were inserted at junction locations from HEC-HMS with flow hydrograph boundary conditions. Figure 55 shows a sample junction with storm event data attributed to the 1%. The internal boundary condition would be placed in the same location as HUC_102_J_204 and the inflow hydrograph would be from storm event R10-Y166-E0001 and include the additional subbasin inflows that contribute to that junction.
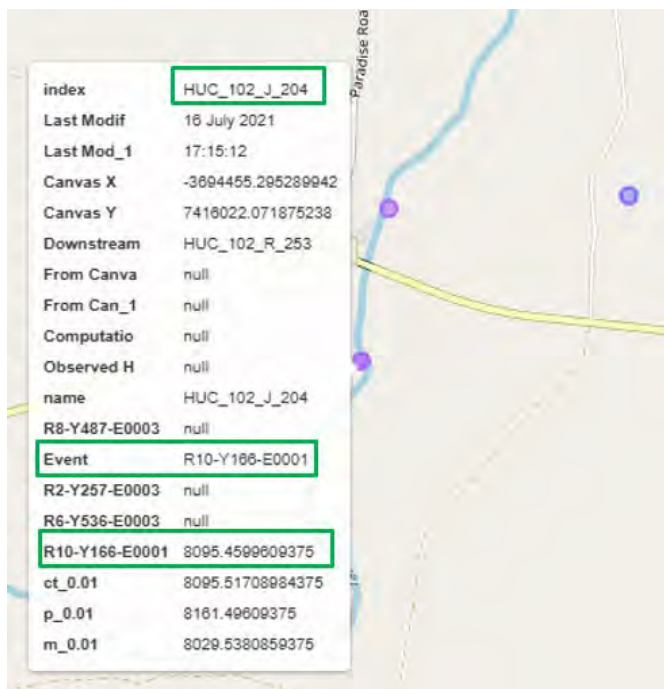
Figure 55. Sample Model Junction with Associated 1% Storm Event Data

Agricultural diversions, as described in Section 5.5.1.7, were incorporated into the hydraulic models as internal boundary conditions. The hydrographs provided negative flow. Figure 56 illustrates the internal boundary condition and associated hydrograph. Models that required this resulted in a high percent volume error because of differences in flow conditions between HEC-HMS and HEC-RAS. The high error is a limitation to the approach, but does not impact the results

because it effectively represents the situation where the diversion is removing more water volume than is physically present within the mesh cells.
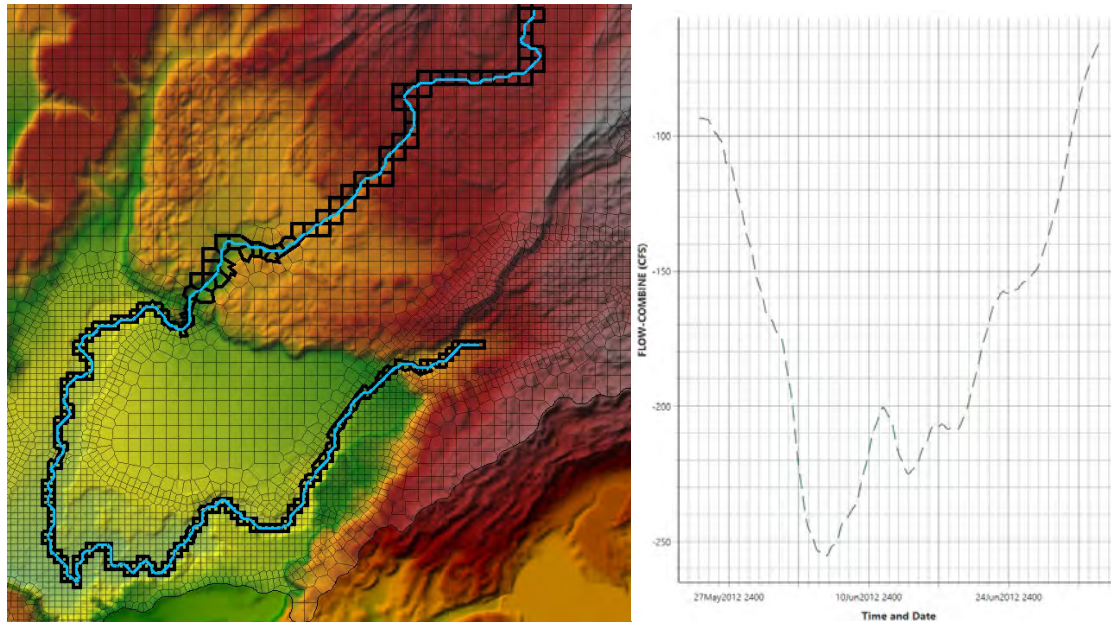

Figure 56. Example of Agricultural Diversions as Internal Boundary Conditions

6.3.4.3   Upstream Boundary Condition

All models with flow from upstream models will have an inflow hydrograph upstream boundary condition. All of these models have a junction in the same location as the inflow, and these junctions will provide the flow used directly from HEC-HMS.

6.3.4.4   Closed Basins

Two of the scoped models are closed basins and do not have downstream boundary conditions. HUC10 1404020007 and 1404020005 do not have any flow leaving the model domain.

6.3.5   Reservoirs

Unlike the rest of the dams in the domain areas, the operation of Fontenelle Dam and Flaming Gorge Dam was considered, requiring a separate approach.

The hydrology incorporated a steady outflow downstream for the reservoirs. Since the flow upstream and downstream of the reservoirs were analyzed separately, the inflow upstream of the dam crest needed to be disassociated with flow downstream of the dam. To recreate these separate conditions in the HEC-RAS model, the perimeter was trimmed and cut through the model domain at the dam, and an external boundary condition is introduced along the spillway, as shown in Figure 57. For Flaming Gorge, a Rating Curve was used, and for Fontenelle, a Normal Depth

was used. This effectively reset the flows at the dam and allowed the RAS model to match the operational flows downstream of the dam specified by HEC-HMS.
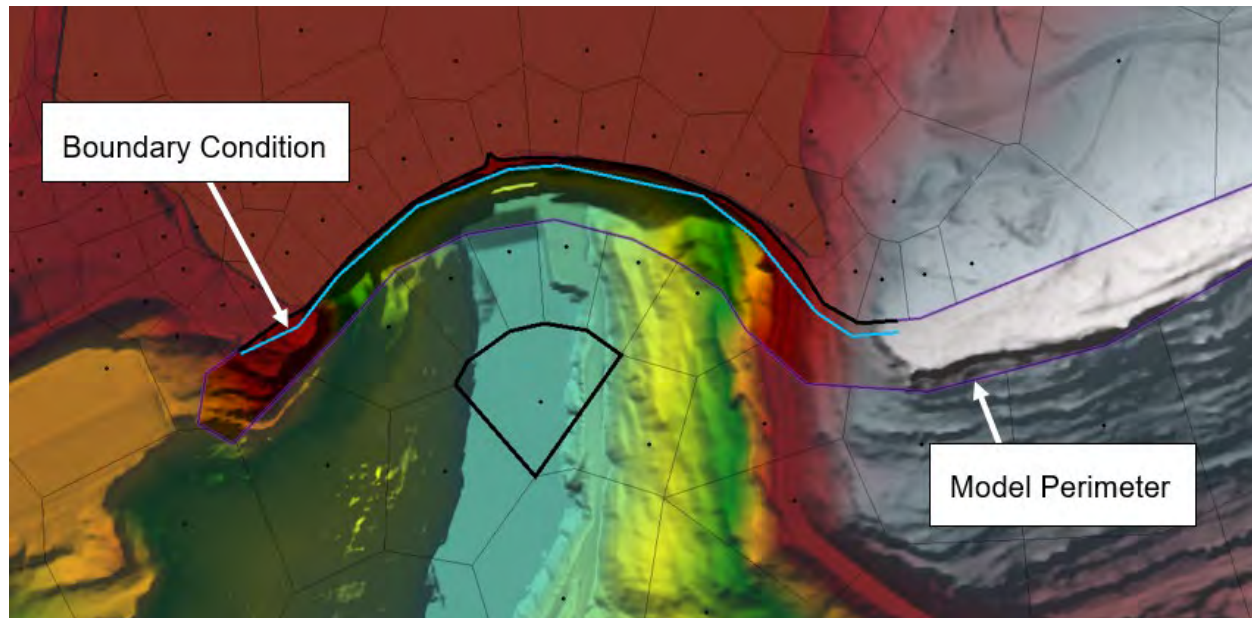

Figure 57. Mesh Adjustment for Reservoirs

6.3.6 Tie-Ins

The general approach to model tie-ins was to achieve continuity in WSEL information from reach to reach within the 0.5-foot tolerance as specified by FEMA SID #65. However, there are instances where the tie-in was greater than the 0.5-foot tolerance and will need to be resolved during the data development phase.

Achieving a tie-in within 0.5 feet was a challenge with the current project workflow because of the following reasons:

1. Flows were not necessarily consistent across model domains at the tie-in location.

2. Several storm events were required to generate a recurrence interval map for the entire basin, sometimes resulting in elevated flows at the tie-in from non-tie-in events.

Inconsistencies in flows across tie-ins existed because HEC-HMS was utilized to provide input flow hydrographs yet outlet flow conditions were based on the routing of basin flows within the HEC-RAS 2D mesh. Although the input into both models was the same, the resulting hydrograph at the boundary condition differed because of difference in flow routing methodologies between the HEC-HMS and HEC-RAS. An example of the differences at a tie-in location is shown in Figure 58. The downstream model uses the HMS hydrograph as input whereas the upstream model condition at the same location is represented by the HEC-RAS output hydrograph.
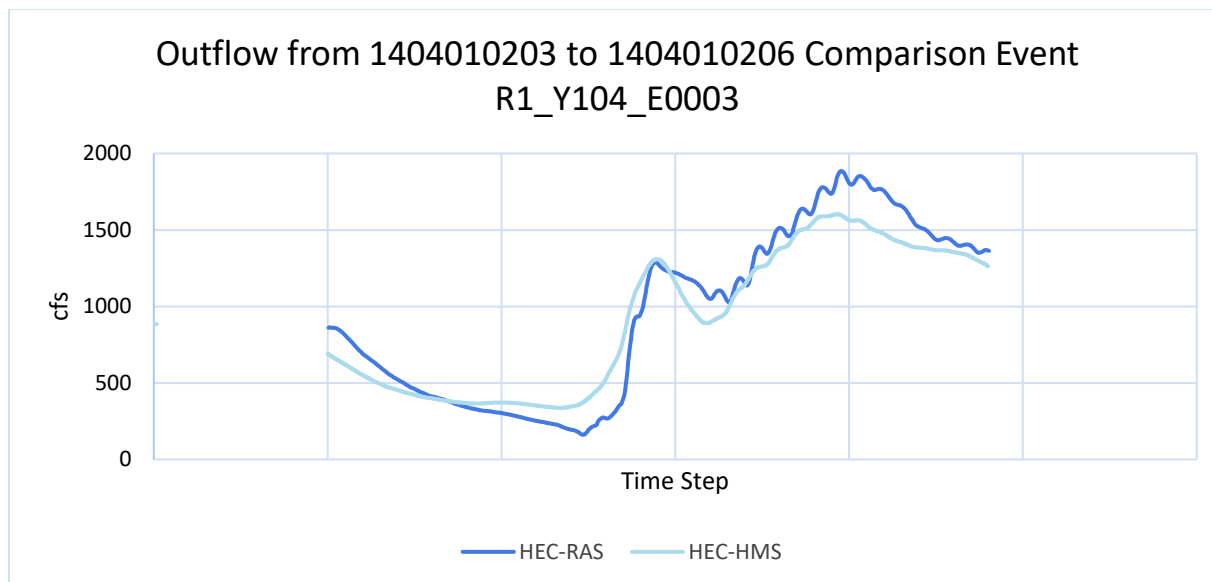
Figure 58. Flow Discrepancies at Boundary Conditions (HMS vs RAS)

The flow differences caused differences in stage. To force a tie-in, a stage hydrograph or rating curve boundary condition approach was used to impose the stage hydrograph of the downstream model onto the upstream model. Supplemental information about this approach is available in the Hydraulic SOP Appendix A. An example showing the location of the boundary condition location is shown in Figure 59.

Figure 59. Model Boundary Map

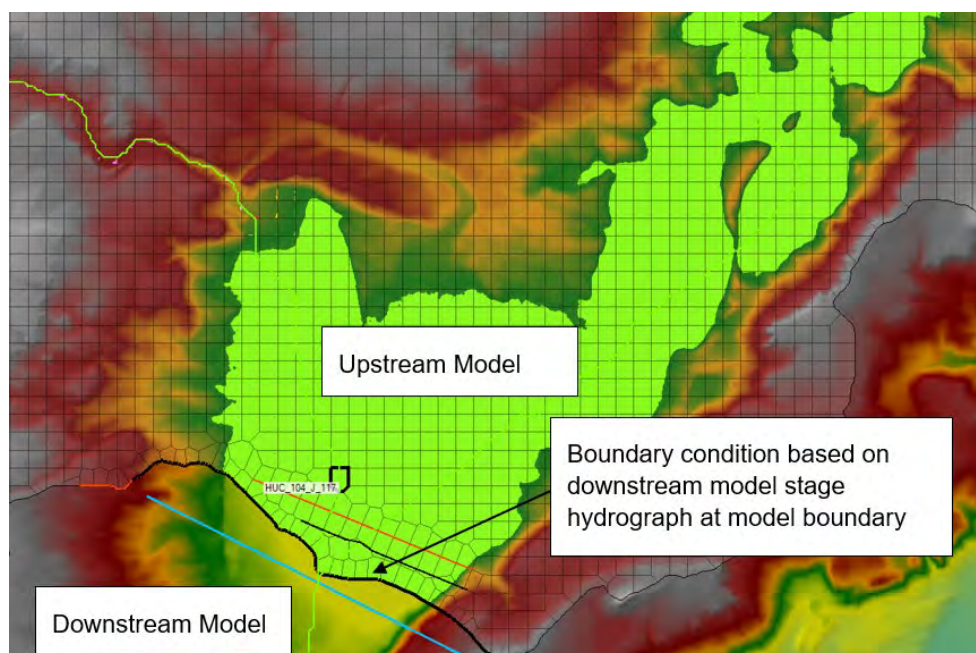Aerial imagery and flow/stage relationships were considered to determine whether the downstream boundary condition of a tie-in model should be based on a rating curve or a stage hydrograph. If it appeared that backwater from the downstream model would dominate the stage into the upstream model, as is the case for lakes, a stage hydrograph should be applied. Otherwise, a rating curve was used.

Additionally, multiple events were often required to represent a single recurrence interval across the basin; therefore, several RAS model plans needed to be combined by maximum water surface elevation. There were cases where storm events that were not intended to produce the maximum water surface elevation at the tie-in ended up controlling the water surface elevations. For these cases, manual tie-ins were achieved as part of post-processing. Additional work on the SST inputs would be required to address this challenge as part of the RAS modeling effort.

6.3.7   Quality Control and Finalization

A comprehensive quality control (QC) process was conducted before finalizing each model, including:

- Model geometry and terrain development

- Hydrologic incorporation

- Results review

These steps provided consistency across the model areas and were used to confirm that the final hydraulic models met project requirements. Particular focus was given to reviewing for consistent application of hydro connectors and breaklines, volume and flow consistency between HEC-HMS and HEC-RAS, and realistic velocities.

6.4   Results

From the process mentioned in Section 1.3, WSEL and depth grids corresponding to the 10%, 4%, 2%, 1%, 1% plus, 1% minus, and 0.2% AEP were produced. Each junction had an associated storm event, which was processed for the entire HUC10 model. Figure 60 and Figure 61 show that different storms represent the main channel and the side tributary flowing into it. To create the final floodplain for 1%, the maximum WSEL is used. Figure 62 shows the final merged 1% floodplain.
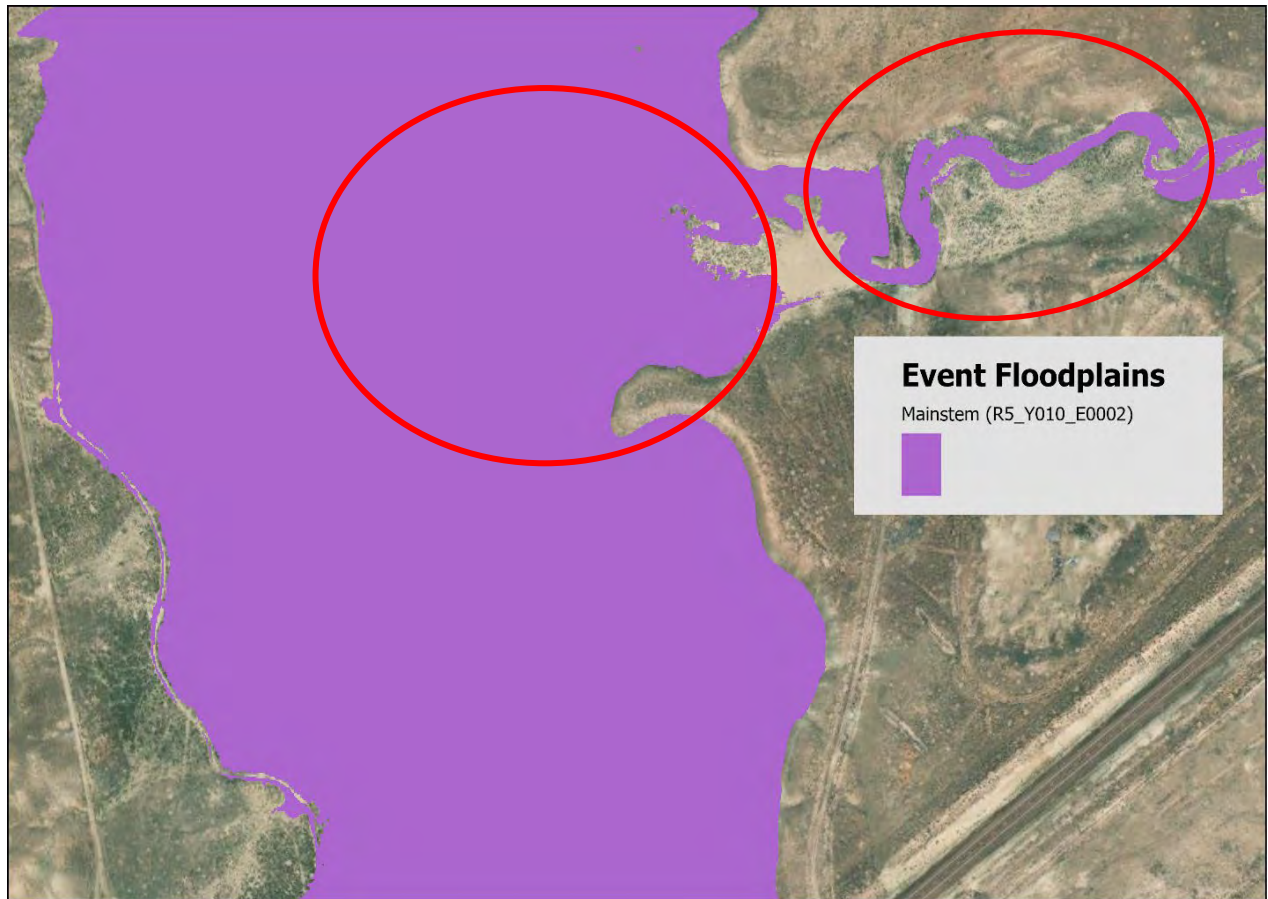
Figure 60. 1% Storm Event for Mainstem

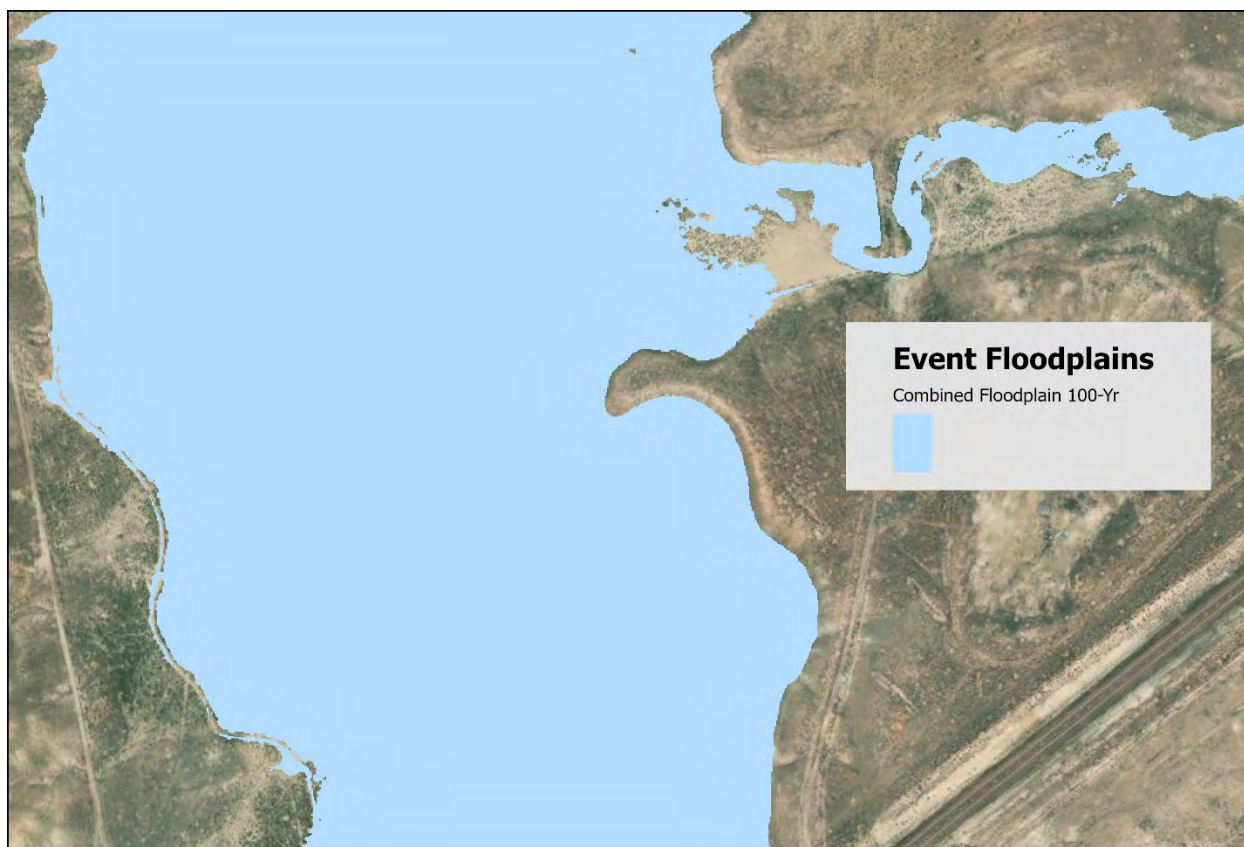**Figure 61. 1% Storm Event for Side Tributary**

Figure 62. Merged 1% Mainstem and Side Tributary Floodplain

7.0   Floodplain Mapping

The BLE 10%, 4%, 2%, 1%, 1%+, 1%-, and 0.2% AEP results were mapped to the DEM terrain used within the Discovery BLE 2D hydraulic models. Floodplains were edited slightly using engineering judgment.

Each AEP consists of data from multiple storm events that are representative of the relevant AEP. To create one grid for each AEP, the maximum WSEL, depth, and velocity is applied for each storm event.

All of the AEP WSEL extents obtained from Discovery BLE 2D hydraulic model results are included in the database deliverable as "S_Fld_Haz_Ln". Floodplains were not modified manually to include water features visible in the aerial photography (e.g., lakes, ponds, stream meanders). Floodplains were not cleaned up in areas of split flow or non-containment. Floodplains were simplified and refined to remove detached polygons and holes. A sample 1% and 0.2% floodplain is shown in Figure 63.

Model tie-ins were determined based on a +/- 0.5-foot threshold. STARR II identified areas where the BLE 1% AEP extents differed from the mapping in the adjacent counties. Where feasible,

STARR II made minor updates to the model perimeters to improve the tie-ins in these areas to limit the amount of border mismatches or unusual gaps in floodplain mapping that are generated (FEMA SID 306).
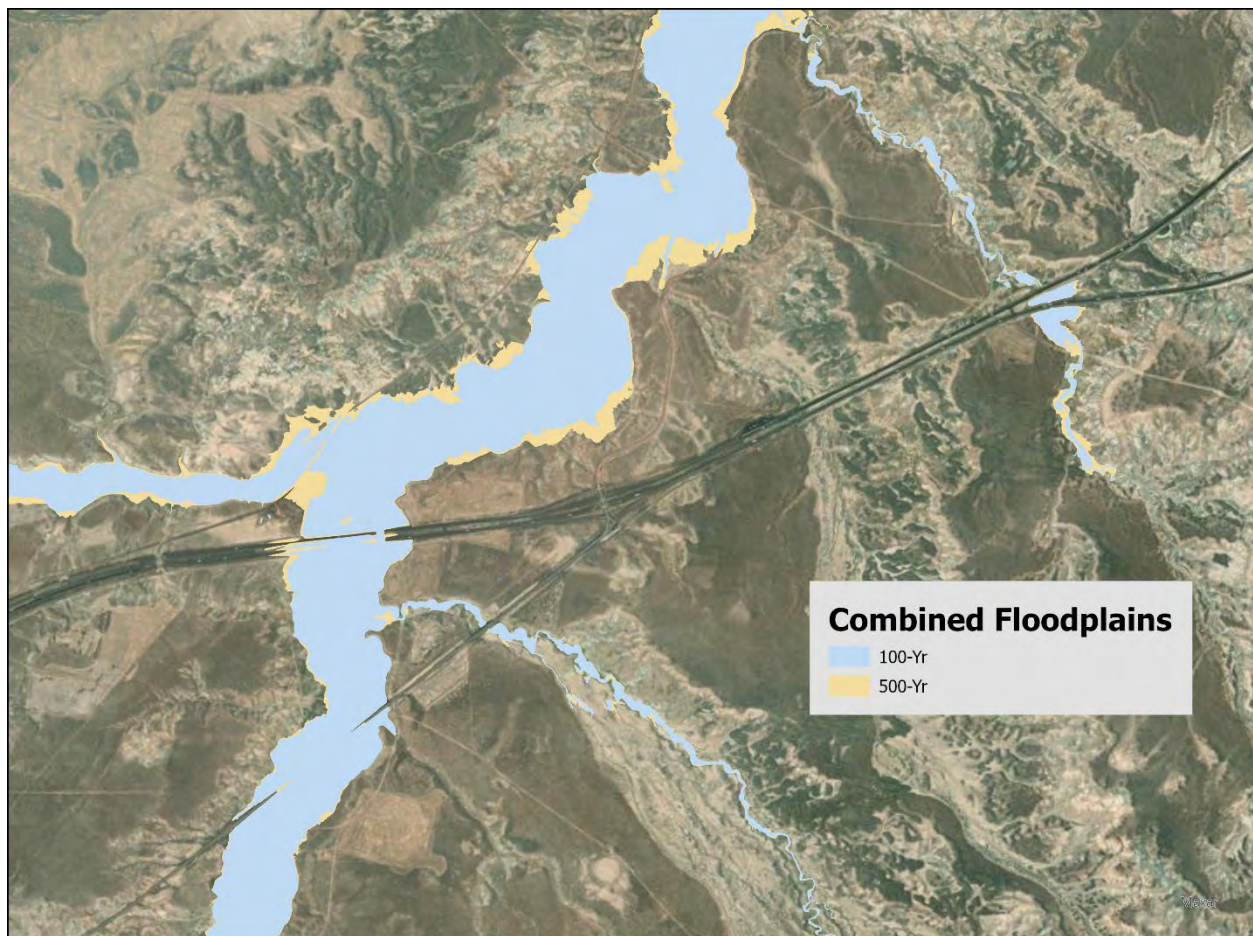
Figure 63. Sample 100-Yr and 500-Yr Floodplain

8.0   Data Capture Submittal Folder Structure

For further details on data capture submittal, see the readme file in the task documentation folder.

9.0   Recommendations

BLE offers a cost-effective and scalable approach for identifying flood hazards, making it a valuable tool for screening, mitigation planning, and emergency preparedness. However, its adoption should align with its intended purpose, technical limitations, and integration with other flood risk management efforts. Key considerations for BLE use include:

- **Supporting non-regulatory applications:** BLE should be leveraged as a screening tool to enhance flood risk awareness, inform mitigation strategies, and support emergency response planning. It can complement existing flood hazard datasets, particularly in areas with limited or outdated flood risk information, but should not replace detailed studies for decision-making related to infrastructure, land use, or regulatory floodplain management.

- **Enhancing climate resilience and study prioritization:** BLE can help identify areas where flood risk may increase over time, supporting proactive adaptation strategies. It also serves as an initial screening tool to prioritize detailed flood studies, ensuring efficient resource allocation to high-risk areas requiring further analysis. By leveraging BLE appropriately, stakeholders can improve flood risk awareness and preparedness while recognizing the need for additional validation and refinement in certain areas.

Advancing a BLE study into a detailed study requires varying levels of effort, depending on factors such as data availability, hydrologic and hydraulic complexities, regulatory requirements, and local flood risk concerns.

10.0   References

Alexander, M.A., Scott, J.D., Swales, D., Hughes, M., Mahoney, K., & Smith, C.A. (2015). Moisture pathways into the US Intermountain West associated with heavy winter precipitation events. Journal of Hydrometeorology, 16(3), 1184–1206. https://doi.org/10.1175/JHM-D-14-0139.1

Lawler, S., Deshotel, M., Dietrich, A.H., et al. (2024). Application of stochastic storm transposition for hydrologic modeling in the mountainous western US. Stochastic Environmental Research and Risk Assessment, 39, 109–127. https://doi.org/10.1007/s00477-024-02853-6

Micovic, Z., Schaefer, M.G., & Taylor, G.H. (2015). Uncertainty analysis for probable maximum precipitation estimates. Journal of Hydrology, 521, 360–373. https://doi.org/10.1016/j.jhydrol.2014.12.033

Nathan, R., Jordan, P., Scorah, M., Lang, S., Kuczera, G., Schaefer, M., & Weinmann, E. (2016). Estimating the exceedance probability of extreme rainfalls up to the probable maximum precipitation. Journal of Hydrology, 543, 706–720. https://doi.org/10.1016/j.jhydrol.2016.10.044

Wright, D.B., Smith, J.A., Villarini, G., & Baeck, M.L. (2013). Estimating the frequency of extreme rainfall using weather radar and stochastic storm transposition. Journal of Hydrology, 488, 150–165. https://doi.org/10.1016/j.jhydrol.2013.03.003

Wright, D.B., Mantilla, R., & Peters-Lidard, C.D. (2017). A remote sensing-based tool for assessing rainfall-driven hazards. Environmental Modelling & Software, 90, 34–54. https://doi.org/10.1016/j.envsoft.2016.12.006

Wright, D.B., Yu, G., & England, J.F. (2020). Six decades of rainfall and flood frequency analysis using stochastic storm transposition: Review, progress, and prospects. Journal of Hydrology, 585, 124816. https://doi.org/10.1016/j.jhydrol.2020.124816

Federal Emergency Management Agency (FEMA). (2023). Guidance for flood risk analysis and mapping: Base level engineering (BLE) analysis and mapping. Available at https://www.fema.gov/sites/default/files/documents/fema_rm-base_level_engineering_guidance_nov_2023.pdf , accessed March 2025.

FEMA. (2024). Guidance for flood risk analysis and mapping, hydrology: Rainfall-runoff analysis. Available at https://www.fema.gov/sites/default/files/documents/fema_guidance_hydrology_rainfall-runoff_analysis_nov_2024.pdf, accessed March 2025.

FEMA. (2022). Guidance for flood risk analysis and mapping, General hydrologic considerations, Available at https://www.fema.gov/sites/default/files/documents/fema_general-hydrologic-considerations_112022.pdf, accessed March 2025.

FEMA. (2022). Guidance for flood risk analysis and mapping, General hydraulics considerations. Available at https://www.fema.gov/sites/default/files/documents/fema_general-hydraulics-guidance_112022.pdf, accessed March 2025.

Bureau of Land Management (BLM). (2023). Wyoming land use & public lands data. U.S. Department of the Interior. Available at https://www.blm.gov/wyoming, accessed March 2025.

Science and Technology Program Research and Development Office, U.S. Bureau of Reclamation (USBR). (2020). Stochastic storm transposition for physically-based rainfall and flood hazard analyses. Final Report No. ST-2020-1735-1, Technical Memo No. ENV-2020-070.

United States Army Corps of Engineers. (2022). Kanawha Pilot Project for Future of Flood Risk Data Initiative.

U.S. Census Bureau. (2024). Annual estimates of the resident population for counties in Wyoming: April 1, 2020 to July 1, 2023. Population Division. Available at https://www2.census.gov/programs-surveys/popest/tables/2020-2023/counties/totals/co-est2023-chg-56.xlsx, accessed March 2025.

National Weather Service, Office of Weather Prediction. (2021). Analysis of record for calibration: Version 1.1, sources, methods, and verification.

National Oceanic and Atmospheric Administration (NOAA). (2025). Analysis of record for calibration (AORC). Available at https://registry.opendata.aws/noaa-nws-aorc/, accessed February 2023.

NOAA. (2025). Analysis of record for calibration: Version 1.1. Available at https://hydrology.nws.noaa.gov/pub/AORC/V1.1/, accessed February 2023.

PRISM Climate Group, Oregon State University. (2022). PRISM climate data. Available at https://prism.oregonstate.edu, accessed February 2023.

U.S. Census Bureau. (2024). TIGER Line datasets, road and railroad shapefiles. Available at https://www2.census.gov/geo/tiger/TIGER2024/ROADS/ and https://www2.census.gov/geo/tiger/TIGER2024/RAILS/, accessed March 2025.

U.S. Bureau of Reclamation (USBR). (2021). Flaming Gorge Reservoir 2019 area and capacity table, Colorado River Storage Project, Utah Upper Colorado Region. Available at https://usbr.gov/tsc/techreferences/reservoir/FlamingGorgeRes2019AreaCapacityTables_final508.pdf, accessed March 2025.

USBR. (2023). Flaming Gorge operation plan May 2023 - April 2024. Available at https://usbr.gov/tsc/techreferences/reservoir/FlamingGorgeRes2019AreaCapacityTables_final508.pdf, accessed March 2025.

USBR. (2023). Fontenelle Dam and Flaming Gorge Dam project pages. Available at https://www.usbr.gov/projects, accessed March 3, 2025.

USBR (2024), RISE website, https://data.usbr.gov, accessed February 2024.

U.S. Geological Survey (USGS). (2023). National Hydrography Dataset (NHD) - Current hydrography and watershed boundaries. Available at https://www.usgs.gov/national-hydrography, accessed March 2025.

USGS. (2004). Water resources of the Upper Colorado River Basin: Hydrology and water quality. Circular 1289. Available at https://pubs.usgs.gov/publication/pp441, accessed March 2025.

USGS National Map. (2023). NHDPlus dataset. Available at TNM Download v2, accessed March 2025.

Wyoming State Geological Survey (WSGS). (2023). Geology of Wyoming. Available at https://main.wsgs.wyo.gov/geology-of-wyoming/geologic-history, accessed March 2025.

Wyoming Water Development Office. (2014). Probable maximum precipitation study for Wyoming. Available at https://wwdc.state.wy.us/PMP/final-report.pdf

Wyoming State Engineer's Office. (2025). Agriculture diversion information. Available at https://seoflow.wyo.gov/, accessed March 2025.

 Wyoming State Engineer's Office. (2025). Real-time discharge data. Available at https://seoflow.wyo.gov/Data/Map/Parameter/Discharge/Statistic/LATEST/Interval/Latest, accessed March 2025.

Wyoming State Geological Survey (WSGS). (2023). Guide to the Green River Basin. Available at https://www.wsgs.wyo.gov/, accessed March 2025.

United States Geological Survey (USGS). (2003). Peak-flow characteristics of Wyoming streams (WRIR 03-4107). Available at https://pubs.usgs.gov/wri/wri034107/pdf/wri034107.pdf

NASA Earth Data. (2022). Daily 4 km gridded SWE and snow depth from assimilated in-situ and modeled data over the conterminous US, Version 1. https://doi.org/10.5067/0GGPB220EX6A

University of Arizona Climate Database. (2025). SWE. Available at https://climate.arizona.edu/data/UA_SWE/ , accessed March 2025.

Wyoming State Geological Survey (WSGS). (2025). GIS groundwater data. Available at https://main.wsgs.wyo.govgis/gis-groundwater.